

1962

The crystal structures and magnetic properties of some red cupric chloride complexes

Roger DuWayne Willett
Iowa State University

Follow this and additional works at: <https://lib.dr.iastate.edu/rtd>

 Part of the [Physical Chemistry Commons](#)

Recommended Citation

Willett, Roger DuWayne, "The crystal structures and magnetic properties of some red cupric chloride complexes " (1962).
Retrospective Theses and Dissertations. 2333.
<https://lib.dr.iastate.edu/rtd/2333>

This Dissertation is brought to you for free and open access by the Iowa State University Capstones, Theses and Dissertations at Iowa State University Digital Repository. It has been accepted for inclusion in Retrospective Theses and Dissertations by an authorized administrator of Iowa State University Digital Repository. For more information, please contact digirep@iastate.edu.

This dissertation has been 63-3011
microfilmed exactly as received

WILLETT, Roger DuWayne, 1936-
THE CRYSTAL STRUCTURES AND MAGNETIC
PROPERTIES OF SOME RED CUPRIC CHLORIDE
COMPLEXES.

Iowa State University of Science and Technology
Ph.D., 1962
Chemistry, physical

University Microfilms, Inc., Ann Arbor, Michigan

THE CRYSTAL STRUCTURES AND MAGNETIC PROPERTIES
OF SOME RED CUPRIC CHLORIDE COMPLEXES

by

Roger DuWayne Willett

A Dissertation Submitted to the
Graduate Faculty in Partial Fulfillment of
The Requirements for the Degree of
DOCTOR OF PHILOSOPHY

Major Subjects: Physical Chemistry
Physics

Approved:

Signature was redacted for privacy.

In Charge of Major Work

Signature was redacted for privacy.

Heads of Major Departments

Signature was redacted for privacy.

Dean of Graduate College

Iowa State University
Of Science and Technology
Ames, Iowa

1962

TABLE OF CONTENTS

	Page
I. INTRODUCTION	1
A. Purpose and Nature of the Problem	1
B. Literature Review	2
1. Structures	2
2. Magnetic properties	5
3. Optical properties	8
II. STRUCTURAL ANALYSIS	12
A. General Remarks	12
1. Computer techniques	12
2. Weighting schemes	16
B. Structure of KCuCl_3	23
1. Preparation and properties	23
2. X-ray data	24
3. Structural determination	26
4. Refinement	34
5. Discussion	35
C. Structure of NH_4CuCl_3	49
1. Preparation and properties	49
2. X-ray data	49
3. Structure determination	50
4. Refinement	50
5. Discussion	63
D. Structure of $\text{Cu}_2\text{Cl}_4(\text{CH}_3\text{CN})_2$	64
1. Preparation and properties	64
2. X-ray data	65
3. Structural determination	66
4. Refinement	71
5. Discussion of structure	78

	Page
E. Structure of $\text{Cu}_3\text{Cl}_6(\text{CH}_3\text{CN})_2$	83
1. Preparation and properties	83
2. X-ray data	83
3. Structural determination	85
4. Refinement	96
5. Discussion	108
F. Structure of $\text{Cu}_5\text{Cl}_{10}(\text{C}_3\text{H}_7\text{OH})$	114
1. Preparation and properties	114
2. X-ray data	115
3. Structure determination	117
4. Refinement	126
5. Discussion	133
III. MAGNETIC SUSCEPTIBILITY MEASUREMENTS	141
A. Introduction	141
B. Magnetic Susceptibility of CuCl_2	145
C. Magnetic Susceptibility of KCuCl_3	149
IV. THEORETICAL ASPECTS	152
A. Introduction	152
B. Electronic Structure of the CuCl_4^- Ion	154
C. Electronic Structure of the Cu_2Cl_6^- Ion	160
D. Conclusion	171
V. LITERATURE CITED	173
VI. ACKNOWLEDGMENTS	178
VII. APPENDIX A: GROUP THEORY APPLICATION TO BONDING IN THE CuCl_4^- ION	179
VIII. APPENDIX B: GROUP THEORY APPLICATION TO BONDING IN THE Cu_2Cl_6^- ION	192

LIST OF TABLES

	Page
Table 1. Final parameters, temperature factors, standard deviations, and R factors for KCuCl_3	36
Table 2. Interatomic distances and bond angles for KCuCl_3	37
Table 3. Least squares plane for the Cu_2Cl_6^- dimer in KCuCl_3	38
Table 4. Comparison of observed and calculated structure factors for $\{hk0\}$ precession data for KCuCl_3	39
Table 5. Final parameters, temperature factors, standard deviations, and R values for NH_4CuCl_3	57
Table 6. Interatomic distances and bond angles for NH_4CuCl_3	58
Table 7. Least squares plane for the Cu_2Cl_6^- dimer in NH_4CuCl_3	59
Table 8. Comparison of observed and calculated structure factors for $\{0kl\}$ data for NH_4CuCl_3	60
Table 9. Comparison of observed and calculated structure factors for $\{hk0\}$ data for NH_4CuCl_3	62
Table 10. Parameters, temperature factors, standard deviations and R factors for $\text{Cu}_2\text{Cl}_4(\text{CH}_3\text{CN})_2$	72
Table 11. Interatomic distances and bond angles for $\text{Cu}_2\text{Cl}_4(\text{CH}_3\text{CN})_2$	73
Table 12. Least squares plane for $\text{Cu}_2\text{Cl}_4(\text{CH}_3\text{CN})_2$	74
Table 13. Comparison of observed and calculated structure factors for $\{0kl\}$ data for $\text{Cu}_2\text{Cl}_4(\text{CH}_3\text{CN})_2$	75

	Page
Table 14. Comparison of observed and calculated structure factors for $\{h0l\}$ data for $\text{Cu}_2\text{Cl}_4(\text{CH}_3\text{CN})_2$	77
Table 15. Final parameters, temperature factors, standard deviations, and R factors for $\text{Cu}_3\text{Cl}_6(\text{CH}_3\text{CN})_2$	100
Table 16. Interatomic distances and bond angles for $\text{Cu}_3\text{Cl}_6(\text{CH}_3\text{CN})_2$	101
Table 17. Least squares plane for $\text{Cu}_3\text{Cl}_6(\text{CH}_3\text{CN})_2$	102
Table 18. Comparison of observed and calculated structure factors for the $\{h0l\}$ data for $\text{Cu}_3\text{Cl}_6(\text{CH}_3\text{CN})_2$	103
Table 19. Chemical analysis	118
Table 20. Final parameters, temperature factors, standard deviations, and R factors for $\text{Cu}_5\text{Cl}_{10}(\text{C}_3\text{H}_7\text{OH})_2$	128
Table 21. Interatomic distances and bond angles for $\text{Cu}_5\text{Cl}_{10}(\text{C}_3\text{H}_7\text{OH})_2$	130
Table 22. Least squares plane for $\text{Cu}_5\text{Cl}_{10}(\text{C}_3\text{H}_7\text{OH})_2$	132
Table 23. Character table for the group D_{4h}	179
Table 24. Character table for the spherical harmonics of the symmetry group D_{4h}	180
Table 25. Decomposition of the Y_1 and Y_2 representations into irreducible representations for the symmetry group D_{4h}	182
Table 26. Matrix representation of the group operations of the symmetry group D_{4h}	183
Table 27. Matrix representation for the interchange of ligands in CuCl_4^- under the symmetry operations of D_{4h}	188
Table 28. Symmetry orbitals for the CuCl_4^- ion	191

	Page
Table 29. Character table for the group D_{2h}	192
Table 30. Characters for the representations of the Y_0 , Y_1 , and Y_2 spherical harmonics and decomposition into their irreducible representations for the group D_{2h}	193
Table 31. Symmetry orbitals for the $Cu_2Cl_6^{=}$ ion	196

LIST OF FIGURES

	Page
Figure 1. Patterson projection onto the (100) plane for KCuCl_3	28
Figure 2. Fourier projection onto the (100) plane for KCuCl_3	29
Figure 3. Patterson projection onto the (001) plane for KCuCl_3	30
Figure 4. Patterson projection onto the (010) plane for KCuCl_3	31
Figure 5. Fourier projection onto the (001) plane for KCuCl_3	33
Figure 6. Comparison of observed and calculated structure factors for KCuCl_3	41
Figure 7. Illustration of the Cu_2Cl_6^- ion and its stacking in KCuCl_3	45
Figure 8. Illustration of the coordination of the potassium ion in KCuCl_3	47
Figure 9. Patterson projection onto the (100) plane for NH_4CuCl_3	52
Figure 10. Patterson projection onto the (001) plane for NH_4CuCl_3	53
Figure 11. Fourier projection onto the (100) plane for NH_4CuCl_3	55
Figure 12. Fourier projection onto the (001) plane for NH_4CuCl_3	56
Figure 13. Patterson projection onto the (100) plane for $\text{Cu}_2\text{Cl}_4(\text{CH}_3\text{CN})_2$	67
Figure 14. Fourier projection onto the (100) plane for $\text{Cu}_2\text{Cl}_4(\text{CH}_3\text{CN})_2$	69
Figure 15. Fourier projection onto the (010) plane for $\text{Cu}_2\text{Cl}_4(\text{CH}_3\text{CN})_2$	70

	Page
Figure 16. Illustration of the $\text{Cu}_2\text{Cl}_4(\text{CH}_3\text{CN})_2$ molecule and its stacking in the crystalline state	80
Figure 17. $\{h0l\}$ precession photograph of $\text{Cu}_3\text{Cl}_6(\text{CH}_3\text{CN})_2$	87
Figure 18. Weighted reciprocal lattice, super lattice, and sub cell for the $[010]$ zone of $\text{Cu}_3\text{Cl}_6(\text{CH}_3\text{CN})_2$	89
Figure 19. Fourier projection onto the (010) plane for $\text{Cu}_3\text{Cl}_6(\text{CH}_3\text{CN})_2$	92
Figure 20. Patterson projection onto the (010) plane for $\text{Cu}_3\text{Cl}_6(\text{CH}_3\text{CN})_2$	93
Figure 21. Patterson projection onto the (100) plane for $\text{Cu}_3\text{Cl}_6(\text{CH}_3\text{CN})_2$	94
Figure 22. Final Fourier projection onto the (010) plane for $\text{Cu}_3\text{Cl}_6(\text{CH}_3\text{CN})_2$	97
Figure 23. Fourier projection onto the (100) plane for $\text{Cu}_3\text{Cl}_6(\text{CH}_3\text{CN})_2$	98
Figure 24. Comparison of observed and calculated structure factors for $\text{Cu}_3\text{Cl}_6(\text{CH}_3\text{CN})_2$	106
Figure 25. Illustration of the $\text{Cu}_3\text{Cl}_6(\text{CH}_3\text{CN})_2$ molecule	109
Figure 26. Stacking of the trimers in $\text{Cu}_3\text{Cl}_6(\text{CH}_3\text{CN})_2$	111
Figure 27. View of the structure of $\text{Cu}_3\text{Cl}_6(\text{CH}_3\text{CN})_2$ from the (001) direction	112
Figure 28. Weighted reciprocal lattice, super lattice, and sub cell for the $[010]$ zone of $\text{Cu}_5\text{Cl}_{10}(\text{C}_3\text{H}_7\text{OH})_2$	121
Figure 29. Fourier projection onto the (010) plane for $\text{Cu}_5\text{Cl}_{10}(\text{C}_3\text{H}_7\text{OH})_2$	122

	Page
Figure 30. Patterson projection onto the (010) plane for $\text{Cu}_5\text{Cl}_{10}(\text{C}_3\text{H}_7\text{OH})_2$	124
Figure 31. Patterson projection onto the (100) plane for $\text{Cu}_5\text{Cl}_{10}(\text{C}_3\text{H}_7\text{OH})_2$	125
Figure 32. Final Fourier projection onto the (010) plane for $\text{Cu}_5\text{Cl}_{10}(\text{C}_3\text{H}_7\text{OH})_2$	134
Figure 33. Comparison of observed and calculated structure factors for $\text{Cu}_5\text{Cl}_{10}(\text{C}_3\text{H}_7\text{OH})_2$	136
Figure 34. Illustration of the $\text{Cu}_5\text{Cl}_{10}(\text{C}_3\text{H}_7\text{OH})_2$ molecule	138
Figure 35. View of the structure of $\text{Cu}_5\text{Cl}_{10}(\text{C}_3\text{H}_7\text{OH})_2$ from a direction perpendicular to the $(10\bar{1})$ plane	139
Figure 36. Wiring diagram for a Hartshorn type mutual inductance magnetic susceptibility apparatus	142
Figure 37. Plot of the molar magnetic susceptibility versus temperature for CuCl_2	146
Figure 38. Plot of the reciprocal molar magnetic susceptibility versus temperature for CuCl_2	147
Figure 39. Plot of the molar magnetic susceptibility versus temperature for KCuCl_3	150b
Figure 40. Plot of the reciprocal molar magnetic susceptibility versus temperature for KCuCl_3	151b
Figure 41. Scheme of the molecular orbital energy levels for the CuCl_4^- ion	157
Figure 42. Illustration of the B_{1g} symmetry and molecular orbitals for the CuCl_4^- ion	158

	Page
Figure 43. Scheme of the molecular orbital energy levels for the Cu_2Cl_6^- ion	164
Figure 44. Illustration of the B_{1g} and B_{2u} symmetry and molecular orbitals for the Cu_2Cl_6^- ion	167

I. INTRODUCTION

A. Purpose and Nature of the Problem

For many years attempts to obtain a theoretical explanation of the structural, magnetic, and optical properties of chemical compounds have been one of the major areas of physical and chemical research. Transition metal complexes have provided a particular fruitful field of research because of the wide variety of physical chemical properties exhibited.

Transition metal complexes are characterized by the presence of one or more transition metal ions containing incompletely filled d-orbitals. It is the presence of these incomplete shells which give rise to the interesting structural, magnetic, and optical properties of these compounds.

This report will describe the results of experimental studies of some copper(II) complexes and the interpretation of the results in terms of the electronic structure which occurs in these compounds. Interest in the copper(II) complexes arose out of a recent investigation of the garnet-red compound $\text{LiCuCl}_3 \cdot 2\text{H}_2\text{O}$ (1, 2, 3). A crystal structure analysis revealed the existence of the previously unknown dimer Cu_2Cl_6^- , and suggested an interesting correlation between the structure and coloration of copper(II) complexes. Magnetic investigations revealed that the compound became

antiferromagnetic at very low temperatures. At about the same time, a structural investigation of the red compound KCuCl_3 by Dwiggens (4) suggested that this compound also contained the dimer Cu_2Cl_6^- .

It was decided to make a more thorough study of the relationship between structural and magnetic properties of the red copper(II) halides. Initially it was hoped that a neutron diffraction study of the magnetic ordering of the unpaired electrons in CuCl_2 could be made, but this was not possible as all attempts to grow single crystals large enough for the neutron investigation ended in failure. During these attempts, however, the existence of several new red copper(II) halide complexes were discovered. It was decided to investigate the structure of these and other red copper(II) halide complexes also.

Section II describes the results of the structural investigations, while section III describes the results of the magnetic investigations. In section IV the electronic structure of these complexes is discussed along with the interpretation of the magnetic and optical properties in terms of the bonding.

B. Literature Review

1. Structures

A large number of structural determinations of copper(II) complexes have been made. Since one of the main

points of interest in this report is the relationship between structure and bonding of the halide complexes, these will be the main type of structures discussed.

The red compound CuCl_2 (5) forms an infinite linear chain of the type $(\text{CuCl}_2)_n$. Each copper atom is bonded to four chlorine atoms at distances of $2.3\overset{\circ}{\text{A}}$, sharing two chlorine atoms with each adjacent copper atom in the chain. The chlorine atoms are located equidistant from the two copper atoms to which they are bonded. Each copper atom completes its distorted octahedral configuration by bonding to chlorine atoms in adjacent chains with a bond distance of $2.95\overset{\circ}{\text{A}}$. CuF_2 (6) and CuBr_2 (7) also have this same type structure. The garnet-red $\text{LiCuCl}_3 \cdot 2\text{H}_2\text{O}$ (1) previously mentioned also contains this symmetrical type of bridging chlorine atoms between the two copper atoms in the dimer. Again the copper-chlorine bond lengths in the dimer are close to $2.3\overset{\circ}{\text{A}}$. In the red compound, CsCuCl_3 (8), infinite helical chains of the formula $(\text{CuCl}_3)_n^{n-}$ exist with each copper atom sharing one chlorine atom with each adjacent copper atom in the chain. The coordination of each copper atom is square planar. A discrete CuCl_4^- ion exists in the yellow compound Cs_2CuCl_4 (9). The ion is not planar, however, but is closer to a distorted tetrahedral structure in which the three-fold axes no longer exist, but where one four-fold inversion axis is retained. The Cu-Cl bond

distances are 2.22Å in this compound. In the yellow compound $\text{Cr}(\text{NH}_3)_6\text{CuCl}_5$, the copper(II) ion has a trigonal bipyramidal configuration (10) with two chlorine atoms at 2.32Å and three chlorine atoms at 2.35Å, in contrast to the normal square planar configuration.

In the green compound $\text{CuCl}_2 \cdot 2\text{H}_2\text{O}$ (11), copper again exhibits its square planar configuration, but with two chlorine atoms at 2.30Å and two oxygen atoms at 2.01Å. These $\text{CuCl}_2(\text{H}_2\text{O})_2$ groups are tied together into infinite chains with long (2.99Å) copper-chlorine bonds between adjacent groups. This leads to an unsymmetrical type of bridge between adjacent copper atoms in which the chlorine atoms are much closer to one copper atom than to the other. This same type arrangement occurs in the dark blue $\text{Cu}(\text{C}_5\text{H}_5\text{N})_2\text{Cl}_2$ (12). The structure of $\text{CuF}_2 \cdot 2\text{H}_2\text{O}$ (13) also contains unsymmetrical bridges between copper atoms with, however, slightly different stacking of the chains than in $\text{CuCl}_2 \cdot 2\text{H}_2\text{O}$. In the isomorphous green salts $\text{K}_2\text{CuCl}_4 \cdot 2\text{H}_2\text{O}$ and $(\text{NH}_4)_2\text{CuCl}_4 \cdot 2\text{H}_2\text{O}$ discrete $\text{CuCl}_4(\text{H}_2\text{O})_2^-$ ions exist (14) with two chlorine atoms at 2.32Å, two oxygen atoms at 1.97Å, and two more chlorine atoms at 2.95Å. In the blue $[\text{Cu}(\text{NH}_2\text{CONHCONH}_2)_2]\text{Cl}_2$ (15), each copper atom is surrounded by four nitrogen atoms at about 1.92Å and two chlorine atoms at about 3.0Å.

2. Magnetic properties

Thorough magnetic studies have been made on very few copper(II) halide complexes, especially at very low temperatures. Part of the reason for this is the extreme difficulty of obtaining satisfactory single crystals for use in neutron diffraction and nuclear resonance studies.

Magnetic susceptibility measurements on $\text{CuCl}_2 \cdot 2\text{H}_2\text{O}$ (16) showed an antiferromagnetic transition at 4.8°K . The proton nuclear magnetic resonance has been studied in single crystals as a function of temperature by Poulis and Hardeman (17, 18) where the Néel temperature was found to be 4.3°K . Both Poulis and Hardeman, and later Rundle (19), postulated an antiferromagnetic arrangement of spins along the CuCl_2 chains, but differed in the type of interaction postulated between chains. The computations by Rundle also showed that it was necessary to distribute some of the unpaired electron of the copper atom over the chlorine and oxygen atoms, thus the unpaired electron is required to be in a molecular orbital. A recent study of the magnetic ordering at 4.2°K in $\text{CuF}_2 \cdot 2\text{H}_2\text{O}$ (20) indicated that a ferromagnetic interaction occurred between adjacent copper atoms in the chain. This compound has a Néel temperature of 10.9°K (21) with the susceptibility showing a maximum at 26°K (22). Above this temperature the susceptibility

follows the Curie-Weiss law¹ with an effective Bohr magneton number μ_{eff} of 1.9 and Curie constant of -37°K . This is somewhat anomalous since a negative Curie constant is usually interpreted as indicating a predominately antiferromagnetic interaction, while the interaction along the chain must be interpreted as the strongest interaction in order to explain the difference between the true Néel temperature and the observed maximum in the magnetic susceptibility (23):

Magnetic susceptibility measurements on CuCl_2 (24, 25, 26) in the range $17\text{-}300^{\circ}\text{K}$ showed an antiferromagnetic transition at about 70°K with $\mu_{\text{eff}} = 2.01$ and $\theta = -93^{\circ}\text{K}$ in the paramagnetic region. The extrapolation of the data in the paramagnetic region was extremely difficult, however, due to the curvature of the $1/\chi$ versus T plot. In $\text{LiCuCl}_3 \cdot 2\text{H}_2\text{O}$, the antiferromagnetic transition in the magnetic susceptibility occurs at 5.9°K (2), while the Néel temperature has been determined to be 4.46°K by nuclear resonance techniques (27). In the region where the salt is

¹The Curie-Weiss law is defined by the relationship

$$\chi_m = C/(T-\theta)$$

where

$$C = (\mu_{\text{eff}}/2.84)^2 = g^2 J(J+1)/2.84^2 .$$

paramagnetic, it follows the Curie-Weiss law with $\theta = -10^{\circ}\text{K}$ and $\mu_{\text{eff}} = 2.86$ (assuming spins paired parallel in the dimers). Again the value of θ is somewhat uncertain due to the difficulty in extrapolation of the $1/\chi$ versus T plot from the paramagnetic region. Preliminary neutron diffraction results at 4.2°K showed that the magnetic unit cell is the same size as the chemical unit cell.¹ Unfortunately the investigation has not proceeded to the point where the actual arrangement of spins can be determined. In $\text{Co}(\text{NH}_3)_6\text{CuCl}_5$, the magnetic susceptibility follows the Curie-Weiss law with $\theta = -2.3^{\circ}\text{K}$ and $\mu_{\text{eff}} = 1.47$ (28). This compound presumably has the same structure as $\text{Cr}(\text{NH}_3)_6\text{CuCl}_5$ (10), and the low moment is probably due to the bipyramidal configuration of the copper(II) ion.

Magnetic susceptibility measurements have been made on many copper(II) compounds at room temperature with the value of the effective Bohr magneton usually being greater than the spin only value of 1.73. It thus appears that the quenching of the orbital angular momentum is not complete in the copper(II) complexes as would be predicted by the Bose-Stoner formula (29). Ray and Sen (30) have compiled an extensive list of magnetic susceptibility data of copper(II)

¹S. C. Abrahams, Brookhaven, N.Y. Data from neutron diffraction study. Private communication. 1962.

complexes. From these data they tried to distinguish between two different classes of compounds, those with moments between 1.73 and 1.90 and those with moments between 1.90 and 2.20. They classified the first class of compounds as essentially covalent with dsp^2 type bonding involving the 3d-orbitals, while the latter class of compounds was classified as essentially ionic with sp^2d type bonding involving the 4d-orbitals. It seems highly unlikely that an appreciable admixture of the 4d-orbital would occur in the bonding since this would leave a 3d-orbital occupied with only one electron and a 4p-orbital unoccupied. They also attempted to draw a parallel between color and magnetic properties, noting that all compounds of the latter group were greenish-blue in coloration, while the first group consisted mainly of compounds with violet coloration.

$CuCl_2 \cdot 2H_2O$ would be a typical example of the latter group, while copper biguanide chloride, $[Cu(C_2H_7N_5)_2]Cl_2 \cdot 2H_2O$ would be a typical example of the first group. It should be noted that the red cupric chloride complexes discussed in this report are not members of this first grouping, since their red coloration is at a still shorter wave length than the violet compounds.

3. Optical properties

Several studies of the absorption spectra of the copper(II) ion in solution have been made. However there

have been very few studies made of the spectra of the copper(II) ion in crystals. This is somewhat unfortunate since the knowledge of the absorption with polarized light in single crystals could be quite helpful in discussing the type of bonding.

Most water solutions of simple copper(II) salts show a broad maximum in the range of 8050 to 8075^oÅ (31, 32) with more than one transition being involved. In ammonium hydroxide solution the maximum shifts to approximately 6200^oÅ (31). In the presence of chloride ion, the maximum shifts down to the region 5000 to 5300^oÅ (33, 34), which has been interpreted as indicating the presence of the $\text{CuCl}_4^{=}$ ion in solution (33). The shift of the absorption maximum -- in ammonium hydroxide solution is in the direction expected in terms of the spectrochemical series (32), but the shift expected in the presence of chloride ion is in the opposite direction of the observed shift.

The spectra of both the water solution and of crystals of Cs_2CuCl_4 have been studied (9) with the solution showing a strong maximum at 3700^oÅ and two weaker maximum at 2700 and 1400^oÅ, while the crystal showed two strong maximum at 2400 and 3200^oÅ and a weaker maximum at 4200^oÅ. The spectrum of single crystals of Cs_2CuCl_4 was examined with polarized light in the region 3000 to 6000^oÅ with maximum observed at 4600 and 4250^oÅ looking down the b and c axes respec-

tively (35).

Felsenfeld (36) accounted for the distorted configuration of the CuCl_4^- ion by taking into account the electrostatic and van der Waals repulsion of the polarized chloride ions, and calculated the energies for the d-orbitals. From these energy levels, the calculated transitions are $d_{z^2} \rightarrow d_{xy}$ at $1730\overset{\circ}{\text{Å}}$, $d_{xz}, d_{yz} \rightarrow d_{xy}$ at $3100\overset{\circ}{\text{Å}}$, and $d_{x^2-y^2} \rightarrow d_{xy}$ at $4450\overset{\circ}{\text{Å}}$, in fair agreement with the observed spectra.

Ballhausen (37) ascribed the maxima in the crystal spectra to charge transfer because of their great intensity, but Felsenfeld (36) suggested that the maxima may be due to transitions between 3d and 4s orbitals. Ballhausen and Liehr (38, 39) also treated the CuCl_4^- ion from the standpoint of the molecular orbital ligand field theory. Unfortunately they considered the ion as being tetrahedral and they were unable to explain the spectra without inclusion of π -bonding. However they were able to show that neither vibronic nor crystal field coupling of the 3d and 4p levels was sufficient to account for the observed spectra.

Mori (40) has studied the reflection spectra of several powdered copper(II) halide complexes and also absorption spectra of solutions of these complexes in the region 3000 to $7000\overset{\circ}{\text{Å}}$ and has interpreted the results in a different manner. The reflection spectrum of $\text{Cr}(\text{NH}_3)_6\text{CuCl}_5$ shows a broad maximum at approximately $3700\overset{\circ}{\text{Å}}$ which Mori attributed

to charge transfer bonds of the CuCl_5^{3-} ion. The absorption spectrum of a solution of CuSO_4 in 10.0 N HCl solution shows a strong maximum at 3850Å and has very nearly the same shape as the reflection spectra of $\text{Cr}(\text{NH}_3)_6\text{CuCl}_5$. Mori suggests that the copper(II) ion in concentrated chloride solutions may exist as the bipyramidal CuCl_5^{3-} ion found in $\text{Cr}(\text{NH}_3)_6\text{CuCl}_5$ (10). The reflection spectrum of KCuCl_3 was studied by Mori also. This shows maxima at 5250Å and also near 4000Å. The peak at 5250Å was not found in the other complexes studied by Mori, and he concluded that the structure of KCuCl_3 must be different from the usual complexes. This has been confirmed by this report.

II. STRUCTURAL ANALYSIS

A. General Remarks

1. Computer techniques

During the past few years the field of crystallography has been aided greatly by the development of large, fast computers and their adaption to crystallographic problems. It is now possible to make full three-dimensional studies of even the largest organic molecules routinely. Structure factors can be computed for thousands of reflections, with each structure factor consisting of a sum of sine and cosine terms of over twenty, thirty or even much larger numbers of atoms. Three dimensional Fourier techniques allow the examination of the electron density distribution over the complete unit cell, and take only a matter of minutes even when thousands of reflections are involved. Thus it has been possible to extend the sharpened Patterson technique and the various minimum function techniques of Patterson interpretation from two-dimensional to three-dimensional applications. It has also become possible to make extensive use of the difference synthesis as a three-dimensional refinement technique. The least squares refinement method has become a standard method of obtaining accurate positional and thermal parameters. In short, a computer has become an indispensable tool in the field of crystallography.

The initial computations performed while working on the structures described in this report were made on the IBM 650 located on the Iowa State University campus. It became necessary, however, to use the IBM 704 operated by the Midwestern Universities Research Association (MURA) and located at Madison, Wisconsin for most of the computations. Fortunately most of the necessary programs, such as the Fourier program, least squares program, and function and error program had been written previously at other laboratories. The IBM 704 is a larger and faster machine than the IBM 650 also, and thus allowed three-dimensional structure analysis to be undertaken conveniently.

The data processing programs for the IBM 704 were not available from other sources, and the writing of these programs was undertaken. A program to process film intensity data obtained by either the precession or Weissenberg technique was written in conjunction with Galen Stucky. The main segment of the program served mainly as an input and output routine, while the majority of the computations were performed by various subroutines. The LP (Lorentz-polarization) correction for Weissenberg data was easy to program; the more complicated LP corrections for precession data were

programmed by Galen Stucky and David Olson.¹ Provision was made for including subroutines for making absorption corrections and sigma calculations, and for Patterson sharpening. A tape, suitable for input into Busing and Levy's least squares program, was obtained as output from the program and optionally, the program would prepare a Patterson tape for input into Sly and Shoemaker's MLFR1 Fourier program. The processed intensity data could also be punched on cards at the option of the operator.

The second data processing program was written to process the intensity data for the compound $\text{Cu}_5\text{Cl}_{10}(\text{C}_3\text{H}_7\text{OH})_2$ obtained on the General Electric XRD-5 equipped with a single crystal orientor and scintillation counter. The logic of the program was essentially the same as a program written earlier by Dr. D. R. Fitzwater. The main change was the inclusion of a subroutine to compute the background correction to each intensity measurement. The actual mathematics of this subroutine will be discussed in the section on the structure of $\text{Cu}_5\text{Cl}_{10}(\text{C}_3\text{H}_7\text{OH})_2$. The streak and unobserved subroutines calculated the LP correction, the standard deviations, and the structure factor value for unobserved reflections. The main features of these

¹Galen Stucky and David Olson, Department of Chemistry, Iowa State University of Science and Technology, Ames, Iowa. Private communication. 1962.

subroutines will be discussed in the section on weighting schemes.

Since the computer programs were of such vital importance in the research discussed in this portion of the thesis, it seems wise to be sure credit is given in the cases where other programs were used. An attempt has been made to give credit throughout the thesis wherever possible. However, to make sure none are missed, a list will be given here of all programs used.

IBM 650

- INCOR IM - Intensity correction. Walken and Jones, as modified by D. R. Fitzwater.¹
- LS IIM - Structure Factor and Least Squares. Senko and Templeton.¹
- TDF-2 - Fourier, D. R. Fitzwater and D. E. Williams.¹
- 1053 - Least Square Plane. J. M. Stewart.²

IBM 704

- ORXLS - Structure Factor and Least Squares. Busing and Levy (41).

¹Copies of these programs may be obtained from the Computer Service group under the direction of Dr. D. R. Fitzwater, Ames Laboratory, Iowa State University, Ames, Iowa.

²This program was obtained from J. M. Stewart, Department of Chemistry, University of Washington, Seattle, Washington.

ORXFE - Function and Error. Busing and Levy (42).

MLFR1 - Fourier. Sly and Shoemaker (43).

Cyclone

SCO-3 - Single Crystal Orientor angles. D. E.

Williams.¹

The use of these programs was appreciated.

2. Weighting schemes

In the least squares refinement technique, one seeks to minimize the function

$$R_3 = \frac{\sum_{hkl} w_{hkl} (|F_o(hkl)| - |F_c(hkl)|)^2}{\sum_{hkl} w_{hkl} |F_o(hkl)|^2} \quad (\text{Eq. 1})$$

where $F_o(hkl)$ = observed structure factor

$F_c(hkl)$ = calculated structure factor

w_{hkl} = weighting factor for each reflection.

The choice of the weighting factor determines the rate and extent of convergence of the least squares process and, in extreme cases, whether or not the least squares process will converge. Thus, it is of extreme importance to make a

¹Copies of these programs may be obtained from the Computer Service group under the direction of Dr. D. R. Fitzwater, Ames Laboratory, Iowa State University, Ames, Iowa.

wise choice of weighting function. The value of the weighting factor is usually input into the least squares program as the standard deviation of the structure factor, the relationship between the two quantities being defined by the equation

$$\sigma = \frac{1}{\sqrt{w}} \quad . \quad (\text{Eq. 2})$$

The discussion of weighting schemes breaks naturally into two portions, depending on whether a film technique or a counter technique is used for recording the intensities. With film methods there are several choices of weighting schemes in general use. The simplest approach is to assume that sigma is the same for all reflections and this is probably the most valid approximation to the actual errors in the initial stages of refinement. The Hughes weighting scheme (44) is defined by the relations

$$\begin{aligned} \sigma &= 4F_{\min} && \text{for } I_o < 16I_{\min} \\ \text{and } \sigma &= F_o && \text{for } I_o > 16I_{\min} \end{aligned} \quad (\text{Eq. 3})$$

where I_{\min} is the minimum observable intensity. This assumes that the per cent probable error is a constant for reflections with intensities of greater than $16I_{\min}$ and that the absolute probable error is a constant for reflections with

intensities of less than $16I_{\min}$. The scheme frequently employed in our laboratory with Senko and Templeton's least squares program on the IBM 650 is defined by the relations

$$\begin{aligned} \sigma &= 4F_{\min} / F_o && \text{for } I_o < 16I_{\min} \\ \text{and } \sigma &= F_o / 4F_{\min} && \text{for } I_o > 16I_{\min}. \end{aligned} \quad (\text{Eq. 4})$$

In this weighting scheme, the errors are assumed to increase as the intensities become very small, primarily because of the increased background on the longer film exposures. The weighting function used frequently with Busing and Levy's least squares program on the MURA IBM 704 is as follows:

$$\begin{aligned} \sigma &= K(I_1)^{\frac{1}{2}}(F)^{-1} && \text{for } I_o < I_1, \\ \sigma &= K && \text{for } I_1 < I_o < I_2, \\ \text{and } \sigma &= K(F)(I_2)^{-\frac{1}{2}} && \text{for } I_o > I_2. \end{aligned} \quad (\text{Eq. 5})$$

This weighting scheme was incorporated into the sigma subroutine of the data processing program for film intensity data previously mentioned on page 13. It was written so that a separate value of K , I_1 , and I_2 could be specified for each layer. By appropriate choice of I_1 and I_2 it is possible to obtain any of the weighting schemes mentioned above.

Another critical point in the least squares refinement process is the treatment of unobserved reflections. Sometimes they are omitted entirely, or what seems a wiser choice, they are included in the input, but with zero weight, so that they are excluded from the least squares process. This latter procedure allows one to examine these reflections to see if there are any serious discrepancies between the calculated and observed structure factors. The procedure usually used in treating unobserved reflections was to set $F_o = F_{\min}$ and $\sigma = KI_1(F_o)^{-1}$. Then, after the structure factor calculation was completed, $\Delta = |F_o| - |F_c|$ was set equal to zero if $|F_c|$ was less than $|F_o|$. This eliminated unobserved reflections from the least squares process for which the calculated structure factor was less than the lowest observable value.

For counter intensity data, the main problem involved is the method of treating very weak reflections. The standard deviation of the intensity is calculated as

$$\sigma^2(I_o) = TC + B + (\%G)^2(I_o)^2 + (\%B)^2(B)^2 \quad (\text{Eq. 6})$$

or some reasonable variation of this. Here TC is the total count, B is the background count, $I_o = TC - B$, %G is a constant representing the overall accuracy of the measured intensities, and %B is a constant representing the accuracy

of the background measurements. The first two terms take into account statistical counting errors, while the latter two terms take into account the systematic errors involved. The constants %G and %B could be determined by computing the standard deviations for several reflections from the results of a large number of measurements of their intensities, and, with the observed values of TC, B, and I_0 , solving Equation 6 for %G and %B.

Starting from the basic relation $I_0 = (LP) F^2$, the variation of each side can be taken and the formula

$$\frac{\sigma(I_0)}{2I_0} = \frac{\sigma(F)}{F} \quad (\text{Eq. 7})$$

is obtained. For larger intensities, $(\%G)^2(I_0)^2$ is the leading term in Equation 6 and $\sigma(I_0)$ is approximately equal to $(\%G)(I_0)$ and the limiting form

$$\sigma(F) = \frac{1}{2}(\%G)F \quad (\text{Eq. 8})$$

is obtained. Equation 7 is not defined as the intensity approaches zero, however, and thus $\sigma(F)$ is undefined. This problem may be avoided by calling all reflections with an intensity less than some predetermined value unobserved, and weighting these reflections with a scheme such as Hamilton's method (45).

If the finite difference method is used instead of the differential method to obtain a relationship between $\sigma(I_0)$ and $\sigma(F)$, it is possible to avoid the problem encountered as I_0 approaches zero. Starting with the relation $I_0 = (LP) F^2$, it is assumed that small finite changes are made in both I_0 and F , that is

$$I_0 + \Delta I_0 = (LP) (F + \Delta F)^2. \quad (\text{Eq. 9})$$

Solving for ΔF , the relation

$$\Delta F = F \left(\sqrt{1 + \Delta I_0 / I_0} - 1 \right) \quad (\text{Eq. 10})$$

is obtained. Under the assumption that $\sigma(F) = \Delta F$ and $\sigma(I_0) = \Delta I_0$, we have

$$\sigma(F) = F \left(\sqrt{1 + \sigma(I_0) / I_0} - 1 \right). \quad (\text{Eq. 11})$$

For reflections with large intensities, the expression

$$\sigma(F) = \frac{1}{2}(\%G)F \quad (\text{Eq. 12})$$

is obtained when the square root is expanded in a power series in $(\%G)$ and terms beyond the first order neglected. This is the same expression as obtained previously in Equation 8. If the expression for $\sigma(F)$ is rearranged in

the form

$$\sigma(F) = (-\sqrt{I_0} + \sqrt{I_0 + \sigma(I_0)}) / \sqrt{LP}, \quad (\text{Eq. 13})$$

it is seen that

$$\sigma(F) = \sqrt{\sigma(I_0)} / \sqrt{LP} \quad (\text{Eq. 14})$$

in the case that $I_0 = 0$. Thus it is possible to treat all intensities in a uniform manner with this approach.

The above discussion of weighting schemes is not intended to be exhaustive, nor to give necessarily the best possible methods. Rather, it is intended to give a brief discussion of the problems involved and to bring together in one place the various types of weighting schemes used instead of spreading them throughout the discussions of the various structures. The specification of the actual weighting scheme used for each compound will be given in the discussion on the refinement process for that compound.

Much of the discussion on the weighting schemes for counter data is based on ideas set forth by D. E. Williams,¹ and this assistance is gratefully acknowledged.

¹D. E. Williams, Department of Chemistry, Iowa State University of Science and Technology, Ames, Iowa. Private communication. 1962.

B. Structure of KCuCl_3 1. Preparation and properties

The compound KCuCl_3 was first prepared by W. Meyerhoffer in 1889 by crystallization from concentrated acetic acid (46). Later, he was able to prepare the compound by melting anhydrous cupric chloride with potassium chloride (47) and from cupric chloride-potassium chloride solutions at temperature above 56.2°C (48). M. Groger, in 1899, prepared the compound by dissolving cupric chloride and potassium chloride in concentrated hydrochloric acid (49).

The unusual deep red coloration of KCuCl_3 , plus the results of the two-dimensional crystallographic study of the compound by Dwiggens (4), aroused interest in this compound. The results of Dwiggens's investigation showed that a dimer of the type Cu_2Cl_6^- existed in the crystal, but the exact structure of the dimer was not determined. Since a planar dimer of this same composition occurs in $\text{LiCuCl}_3 \cdot 2\text{H}_2\text{O}$ (1), which also has the garnet-red coloration, it appeared that a study of the structure of KCuCl_3 could yield valuable information in helping to understand the properties of these red cupric complexes.

The crystals of KCuCl_3 used for crystallographic investigation were prepared from a $\text{KCl-CuCl}_2 \cdot 2\text{H}_2\text{O-HCl}$ solution at room temperature as in the method described by Groger

(49). A concentrated hydrochloric acid solution was saturated with equi-molar quantities of KCuCl_3 and $\text{CuCl}_2 \cdot 2\text{H}_2\text{O}$, and allowed to evaporate slowly over anhydrous magnesium perchlorate. The red-brown crystals crystallized as long needles, which showed a marked tendency to twin.

The crystals grew with $\{010\}$, $\{011\}$, $\{01\bar{1}\}$ and $\{100\}$ faces developed, when the a axis has been chosen as the needle axis. Occasionally the $\{101\}$ face was developed instead of the $\{100\}$ face. The crystals showed strong pleochroism when examined under a polarizing microscope. When observed with polarized light parallel to the $[010]$ direction, the crystals appeared garnet-red when the electric vector was at an angle of 41° to the a-axis and 56° to the c-axis and a light yellowish green when the electric vector was perpendicular to this direction.

The crystals are unstable to water, and on moist summer days they absorb moisture rapidly from the air but are not nearly as unstable to moisture as $\text{LiCuCl}_3 \cdot 2\text{H}_2\text{O}$ (3). The density of the crystals was determined to be 2.85 g/cc by flotation in a mixture of methylene iodide and methylene bromide.

2. X-ray data

A crystal of KCuCl_3 was mounted in a glass capillary such that the needle axis was parallel to the capillary

axis. Oscillation, precession and Weissenberg pictures were taken in order to determine the crystal class and space group. It was found that there was a two-fold axis perpendicular to a mirror plane. Thus the Laue symmetry was C_{2h} and that the crystal class was monoclinic. The following systematic extinctions were observed:

$\{h0l\}$	$l \neq 2n$
$\{0k0\}$	$k \neq 2n$
$\{hkl\}$	none

This implied that the space group was $P2_1/c$. The lattice constants, determined by a back reflection Weissenberg method (50), are $\underline{a} = 4.029 \pm .005\overset{\circ}{\text{A}}$, $\underline{b} = 13.785 \pm .003\overset{\circ}{\text{A}}$, $\underline{c} = 8.736 \pm .004\overset{\circ}{\text{A}}$, $\beta = 97^\circ 20' \pm 4'$. The crystallographic a-axis was chosen parallel to the needle axis. The calculated density, with four formula units in the unit cell, is 2.88 g/cc.

Intensity data for diffraction of planes in the $[001]$ and $[010]$ zones were taken on a precession camera with a timed exposure technique. The intensity of each reflection was visually estimated twice, each time against a different standard reflection chosen from among the reflections of the zone. The LP correction was estimated for each reflection using the standard graphical method (51).

Three dimensional intensity data were taken on the

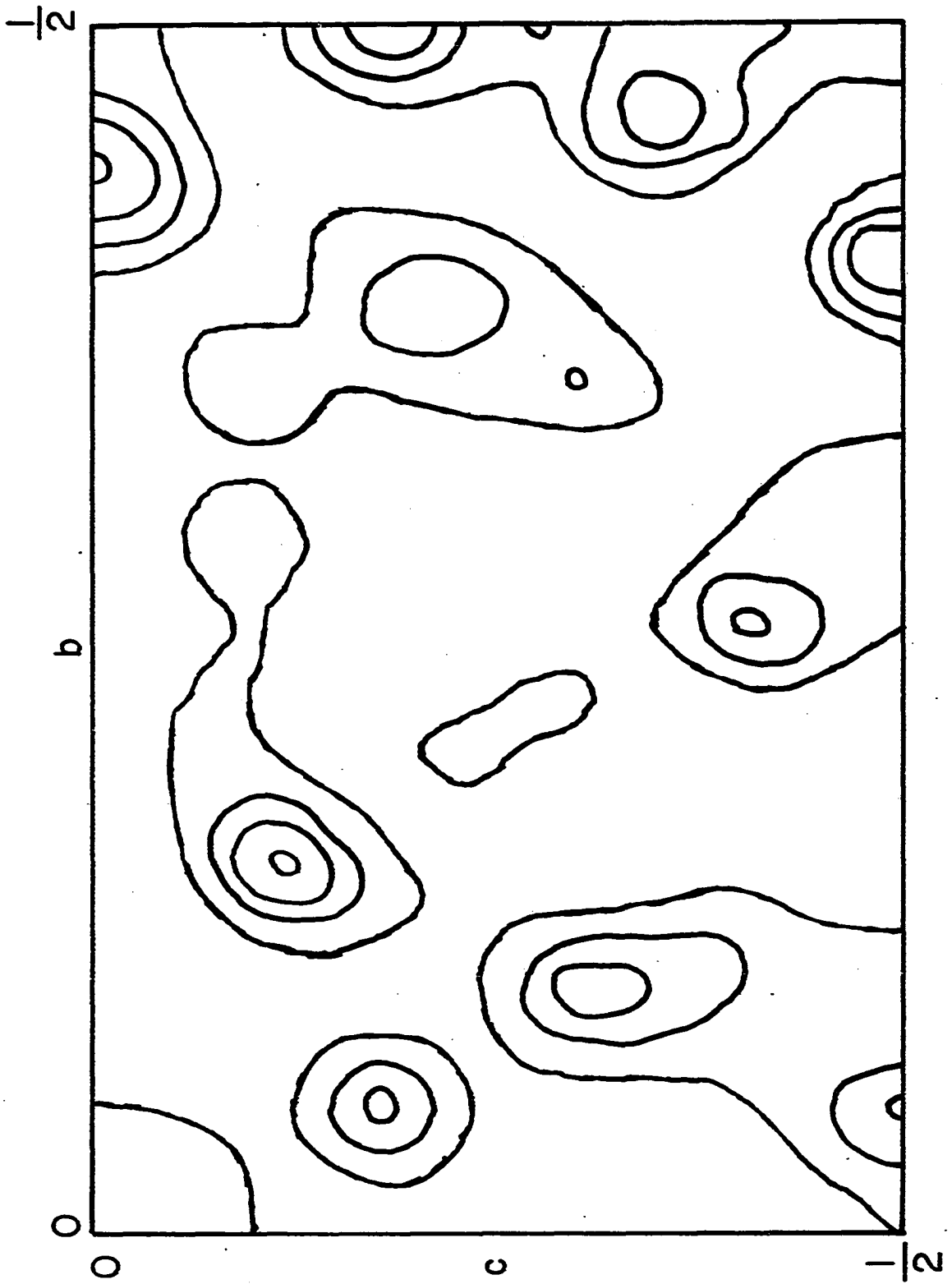
Weissenberg camera with Mo K_{α} radiation and the multiple film technique. The LP corrections were initially computed on an IBM 650 with the program written by Walken and Jones but they were later recalculated on the MURA IBM 704 in order to make use of the weighting routine included in the LP program. A total of 2206 reflections was obtained, of which approximately 1320 reflections were observed.

3. Structural determination

A Patterson projection onto (100) was computed using an IBM 650 and the TDF-2 Fourier Program written by Fitzwater and Williams. This Patterson projection was essentially the same as that given by Dwiggens (4), and the same interpretation was made. The $\{0kl\}$ data were then refined on the IBM 650 using the y- and z-parameters assigned by Dwiggens. This refinement showed that the correct assignment of atomic parameters had been given. The associated electron density projection is given in Figure 2.

The next step necessary in the structure determination was the determination of the x-parameters. Computation of Patterson projections onto (001) and (010) only showed Patterson peaks at or near $U = 0$ or $U = \frac{1}{2}$. This means that the possible values of x are limited to approximately 0 and $\frac{1}{2}$, or to $\frac{1}{4}$ and $\frac{3}{4}$. In the space group $P 2_1/c$, Patterson peaks are expected at $(U, V) = (2x, \frac{1}{2})$ and $(2\bar{x}, \frac{1}{2})$ in the

Figure 1. Patterson projection onto the (100) plane for KCuCl_3
The origin peak has not been drawn in.



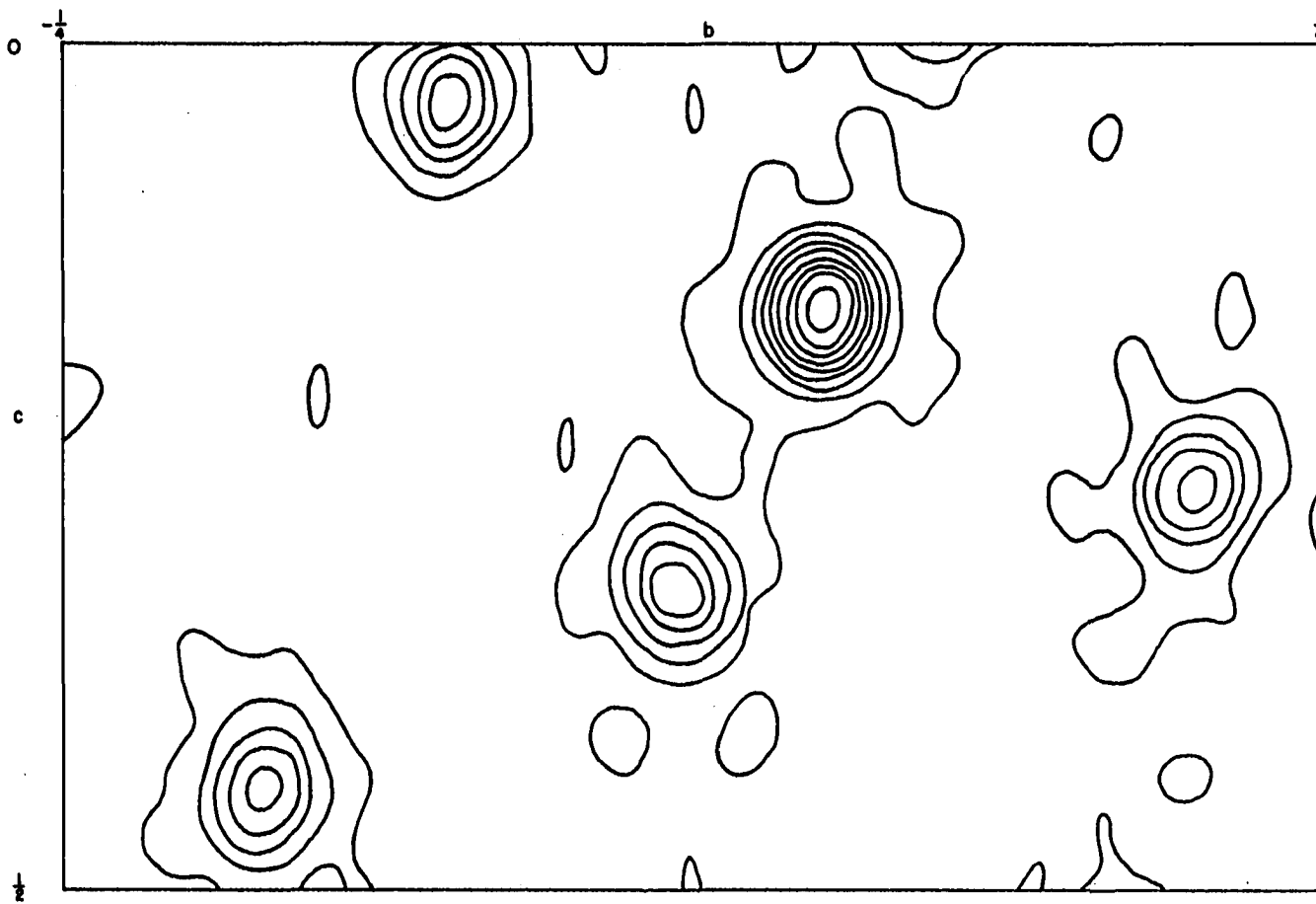


Figure 2. Fourier projection onto the (100) plane for KCuCl_3

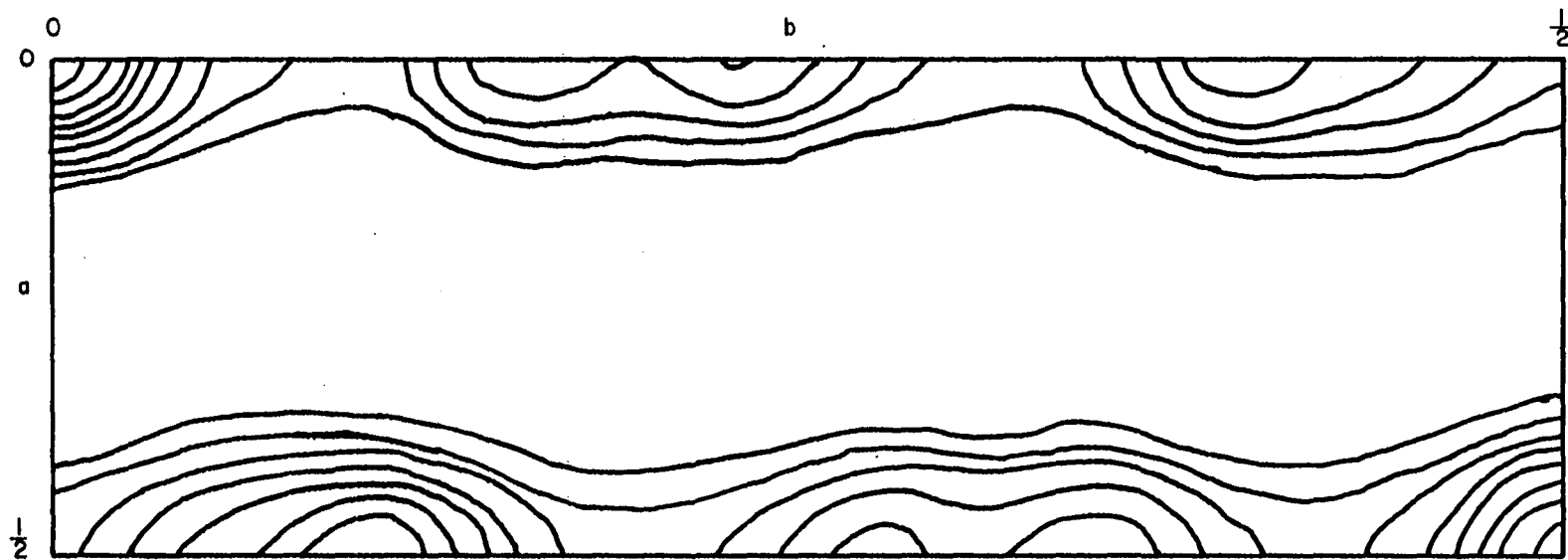


Figure 3. Patterson projection onto the (001) plane for KCuCl_3

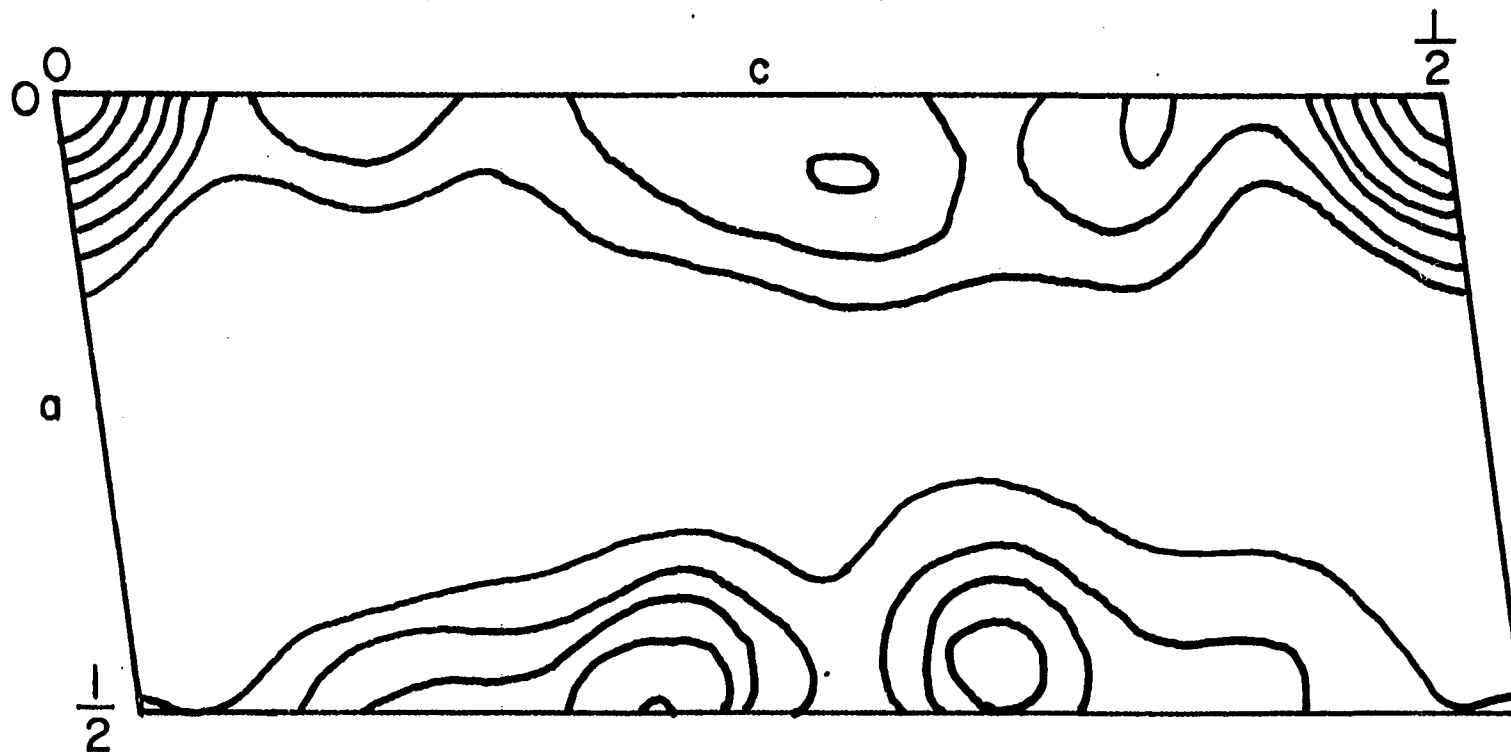
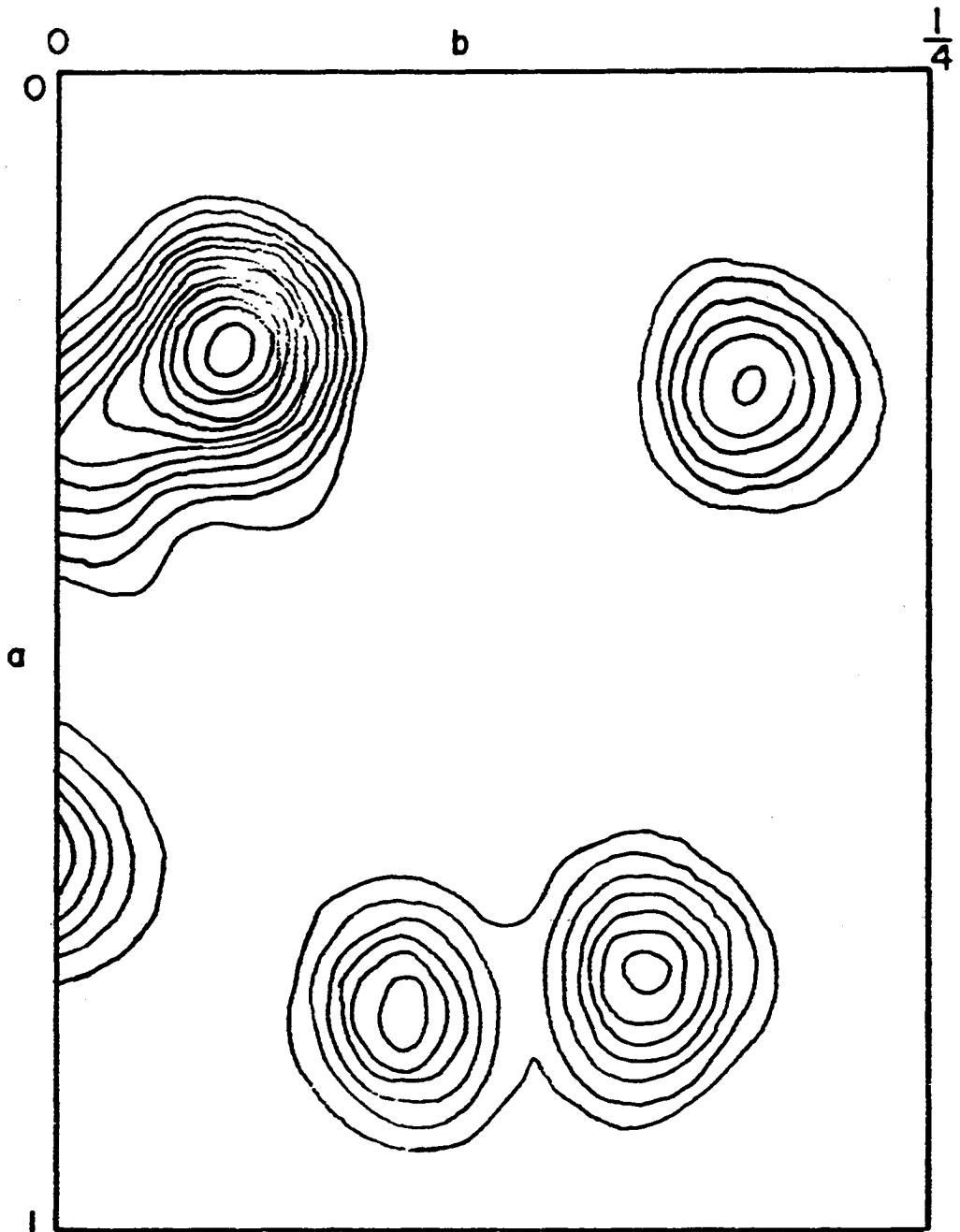


Figure 4. Patterson projection onto the (010) plane for KCuCl_3

Figure 5. Fourier projection onto the (001) plane
for KCuCl_3



projection onto (001). However, for the Patterson projection of KCuCl_3 onto (001), a peak was observed at $(U, V) = (\frac{1}{2}, \frac{1}{2})$ but not at $(U, V) = (0, \frac{1}{2})$. This suggested the atoms lay approximately in the planes $x = 1/4$ and $x = 3/4$.

With the knowledge of interatomic distances, plus the y- and z-parameters determined by the refinement of the $\{0kl\}$ data, approximate x-parameters were assigned to each atom, and the $\{hk0\}$ precession data was refined on the IBM 650 with Senko and Templeton's least squares program.

4. Refinement

The final refinement of the three-dimensional Weissenberg data was made on the MURA IBM 704 at Madison, Wisconsin, using Busing and Levy's least squares program. The weighting scheme given in Equation 5 was used. I_2 was chosen as the median value of the observed intensity and I_1 was chosen as $2I_{\min}$, since this was the approximate dividing point between those reflections where only one estimation of intensity was made from those for which two or more estimations were made. The following choice was made for the parameter K:

<u>layer</u>	<u>K</u>
$0kl$.050
$1kl, \bar{1}kl$.055
$2kl, \bar{2}kl$.060

$3kl, \bar{3}kl$.065
$4kl$.070
$\bar{4}kl$.060

Approximate scale factors for each layer were obtained by comparison with the $\{hk0\}$ precession data. The scale factors were varied each cycle, along with the atomic parameters and the temperature factors during the isotropic refinement. During the anisotropic refinement, the anisotropic temperature factors and the scale factors were not varied simultaneously, since this procedure leads to a singular least squares matrix. During the final refinement also, Busing and Levy's program was modified to omit unobserved reflections from the least squares matrix for which $|F_{\text{cal}}| < |F_{\text{obs}}|$, where F_{cal} is the calculated value of the structure factor, and F_{obs} is the observed value. A final value of $R_1 = 0.111$ was obtained for observed reflections only.

5. Discussion

The three-dimensional structure determination confirmed the existence of the planar dimer Cu_2Cl_6^- . This is the second compound in which this dimer exists, the other being the garnet-red compound $\text{LiCuCl}_3 \cdot 2\text{H}_2\text{O}$. Each dimer is located on a center of symmetry and has approximately D_{2h} symmetry. The two copper atoms in the dimer are bridged by two

Table 1. Final parameters, temperature factors, standard deviations, and R factors for KCuCl_3^a

Atom	x	y	z	B_{11}	B_{22}	B_{33}	B_{12}	B_{13}	B_{23}
Cu	.2408 (0003)	.04976 (00008)	.15750 (00014)	.0136 (0009)	.00184 (00004)	.00601 (00013)	.00085 (00009)	-.00177 (00023)	-.00038 (00006)
Cl ₁	.2754 (0006)	.19875 (00016)	.26300 (00030)	.0195 (0015)	.00205 (00008)	.00744 (00026)	.00111 (00019)	-.00263 (00040)	.00063 (00011)
Cl ₂	.6782 (0005)	-.00745 (00017)	.32171 (00026)	.0132 (0013)	.00244 (00009)	.00588 (00022)	.00087 (00019)	.00096 (00035)	.00015 (00011)
Cl ₃	-.1797 (0005)	.09875 (00015)	.03369 (00028)	.0205 (0014)	.00215 (00008)	.00594 (00023)	.00086 (00019)	-.00002 (00037)	-.00036 (00010)
K	.7825 (0006)	.17081 (00018)	.55692 (00033)	.0180 (0015)	.00283 (00010)	.00927 (00029)	-.00071 (00021)	-.00033 (00043)	-.00039 (00013)

$R_1 = 0.151$ for all reflections

$R_1 = 0.111$ for observed reflections only

$R_3 = 0.232$

^aStandard deviations are given in the parentheses.

Table 2. Interatomic distances and bond angles for KCuCl_3^a

Bond	Distance	Bond	Distance
Cu-Cl_1	$2.248 \pm .003\text{\AA}$	K-Cl_3	$3.282 \pm .003\text{\AA}$
Cu-Cl_2	$2.267 \pm .003\text{\AA}$	K-Cl_2	$3.196 \pm .004\text{\AA}$
Cu-Cl_3	$2.322 \pm .003\text{\AA}$	K-Cl_1	$3.462 \pm .005\text{\AA}$
Cu-Cl_3	$2.314 \pm .003\text{\AA}$	K-Cl_1^{\dagger}	$3.095 \pm .004\text{\AA}$
Cu-Cu	$3.443 \pm .003\text{\AA}$	K-Cl_1^*	$3.083 \pm .004\text{\AA}$
$\text{Cu}^{\dagger}-\text{Cl}_2$	$2.941 \pm .004\text{\AA}$	$\text{K-Cl}_1^{*\dagger}$	$3.404 \pm .005\text{\AA}$
$\text{Cu}^{\dagger}-\text{Cl}_3$	$3.113 \pm .004\text{\AA}$	K-Cl_2^*	$3.214 \pm .004\text{\AA}$
K-Cl_3^*	$3.696 \pm .004\text{\AA}$	$\text{K-Cl}_2^{*\dagger}$	$3.185 \pm .004\text{\AA}$
<u>Angle</u>	<u>Value</u>	<u>Angle</u>	<u>Value</u>
$\text{Cl}_3-\text{Cu}-\text{Cl}_3$	$84.07 \pm .09^\circ$	$\text{Cl}_2^{\dagger}-\text{Cu}-\text{Cl}_1$	$93.23 \pm .10^\circ$
$\text{Cl}_3-\text{Cu}-\text{Cl}_2$	$90.90 \pm .09^\circ$	$\text{Cl}_2^{\dagger}-\text{Cu}-\text{Cl}_2$	$100.56 \pm .12^\circ$
$\text{Cl}_2-\text{Cu}-\text{Cl}_1$	$93.20 \pm .09^\circ$	$\text{Cl}_2^{\dagger}-\text{Cu}-\text{Cl}_3$	$83.79 \pm .11^\circ$
$\text{Cu}_1-\text{Cu}-\text{Cl}_3$	$91.75 \pm .09^\circ$	$\text{Cl}_2^{\dagger}-\text{Cu}-\text{Cl}_3$	$87.02 \pm .09^\circ$
$\text{Cu}_3-\text{Cu}-\text{Cl}_1$	$175.77 \pm .09^\circ$	$\text{Cl}_3^*-\text{K}-\text{Cl}_2$	$126.54 \pm .11^\circ$
$\text{Cu}_3-\text{Cu}-\text{Cl}_2$	$173.20 \pm .11^\circ$	$\text{Cl}_2-\text{K}-\text{Cl}_3$	$113.65 \pm .09^\circ$
$\text{Cl}_3^{\dagger}-\text{Cu}-\text{Cl}_3$	$94.55 \pm .09^\circ$	$\text{Cl}_3-\text{K}-\text{Cl}_3^*$	$119.74 \pm .09^\circ$
$\text{Cl}_3^{\dagger}-\text{Cu}-\text{Cl}_1$	$90.57 \pm .09^\circ$	$\text{Cl}_1^*-\text{Cl}_2-\text{Cl}_1^*$	$64.42 \pm .05^\circ$
$\text{Cl}_3^{\dagger}-\text{Cu}-\text{Cl}_2$	$80.75 \pm .11^\circ$	$\text{Cl}_2^*-\text{Cl}_1^*-\text{Cl}_1$	$61.43 \pm .07^\circ$
$\text{Cl}_3^{\dagger}-\text{Cu}-\text{Cl}_3$	$89.05 \pm .09^\circ$	$\text{Cl}_1^*-\text{Cl}_1-\text{Cl}_2^*$	$54.15 \pm .05^\circ$

^aAn atom displaced one unit cell in the x-direction is denoted by \dagger .

Table 3. Least squares plane^a for the Cu_2Cl_6^- dimer in KCuCl_3

A	B	C	$\Sigma d_i / n$	Σd_i^2	$\sqrt{\Sigma d_i^2 / n}$
.24820	.09394	-.20355	.03669	.01272	.03988
<u>Distance from plane</u>					
		Cu	.0499 ^o A		
		Cl ₁	.0112 ^o A		
		Cl ₂	-.0366 ^o A		
		Cl ₃	-.0509 ^o A		

^aThe dimer was fit to the plane $Ax + By + Cz = 0$.

chlorine atoms (designated Cl₃) at distances of 2.322 and 2.314^oA. The normal square planar configuration exhibited by copper(II) complexes is completed with each copper atom bonded to two more chlorine atoms (Cl₁ and Cl₂) at distances of 2.248 and 2.267^oA respectively. The standard deviations of the bond lengths are approximately .003^oA and it is seen that two bridging Cu-Cl bonds are significantly longer than the two terminal Cu-Cl bonds. The two lengths of the two bridging bonds are longer than the corresponding bonds in $\text{LiCuCl}_3 \cdot 2\text{H}_2\text{O}$ (2.301 and 2.307^oA), while the lengths of the

Table 4. Comparison of observed and calculated structure factors for $\{hk0\}$ precession data for KCuCl_3

h	k	F_{obs}	F_{calc}	h	k	F_{obs}	F_{calc}	h	k	F_{obs}	F_{calc}
0	2	129	124	2	1	65	59	3	10	18	19
0	4	49	42	2	2	69	-58	3	11	16	16
0	6	54	57	2	3	24	26	3	13	53	-53
0	8	109	-101	2	4	28	-26	3	14	39	37
0	10	17	16	2	5	16	-17	3	15	26	-25
0	12	8	-8	2	6	32	-32	3	16	31	25
0	14	31	-29	2	8	90	87	4	0	82	80
0	16	14	13	2	9	19	-20	4	1	41	-42
0	18	37	39	2	10	8	5	4	3	8	-10
1	2	13	-15	2	11	20	21	4	4	8	9
1	3	20	-20	2	12	15	15	4	5	17	16
1	4	61	-56	2	13	34	34	4	6	8	8
1	5	198	-188	2	14	22	21	4	8	54	-58
1	6	29	-31	2	15	14	14	4	9	19	19
1	7	115	-122	2	16	12	-12	4	10	24	-24
1	8	12	-14	3	0	16	-18	4	11	14	-13
1	9	33	-38	3	1	19	17	4	12	20	-19
1	10	7	-9	3	2	13	12	4	13	24	-27
1	11	27	-28	3	3	31	32	5	0	13	10
1	13	93	92	3	4	71	64	5	1	15	-14
1	14	20	-22	3	5	96	87	5	3	19	-21
1	15	27	29	3	6	41	37	5	4	26	-26
1	16	16	-15	3	7	46	47	5	5	25	-28
1	17	18	-18	3	8	22	20	5	6	11	-10
2	0	294	-295	3	9	8	7	5	7	6	-7
								5	8	9	-10

Scale factor = 3.06

Figure 6. Comparison of observed and calculated structure factors for KCuCl_3

The reflections are grouped into sections of constant k and l . The first column is the running index h ; the second column is $10|F_o|$; the third column is $10F_c$. An asterisk following the running index denotes an unobserved reflection.

Figure 6. (Continued)

Figure 6. (Continued)

9 33 -37	4, 5, L		C 37 -41	4 35 34	1 38 48	6 23 15	2 16 20	8 55 -55	7 60 -66	
10 43 42		0 124 -132	1 33 -34	5 19 -23	2* 11 -2	8 19 -10	3 14 -18	9 46 45	8* 15 9	-4, 16, L
	4, 2, L	0 39 39	1 59 57	2 65 65	6 18 -21	3 18 17	10 87 -109	4 33 -31	10 30 28	4 29 28
		2 40 -47	3 18 17	4 37 -35	8* 12 -6	5* 12 8	6 51 48	-4, 8, L	-4, 12, L	1* 1, 11
1 55 -72	3* 7 4	4 81 84	5 16 13	9 12 13	6 12 13	-4, 1, L	7 111 -102			2* 10 14
2 18 -18	4 65 71	5 95 93	6* 10 1	10 13 11	7 12 6		8 54 51	1 93 -95	1 25 27	4* 15 1
3 14 -7	5 60 -62	6 20 -22	7 26 21		8 12 -6	3* 144 -154	9* 13 -8	2 67 73	2 52 102	5* 55 -55
4 14 -11	6 33 34	7 20 -19	8* 11 -5	4, 15, L		4 19 25	10 24 -19	3 18 -18	1 84 60	6 25 10
5 32 32	7 49 50	8* 10 1	9 27 26		4, 19, L	5 35 33	12 29 29	4 65 -64	4 21 -11	7 24 21
6 68 69	8 57 -56	9 31 -32	10* 12 2	0 27 -26		6 33 -31	11* 15 3	5 54 51	5 45 -38	8 2* 24
7 23 -22	9 55 -55	10 59 53	11 23 22	1* 10 7	0 13 -4	7 34 -30		6 30 -27	6 25 -20	
8 16 16	10* 11 -6	11* 12 6	12 17 -17	2 57 66	1 23 31	8 47 -44	-4, 5, L	7 29 -19	7 22 29	-4, 17, L
9 35 -35	11* 11 3	12 22 -22		3* 10 -4	2* 11 5	9 43 -40		8 18 11	8* 15 -7	
10* 11 -2	12 14 16		4, 12, L	4 18 -18	3 20 -23	10* 14 -5	1 29 -25	9 42 33	9* 16 C	1 19 -25
11 17 19		4, 9, L	0 47 -57	5 56 -56	4* 12 5	11* 15 13	2 71 -83	10 23 17		2* 10 -22
	4, 6, L		1 10 -11	6 27 -29	5 12 2	12* 16 -4	3 9 -13		-4, 13, L	3 22 -22
	4, 3, L	0 44 46	1 10 -11	7* 11 -0	6 21 -22		4 103 89	-4, 9, L		4 41 -14
0 15 -16	1 59 -61	2 65 -65	3* 9 -3	8 39 41	7 35 37	-4, 2, L	5 79 72		1 34 -45	5* 16 13
1 119 150	2 43 -42	3 53 57	4 40 42	9 39 -37	8 30 26		6 47 44	1 27 -27	2 65 66	6 22 16
2 114 -137	3 17 11	4 55 65	5 32 -36	4, 16, L	4, 20, L	3* 77 77	7* 12 -3	2 27 -24	3 46 41	
3 121 -125	4 20 24	5 35 -30	6 46 -49			4 145 -149	8 34 -33	3 86 76	4 57 -50	-4, 18, L
4 27 32	5 70 80	6 11 -13	7* 11 8	0 24 23	0 26 30	5 65 60	9 39 42	4* 11 -6	5* 14 3	
5 32 -31	6 96 -99	7 20 -19	8 22 -15	1* 10 7	1* 12 13	6 87 76	10 27 26	5* 12 -2	6* 14 -3	2 19 21
6* 8 -6	7 11 -9	8 16 17	9* 12 7	2 33 -25	2 19 -20	7 21 12	11 32 32	6 17 21	7 30 -27	3* 16 -6
7* 9 -2	8 44 -47	9 16 14	10 36 38	3* 11 7	3* 12 -3	8 18 -12		7 78 -84	8* 16 -4	4 36 -31
8 26 -27	9 40 -40	10 26 -23	11 12 -5	4* 11 3	4 12 4	9 17 -18	-4, 6, L	8* 14 -12	9 28 28	5 20 -16
9 43 -40	10* 11 8	11 20 22		5 36 -37	5 12 11	10 32 -33		9* 15 16		6 34 35
10* 11 0	11 28 29	12 12 9	4, 13, L	6* 11 -12	6 29 30	11 22 8	1 138 -156		-4, 14, L	-4, 17, L
11 22 -25	12 19 -20		4, 10, L	7 16 19	7 12 -5		2 102 114	-4, 10, L		
12 35 35			C 59 -67	8 14 -12		-4, 3, L	3 55 43		1 56 69	
	4, 7, L	0 54 -63	1 17 17	9 12 17	4, 21, L		4 61 50	1* 7 2	2 24 21	2* 11 1
	4, 4, L	1 23 -24	2* 9 -5			1 7 11	5 25 22	2 13 11	3 18 8	3 45 -42
0 23 23	0* 6 -5	2 27 -25	3* 9 4	4, 17, L	1 25 27	2 11 11	6 21 15	3* 11 3	4 22 -7	4 3* -33
1 89 -163	1 26 27	3 49 -49	4 52 -53		2 12 10	3 18 17	7 18 -11	4* 12 -6	5* 15 -7	
2 49 -54	2 38 -41	4 131 131	5 12 12	0 12 -3	3 16 -20	4 79 74	8 38 43	5 46 -33	6* 15 1	-4, 20, L
3 129 -139	3* 7 -0	5* 9 1	6 48 -53	1 24 33	6 12 6	5 94 88	9* 14 -11	6 98 -161	7 15 14	
4 28 21	4 13 11	6 36 -43	7 57 53	2 73 83	7 30 29	6 29 24	10 24 -22	7 39 -30	8 35 34	2 37 -43
5 66 68	5* 8 11	7* 10 -1	8 14 15	3 36 -40	4* 11 -9	7 17 -9	11 34 41	8 28 25	9 27 28	3* 17 5
6 23 -19	6 44 48	8 19 18	9 14 15	4* 11 -9	4, 22, L	8 56 -52		9* 15 1		4 31 -27
7 37 -38	7 23 -26	8 19 18	9* 11 6	5* 11 11		9 21 -21	-4, 7, L		-4, 15, L	
8 14 -14	8 34 -36	9* 11 6	10 13 -2	6* 12 -6	1 35 -35	10* 14 3	1 90 -84		-4, 11, L	
9 11 -12	9 16 15	10 62 56	4, 14, L	7 18 18	3 22 -23	12* 16 -2	2 99 -103	1 64 -78	1 29 30	
10* 11 -8	10 23 24	11 17 16		8 14 18	6 21 19	11* 15 -1	3 62 57	2* 8 5	2 32 36	
11 51 51	11 12 -12	12 17 -18	0 24 -29				4* 10 11	3 22 14	4 35 -34	
12 17 -16	12 12 9		1 53 58	4, 18, L	-4, 0, L	-4, 4, L	5 20 13	4* 12 6	5 45 47	
	4, 8, L	4, 11, L	2 27 -22	3 13 -14	0 19 21	4 42 -54	6 22 -17	5 45 -36	7* 16 1	
			3 13 -14				7 47 -37	6 16 23	8 30 25	

two terminal bonds are shorter than the ones in $\text{LiCuCl}_3 \cdot 2\text{H}_2\text{O}$ (2.259 and 2.285Å). It is doubtful if these differences are truly significant. The $\text{Cl}_3\text{-Cu-Cl}_3$ bond angle is 84.1° , compared with 84.9° in $\text{LiCuCl}_3 \cdot 2\text{H}_2\text{O}$. The $\text{Cl}_3\text{-Cu-Cl}_2$, $\text{Cl}_2\text{-Cu-Cl}_1$ and $\text{Cl}_1\text{-Cu-Cl}_3$ bond angles are 90.9° , 93.2° and 91.8° respectively. The standard deviations of the bond angles are approximately 0.1° and so the copper atom does not have a rigorous square planar coordination. The dimer is essentially planar, with a maximum deviation from the plane of about 0.05Å, compared with its length of approximately 6Å and its width of 3Å.

The dimers are stacked above each other along the a-axis in such a manner that each copper atom is bonded to one chlorine atom in the dimer directly above it along the a-axis and to a second chlorine atom in the dimer below it. An infinite chain of the type $(\text{Cu}_2\text{Cl}_6^-)_n$ is formed in this manner. These long copper-chlorine bond lengths are 2.941Å for the Cu-Cl_2 bond and 3.113Å for the Cu-Cl_3 bond.

The potassium atom lies at the center of a trigonal prism of chlorine atoms, with three more chlorine atoms located outside the three faces of the trigonal prisms. This leads to a ninefold coordination for the potassium atom. All of the K-Cl bonds are equal to, or greater than, the sum of the ionic radii of potassium and chlorine. There is considerable deviation from ideality in this coordination,

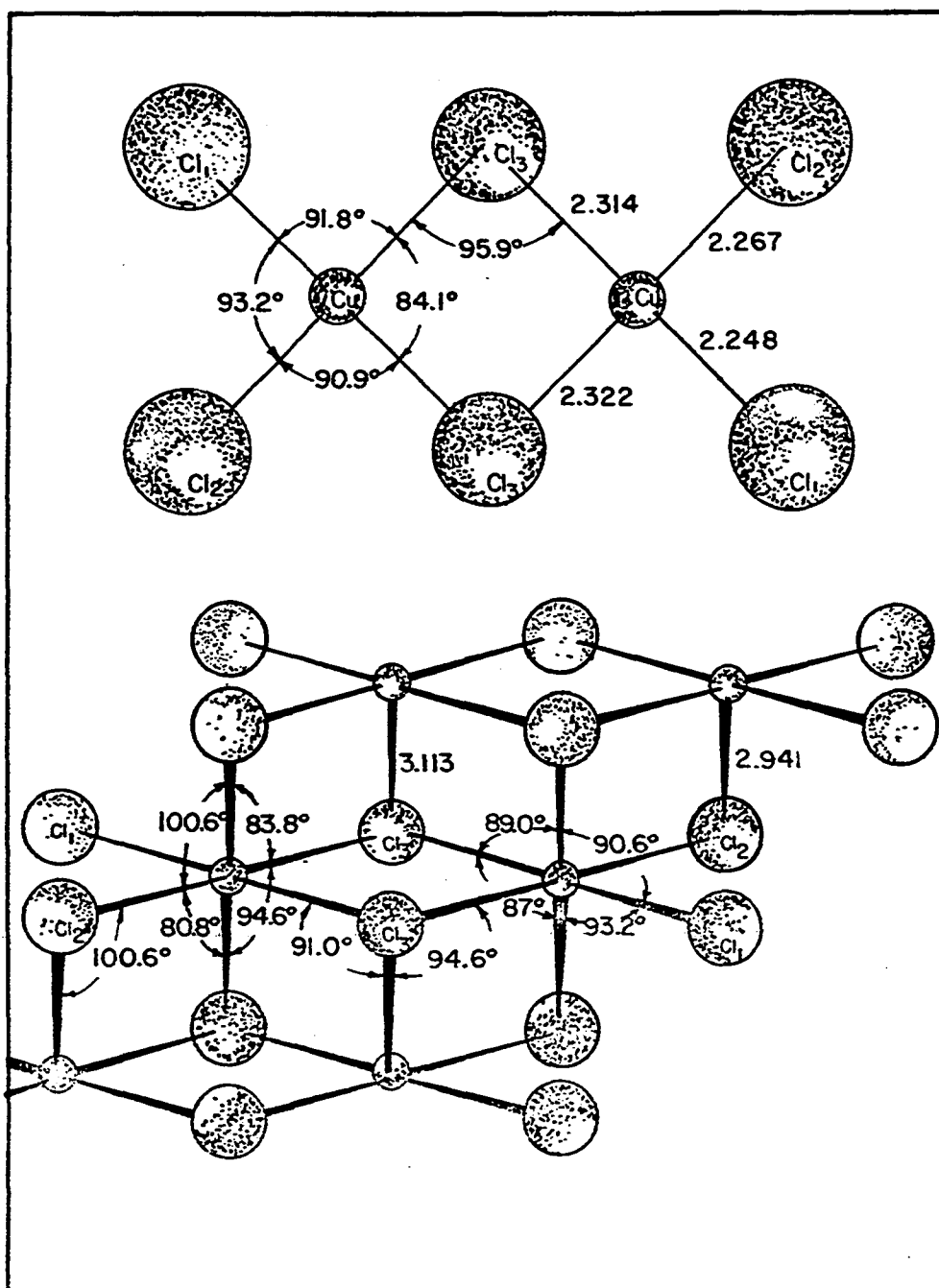
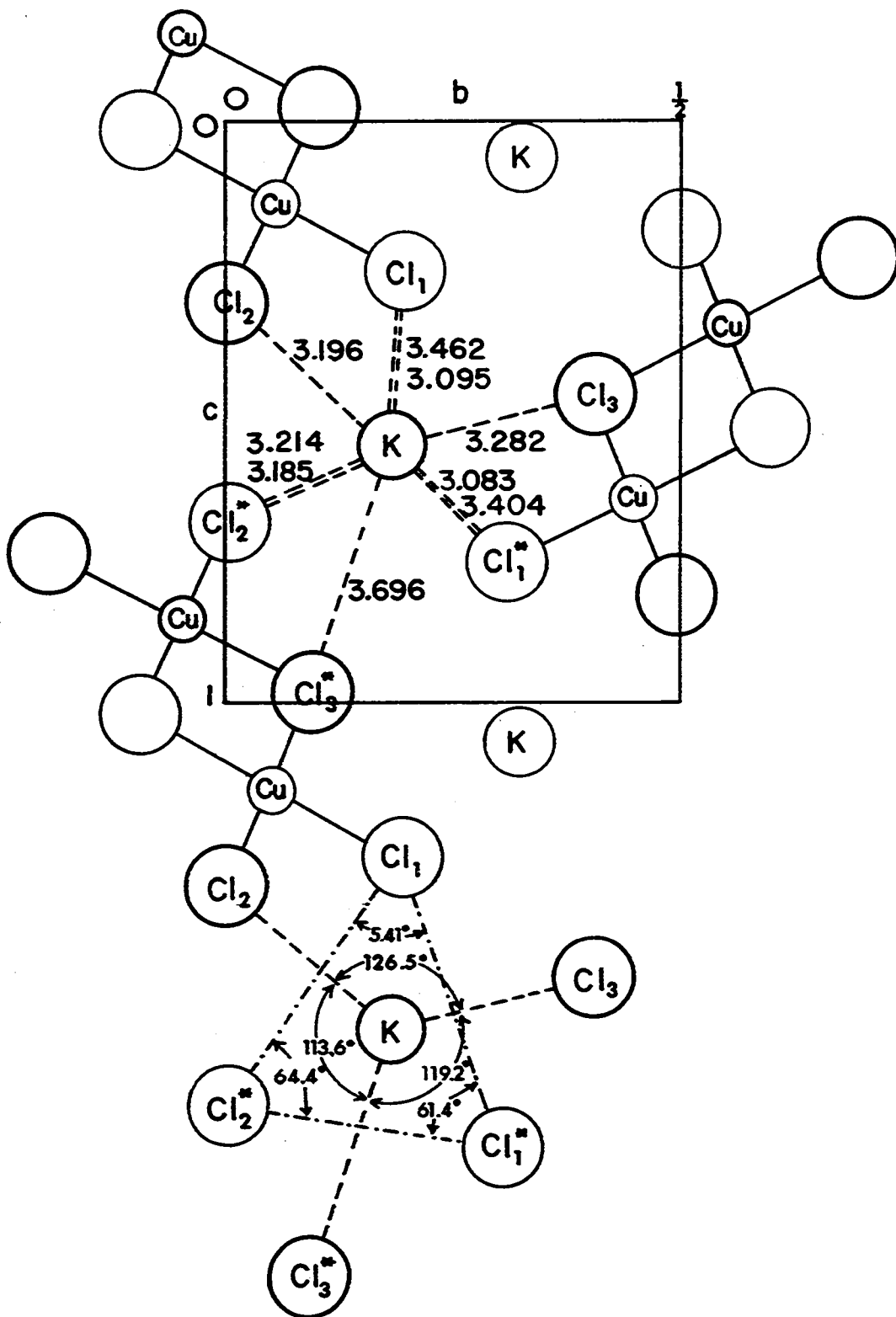


Figure 7. Illustration of the $\text{Cu}_2\text{Cl}_6^=$ ion and its stacking in KCuCl_3

Figure 8. Illustration of the coordination of the potassium ion in KCuCl_3



which is to be expected since the covalent Cu-Cl bonds have a much stronger directional character than the ionic K-Cl bonds, and thus the chlorine atoms tend to lie in the positions prescribed by the square planar character of the Cu-Cl bonds.

It is interesting to note the effect that the cation has upon the crystal structure in the series $MCuCl_3 \cdot xH_2O$. In $CsCuCl_3$ (8), the salt is anhydrous, and can be grown directly from water solutions at room temperatures. This compound forms an infinite helical chain of the type $(CuCl_3)_n^{n-}$. $KCuCl_3$ is anhydrous, but it is necessary to grow the crystals at higher temperatures or from hydrochloric acid solutions. In this compound the planar dimer is found, and the stacking is such that each copper atom completes its distorted octahedral coordination by bonding to chlorine atoms in adjacent dimers. In $LiCuCl_3 \cdot 2H_2O$, the same dimer exists, but the stacking of the dimers is such that the octahedral positions of each copper atom are occupied by an oxygen atom and by one chlorine atom in an adjacent dimer. The compound $HCuCl_3 \cdot 3H_2O$ (52, 53) has been reported, and it would be interesting to see how this fits into the above series of compounds.

C. Structure of NH_4CuCl_3

1. Preparation and properties

The compound NH_4CuCl_3 has been prepared by Foote and Walden (54), who reported it to have a red coloration similar to that of KCuCl_3 . Because of the similar ionic radii of the K^+ ion and the NH_4^+ ion, it was assumed that the structures were isomorphous.

The crystals were prepared by slow evaporation of an equimolar mixture of NH_4Cl and CuCl_2 in anhydrous ethyl alcohol. The crystals show almost exactly the same physical characteristics as the crystals of KCuCl_3 , such as the deep red coloration, the pleochroic effect when observed under the polarized microscope, the ease with which twinned crystals were formed, and the instability with respect to moisture.

2. X-ray data

Examination of oscillation, precession and Weissenberg pictures established that the Laue symmetry was C_{2h} and that the crystal class was monoclinic. The systematic extinctions again implied that the space group was $P 2_1/c$. The lattice constants, determined by the back reflection Weissenberg method, are $\underline{a} = 4.066 \pm .005\overset{\circ}{\text{A}}$, $\underline{b} = 14.189 \pm .003\overset{\circ}{\text{A}}$, $\underline{c} = 9.003 \pm .004\overset{\circ}{\text{A}}$, and $\beta = 97^\circ 30' \pm 4'$. The calculated density was

2.42 g/cc, assuming four formula units in the unit cell.

Intensity data for diffraction of planes in the [100] and [001] zones were collected on a General Electric XRD-5 equipped with a single crystal orientor and scintillation counter. The LP corrections were computed on an IBM 650 using the INCOR IM program as modified by Gordon Engebretson¹ for counter data.

3. Structure determination

Since the lattice constants were quite similar to those of KCuCl_3 , the atomic parameters found for KCuCl_3 were assumed. Initial structure factor computations gave excellent agreement between observed and calculated structure factors.

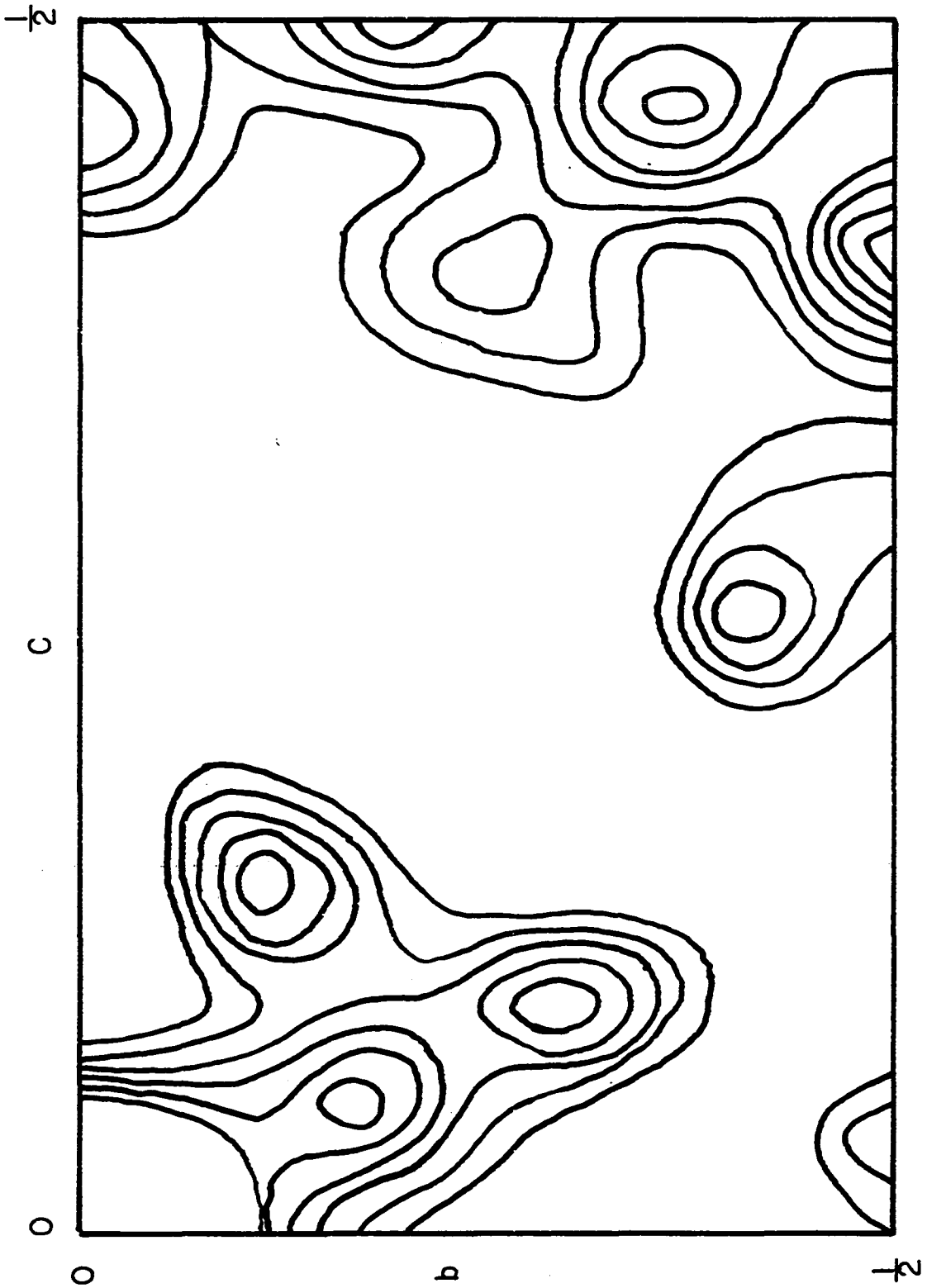
4. Refinement

Refinement was carried out on the MURA IBM 704 computer using Busing and Levy's least squares program. The relationships defined by Equations 6 and 7 were used to obtain $\sigma(F)$. If I_o was less than three times $\sigma(I_o)$, the reflection was called unobserved and Hamilton's weighting scheme was used.

Only isotropic temperature factor refinement was

¹Gordon Engebretson, Department of Chemistry, Iowa State University of Science and Technology, Ames, Iowa. Private communication. 1962.

Figure 9. Patterson projection onto the (100) plane for NH_4CuCl_3
The origin peak has not been drawn in.



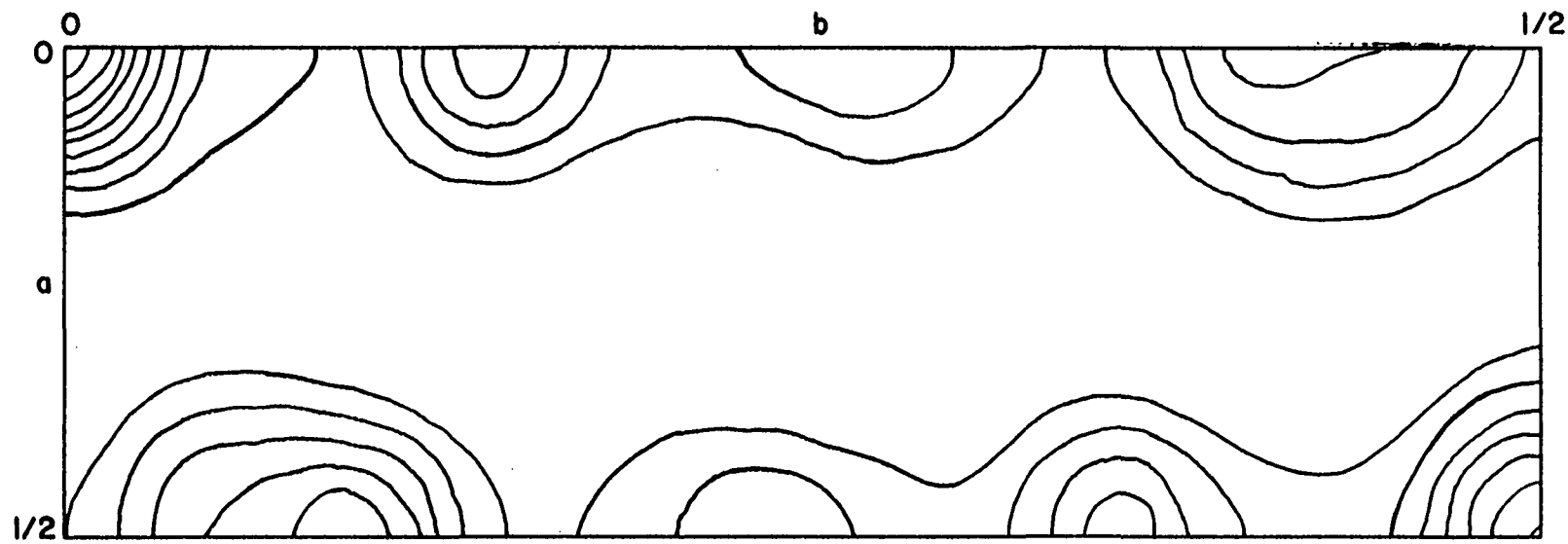
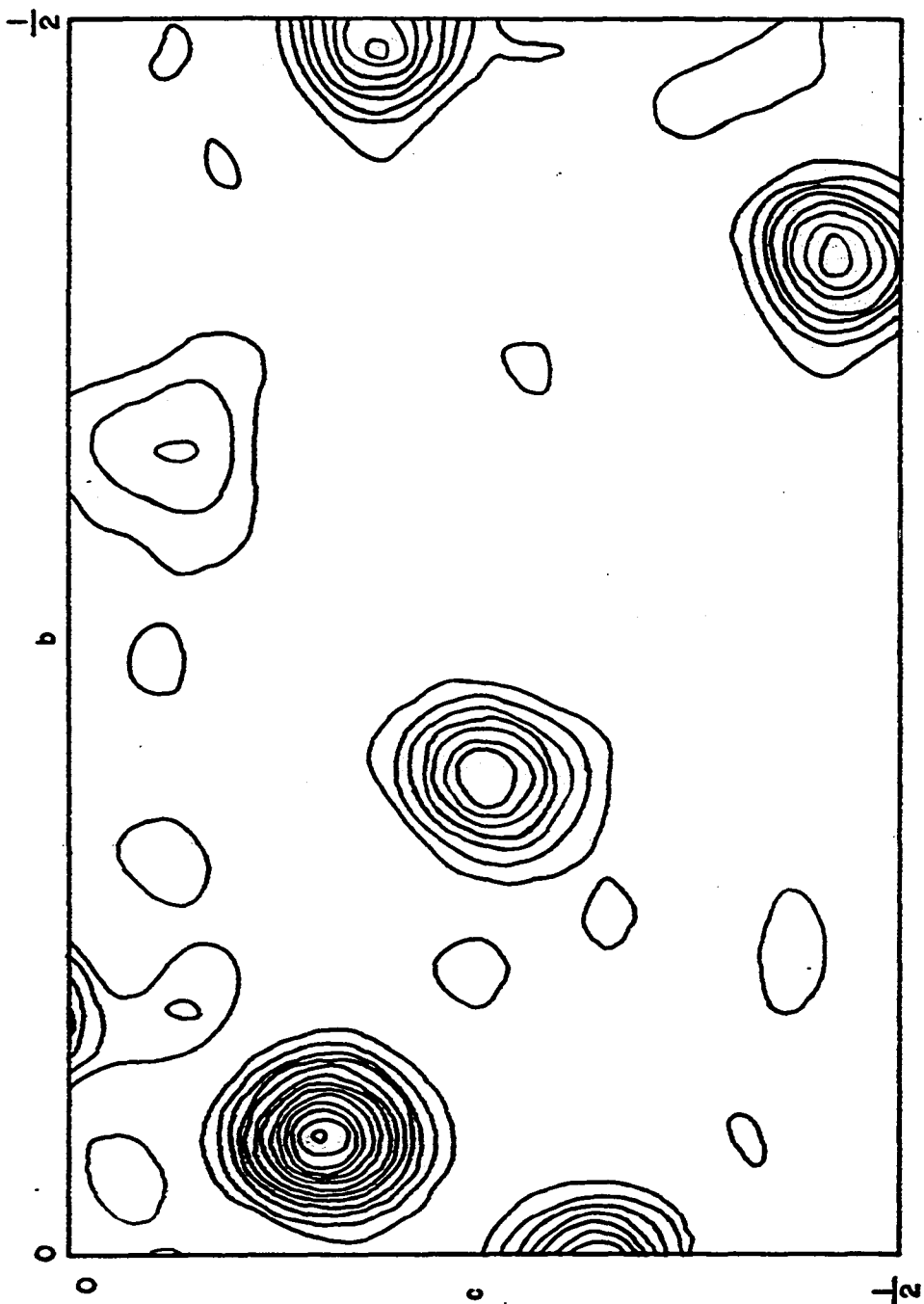


Figure 10. Patterson projection onto the (001) plane for NH₄CuCl₃

Figure 11. Fourier projection onto the (100) plane for NH_4CuCl_3



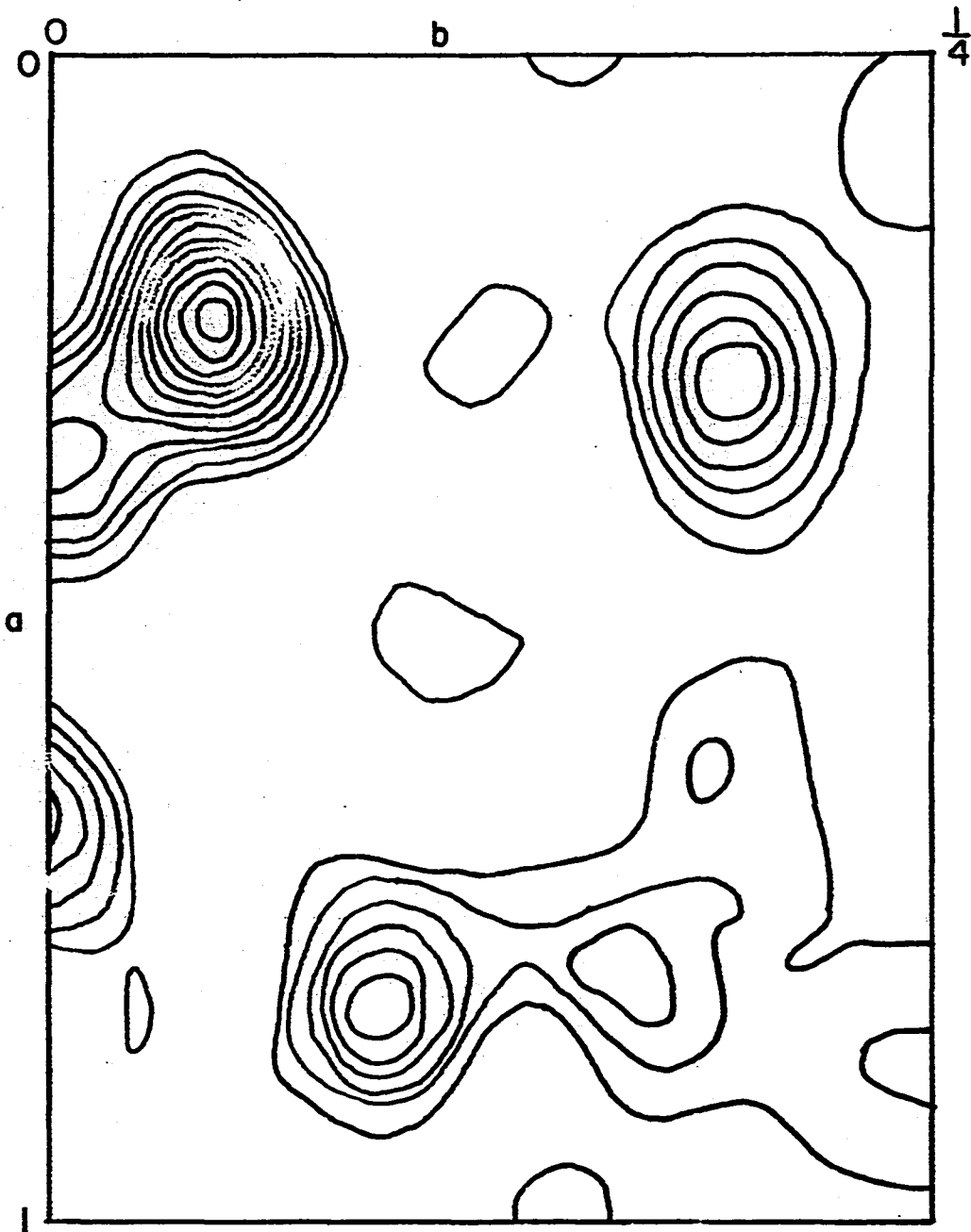


Figure 12. Fourier projection onto the (001) plane
for NH_4CuCl_3

Table 5. Final parameters, temperature factors, standard deviations, and R values for NH_4CuCl_3 ^a

Atom	[001] zone			[100] zone		
	x	y	B	y	z	B
Cu	.2324 (0013)	.0483 (0004)	2.329 (193)	.0489 (0003)	.1530 (0005)	1.443 (184)
Cl ₁	.2670 (0021)	.1942 (0007)	1.957 (276)	.1938 (0007)	.2534 (0011)	1.856 (257)
Cl ₂	.6630 (0034)	-.0066 (0008)	2.846 (299)	-.0065 (0006)	.3129 (0010)	1.910 (264)
Cl ₃	-.1774 (0028)	.0972 (0007)	2.196 (245)	.0966 (0007)	-.0352 (0011)	1.931 (247)
N	.7782 (0083)	.1741 (0025)	2.229 (928)	.1759 (0020)	.5584 (0030)	0.939 (606)
			<u>[001] zone</u>	<u>[100] zone</u>		
		R ₁	.117	.123		
		R ₃	.151	.205		

^aStandard deviations are given in parentheses.

undertaken and each of the two zones was refined separately. Values of $R_1 = 0.123$ and 0.117 were obtained for the [100] zone and the [001] zone respectively. The scale factors obtained in the refinement of the two zones were 3.16 and 3.14 respectively, with the standard deviation being approximately 0.10, so that the agreement between the two zones was

Table 6. Interatomic distances and bond angles for $\text{NH}_4\text{CuCl}_3^a$

Bond	Distance	Bond	Distance
$\text{Cu}-\text{Cl}_1$	2.25A	$\text{N}-\text{Cl}_3$	3.36A
$\text{Cu}-\text{Cl}_2$	2.26A	$\text{N}-\text{Cl}_2$	3.39A
$\text{Cu}-\text{Cl}_3$	2.32A	$\text{N}-\text{Cl}_1$	3.60A
$\text{Cu}-\text{Cl}_3$	2.32A	$\text{N}-\text{Cl}_1^{\prime}$	3.23A
$\text{Cu}-\text{Cu}$	3.42A	$\text{N}-\text{Cl}_1^*$	3.09A
$\text{Cu}^{\prime}-\text{Cl}_2$	2.99A	$\text{N}-\text{Cl}_1^{*\prime}$	3.44A
$\text{Cu}^{\prime}-\text{Cl}_3$	3.19A	$\text{N}-\text{Cl}_2^*$	3.40A
$\text{N}-\text{Cl}_3^*$	3.80A	$\text{N}-\text{Cl}_2^{*\prime}$	3.29A

Angle	Value	Angle	Value
$\text{Cl}_3-\text{Cu}-\text{Cl}_3$	84.9°	$\text{Cl}_2^{\prime}-\text{Cu}-\text{Cl}_1$	93.4°
$\text{Cl}_3-\text{Cu}-\text{Cl}_2$	90.2°	$\text{Cl}_2^{\prime}-\text{Cu}-\text{Cl}_2$	100.8°
$\text{Cl}_2-\text{Cu}-\text{Cl}_1$	93.4°	$\text{Cl}_2^{\prime}-\text{Cu}-\text{Cl}_3$	84.3°
$\text{Cl}_1-\text{Cu}-\text{Cl}_3$	91.36°	$\text{Cl}_2^{\prime}-\text{Cu}-\text{Cl}_3$	87.3°
$\text{Cu}_3-\text{Cu}-\text{Cl}_2$	172.8°	$\text{Cl}_3^*-\text{N}-\text{Cl}_2$	125.3°
$\text{Cu}_3-\text{Cu}-\text{Cl}_1$	176.2°	$\text{Cl}_2-\text{N}-\text{Cl}_3$	113.0°
$\text{Cl}_3^{\prime}-\text{Cu}-\text{Cl}_3$	93.8°	$\text{Cl}_3-\text{N}-\text{Cl}_3^*$	121.7°
$\text{Cl}_3^{\prime}-\text{Cu}-\text{Cl}_1$	90.3°	$\text{Cl}_1^*-\text{Cl}_2-\text{Cl}_1^*$	63.8°
$\text{Cl}_3^{\prime}-\text{Cu}-\text{Cl}_2$	80.7°	$\text{Cl}_2^*-\text{Cl}_1^*-\text{Cl}_1$	62.1°
$\text{Cl}_3^{\prime}-\text{Cu}-\text{Cl}_3$	89.0°	$\text{Cl}_1^*-\text{Cl}_1-\text{Cl}_2^*$	54.0°

^aAn atom displaced one unit cell in the x-direction is denoted by \prime .

Table 7. Least squares plane^a for the Cu_2Cl_6^- dimer in NH_4CuCl_3

A	B	C	$\Sigma d_i / n$	Σd_i^2	$\sqrt{\Sigma d_i^2 / n}$
.19201	.07048	-.15397	.04170	.01667	.04564
<u>Distance from plane</u>					
			o		
		Cu	.0575A		
			o		
		Cl ₁	.0114A		
			o		
		Cl ₂	-.0418A		
			o		
		Cl ₃	-.0562A		

^aThe dimer was fit to the plane $Ax + By + Cz = 0$.

excellent. The y-parameters obtained from the two different zones agreed very well; the difference was less than the standard deviation for all atoms except the copper atom, in which case the difference was less than two times the standard deviation. There was considerable variation between the temperature factors for the two zones, but this is to be expected when the thermal ellipsoids are quite anisotropic. Also, in the case of the nitrogen atom, the presence of the hydrogen atoms would affect the temperature factors and might account for the large discrepancy in this case. A weighted average of the y-parameters from the two

Table 8. Comparison of observed and calculated structure factors for $\{0kl\}$ data for NH_4CuCl_3

k	l	F _{obs}	F _{calc}	k	l	F _{obs}	F _{calc}	k	l	F _{obs}	F _{calc}
2	0	163	171	2	2	31	-26	11	3	136	126
4	0	70	75	3	2	94	-81	12	3	58	58
6	0	34	32	4	2	152	-139	13	3	65	64
8	0	94	-96	5	2	129	-119	14	3	13	-4
10	0	36	34	6	2	102	-97	15	3	13	10
12	0	27	-22	7	2	138	-136	16	3	16	10
14	0	32	-36	8	2	43	38	0	4	6	11
1	1	119	116	9	2	64	-58	1	4	29	28
2	1	111	-101	10	2	11	2	2	4	127	-114
3	1	50	32	11	2	22	16	3	4	130	122
4	1	24	-18	12	2	46	40	4	4	60	-49
5	1	120	-120	13	2	49	42	5	4	138	101
6	1	154	-148	14	2	23	-24	6	4	24	20
7	1	96	-87	15	2	45	49	7	4	22	14
8	1	36	-32	16	2	60	-54	8	4	19	14
9	1	29	-24	17	2	24	22	9	4	24	23
10	1	22	20	18	2	3	5	10	4	123	117
11	1	32	-37	1	3	17	-13	11	4	25	17
12	1	24	26	2	3	98	91	12	4	46	40
13	1	39	-35	3	3	22	-19	13	4	11	-3
14	1	97	99	4	3	104	-97	14	4	3	0
15	1	47	-33	5	3	2	-8	15	4	11	-5
16	1	36	38	6	3	15	5	1	5	19	-20
17	1	19	-14	7	3	85	81	2	5	76	86
18	1	30	33	8	3	63	-58	3	5	38	-47
0	2	64	-102	9	3	156	148	4	5	134	154
1	2	49	-43	10	3	37	-41	5	5	52	-64

Table 8. (Continued)

k	l	F _{obs}	F _{calc}	k	l	F _{obs}	F _{calc}	k	l	F _{obs}	F _{calc}
6	5	37	33	1	7	85	93	9	8	36	-33
7	5	51	-47	2	7	51	50	10	8	17	-14
8	5	37	31	3	7	46	42	11	8	17	17
9	5	27	-29	4	7	40	-44	12	8	37	-42
10	5	10	-4	5	7	23	28	1	9	31	-38
11	5	23	-18	6	7	14	-7	2	9	16	-22
12	5	38	-35	7	7	33	-25	3	9	9	-16
13	5	22	-22	8	7	54	-46	4	9	3	2
14	5	3	-9	9	7	55	-48	5	9	21	21
0	6	35	72	10	7	18	-12	6	9	71	-76
1	6	36	32	11	7	33	-30	7	9	38	38
2	6	145	143	12	7	62	66	8	9	43	-44
3	6	81	73	13	7	26	-26	9	9	33	27
4	6	52	45	0	8	7	-6	0	10	65	-81
6	6	32	-28	1	8	16	-10	1	10	21	24
7	6	25	-14	2	8	45	-45	2	10	9	-8
8	6	3	15	3	8	17	-20	3	10	22	25
9	6	23	-19	4	8	19	-15	4	10	8	8
10	6	36	-58	5	8	55	-59	5	10	12	11
11	6	8	0	6	8	25	-20	6	10	22	21
12	6	11	-14	7	8	81	-81	7	10	10	4
13	6	30	-11	8	8	59	-52	1	11	46	-46
								2	11	42	44
								0	12	18	19

Scale factor = 3.16

Table 9. Comparison of observed and calculated structure factors for {hk0} data for NH_4CuCl_3

h	k	F_{obs}	F_{calc}	h	k	F_{obs}	F_{calc}	h	k	F_{obs}	F_{calc}
0	4	70	73	2	5	14	-15	3	14	33	29
0	6	34	33	2	6	12	-10	3	15	42	-35
0	8	94	-86	2	7	24	-24	3	16	31	25
0	10	36	36	2	8	79	83	4	0	64	58
0	12	27	-22	2	9	24	-26	4	1	26	-25
0	14	32	-34	2	10	3	-2	4	2	3	-1
1	2	12	-14	2	11	25	27	4	3	3	-4
1	3	19	-15	2	12	31	34	4	4	3	10
1	4	54	-59	2	13	37	39	4	5	12	19
1	5	130	-135	2	14	26	30	4	6	3	1
1	6	50	-54	2	15	23	17	4	7	15	19
1	7	162	-169	2	16	20	-15	4	8	52	-60
1	8	25	-24	3	0	25	-21	4	9	26	26
1	9	37	-36	3	1	48	44	4	10	26	-25
1	10	18	-13	3	2	3	-4	4	11	14	-19
1	11	20	-18	3	3	31	30	4	12	31	-35
1	12	16	-9	3	4	52	56	4	13	25	-28
1	13	75	67	3	5	58	63	5	0	20	18
1	14	35	-20	3	6	57	64	5	1	21	-27
1	15	60	47	3	7	63	71	5	2	16	18
1	16	29	-17	3	8	20	27	5	3	20	-22
2	0	266	-252	3	9	3	-2	5	4	13	-13
2	1	42	40	3	10	3	19	5	5	18	-22
2	2	75	-72	3	11	7	10	5	7	13	-16
2	3	23	22	3	12	12	10	5	8	3	-7
2	4	37	-36	3	13	42	-36				

Scale factor = 3.14

zones was used for the computation of interatomic distances, bond angles, and the least squares plane.

5. Discussion

The geometry of the Cu_2Cl_6^- dimer is exactly analogous to the dimer in KCuCl_3 . With standard deviations of approximately 0.01\AA for copper-chlorine distances, there is no significant difference in the bond lengths within the dimers in KCuCl_3 and NH_4CuCl_3 . However, the interdimer Cu-Cl distances are significantly longer in NH_4CuCl_3 , as would be expected due to the longer a-axis. Again the terminal Cu-Cl bonds are significantly shorter than the bridging Cu-Cl bonds (2.25 and 2.26\AA as compared with 2.32\AA) and the $\text{Cl}_3\text{-Cu-Cl}_3$ bond angle (the bond angle between the two bridging chlorines) is considerably less than 90° , with an observed value of 84.9° as compared with 84.07° in KCuCl_3 . The standard deviation of the bond angles is approximately 0.3 to 0.4 degrees in NH_4CuCl_3 .

The ammonium ion exhibits the same nine-fold coordination as does the potassium ion in KCuCl_3 with the N-Cl bonds being significantly longer than the K-Cl bonds in most cases. This is consistent with the increase of 0.15\AA when the ionic radii of the potassium ion is compared with the ammonium ion (1.33\AA vs. 1.48\AA). The standard deviations of the N-Cl distances are approximately 0.3 to 0.4\AA . A complete list of

interatomic distances and bond angles for NH_4CuCl_3 is given in Table 6. The notation is consistent with that used in Table 2 for KCuCl_3 .

D. Structure of $\text{Cu}_2\text{Cl}_4(\text{CH}_3\text{CN})_2$

1. Preparation and properties

Compounds with the formulas $\text{CuCl}_2 \cdot \text{CH}_3\text{CN}$ and $\text{CuCl}_2 \cdot 2\text{CH}_3\text{CN}$ were first reported by Naumann (55) in 1914. The first compound, which was formed at room temperature, had a light brown coloration, while the second compound had a light blue coloration. This latter compound was the stable form in solution below 18°C .

Crystals of $\text{CuCl}_2 \cdot \text{CH}_3\text{CN}$ were grown by slow evaporation of a saturated solution of anhydrous cupric chloride in acetonitrile, or by cooling a solution which had been saturated at $30^\circ - 40^\circ\text{C}$. The compound crystallized out as long yellow or light brown needles, the color becoming darker as the thickness of the crystals increased. The crystals exhibited a tendency to twin with perhaps one single crystal obtained from a thousand. They were hygroscopic, absorbing water very rapidly when exposed to air. These crystals were also pleochroic when observed under a polarizing microscope.

The density of the crystals was obtained by the method of flotation, using a mixture of methyl bromide and methyl iodide as the flotation liquids. The observed density was

1.96 g/cc.

2. X-ray data

A crystal of $\text{CuCl}_2 \cdot \text{CH}_3\text{CN}$ was mounted in a glass capillary with the needle axis of the crystal parallel to the capillary axis. Oscillation, precession, and Weissenberg pictures revealed the existence of a two-fold axis perpendicular to a mirror plane. This established the Laue symmetry as C_{2h} and the crystal class as monoclinic. The observed systematic extinctions,

$$\begin{array}{ll} \{h0l\} & l \neq 2n \\ \{0k0\} & k \neq 2n \\ \{hkl\} & \text{none,} \end{array}$$

implied that the space group was $P 2_1/c$. The lattice constants are $\underline{a} = 3.84 \pm .01\text{\AA}$, $\underline{b} = 7.91 \pm .01\text{\AA}$, $\underline{c} = 18.35 \pm .01\text{\AA}$, and $\beta = 91.1 \pm .1^\circ$, where the a-axis was chosen parallel to the needle axis. The \underline{b} and \underline{c} lattice constants were determined with the back reflection Weissenberg technique (50) while \underline{a} and β were taken from precession camera photographs. The calculated density is $.52 n$, where n is the number of formula units in the unit cell. Thus, with four formula units per unit cell, the calculated density is 2.08 g/cc.

Intensity data for planes in the $[100]$ zone were taken on a Weissenberg camera using the multiple film technique and $\text{Cu } K_\alpha$ radiation. These data were corrected for the LP

correction using the MURA IBM 704. Intensity data for the planes in the [010] zone were taken on a precession camera with Mo K_{α} radiation using the same crystal. The LP correction was estimated for each reflection using the standard graphical technique (51).

3. Structural determination

Early in the course of the structural determination, it was observed that the a-axis length was almost identical to that of $\text{CuCl}_2 \cdot 2\text{H}_2\text{O}$ (8). Since that structure contains unsymmetrical $\text{Cu}(\text{Cl})_2\text{-Cu}$ chains along the a-axis, it seemed likely that the compound $\text{CuCl}_2 \cdot \text{CH}_3\text{CN}$ did also.

As the first step in the solution of the structure, a Patterson projection onto (100) was computed using an IBM 650 along with the TDF-2 Fourier program. It was observed immediately that the basic details in the vicinity of the origin of this Patterson were very similar to that of the Patterson projection of KCuCl_3 onto (100) except for orientation with respect to the crystal axis. It was assumed that a dimer of the type $\text{Cu}_2\text{Cl}_4(\text{CH}_3\text{CN})_2$ existed in the compound, similar to the dimer Cu_2Cl_6^- which exists in KCuCl_3 , but with two of the chlorines replaced by acetonitrile groups. With this assumption, the following parameters were deduced from the Patterson projection onto (100):

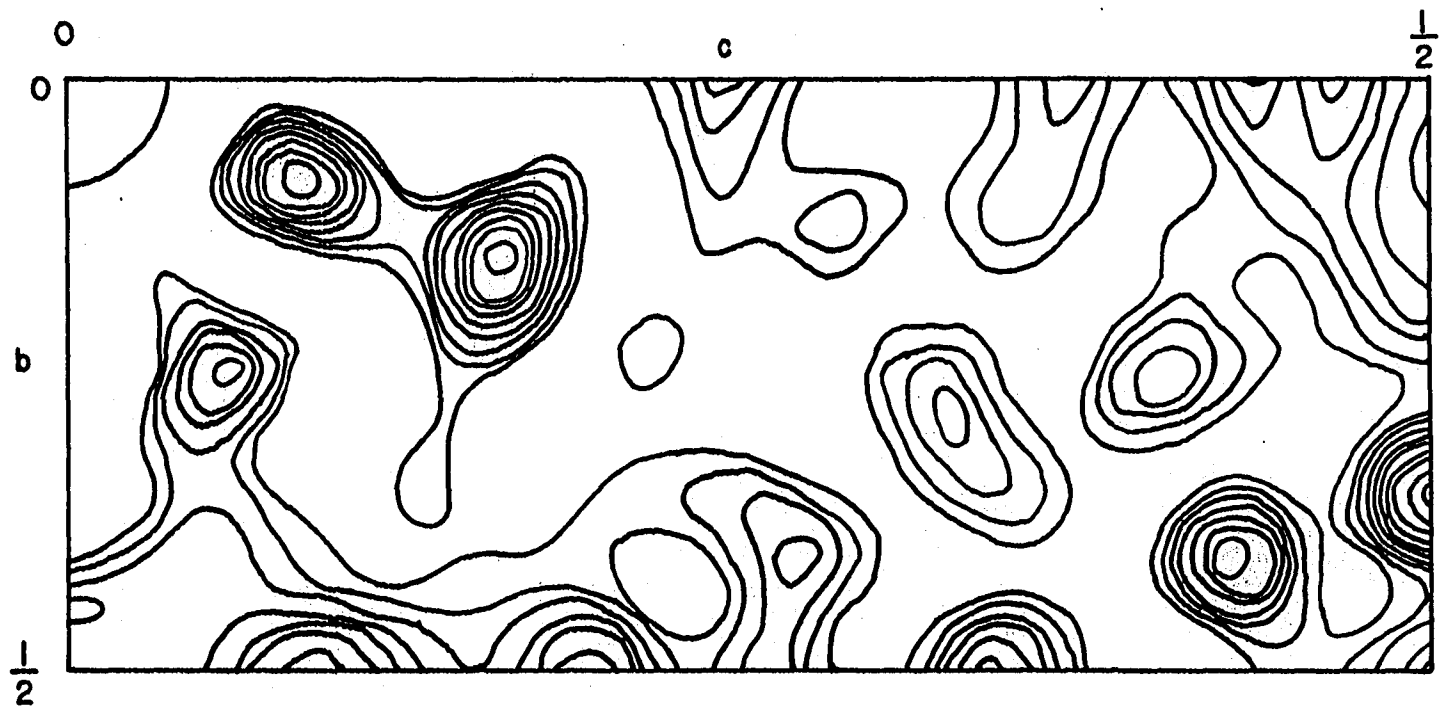


Figure 13. Patterson projection onto the (100) plane for $\text{Cu}_2\text{Cl}_4(\text{CH}_3\text{CN})_2$
The origin peak has not been drawn in.

	<u>y</u>	<u>z</u>
Cu	.088	.067
Cl ₁	.162	-.017
Cl ₂	-.012	.160
N	.312	.111

In the next step, structure factors were computed using an IBM 650 with Senko and Templeton's least squares program, and a Fourier projection onto (100) was computed with the TDF-2 program. All atoms were resolved in this projection and approximate coordinates for the two carbon atoms were obtained.

A Patterson projection onto (010) was not computed, but an estimate of the x-parameters was made from bond length considerations. Structure factors were computed with Busing and Levy's least squares program on the MURA IBM 704. It was observed that the calculated structure factors for the $\{h0l\}$ reflections agreed with the observed structure factors for the $\{\bar{h}0l\}$ reflections, and vice versa. This meant that the signs should be changed on all x-parameters. A Fourier projection onto (010) resolved the copper and chlorine atoms, but it was not possible to resolve the atoms in the acetonitrile group. Further least squares and Fourier refinement of this projection was not able to clearly resolve these atoms either.

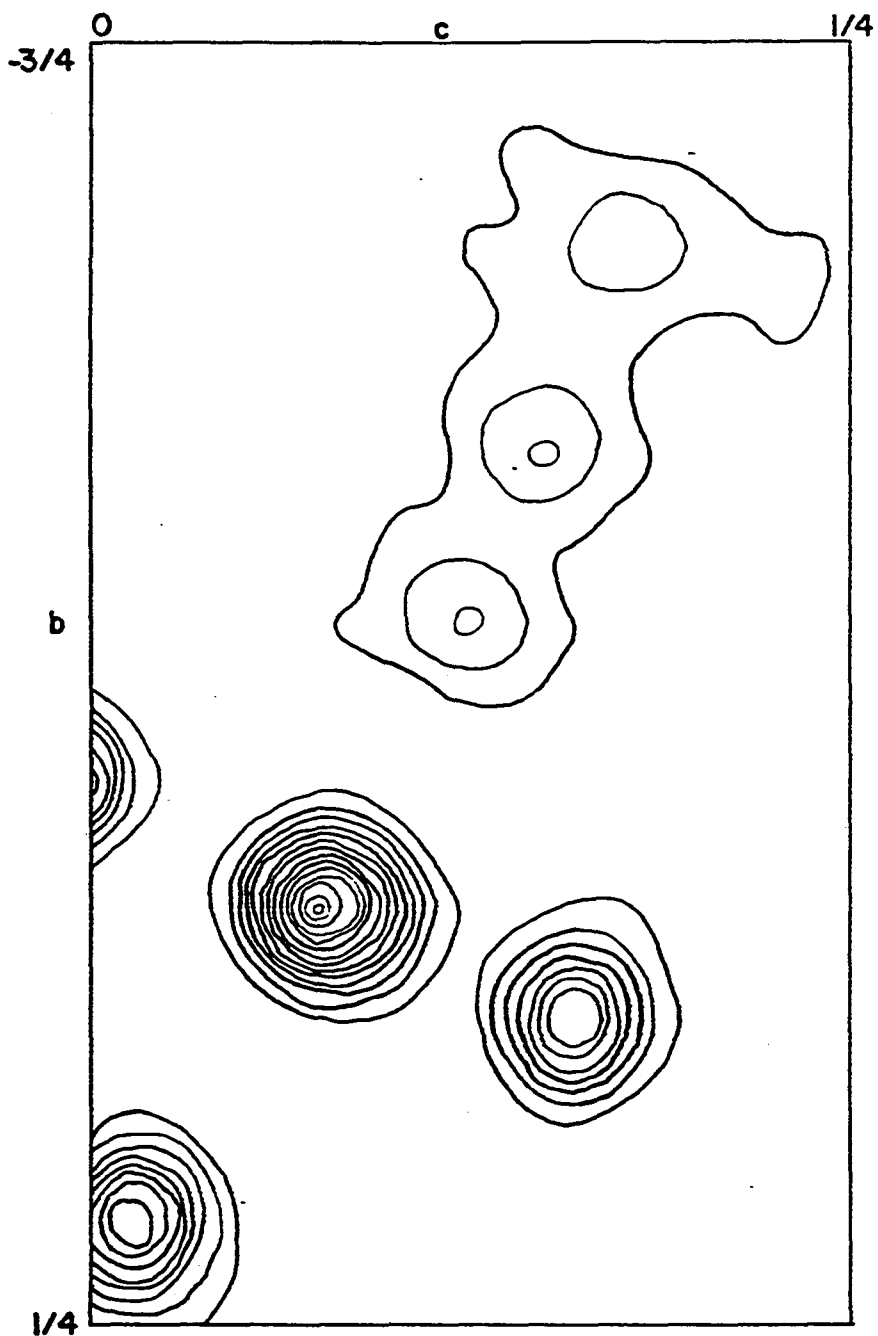


Figure 14. Fourier projection onto the (100) plane for $\text{Cu}_2\text{Cl}_4(\text{CH}_3\text{CN})_2$

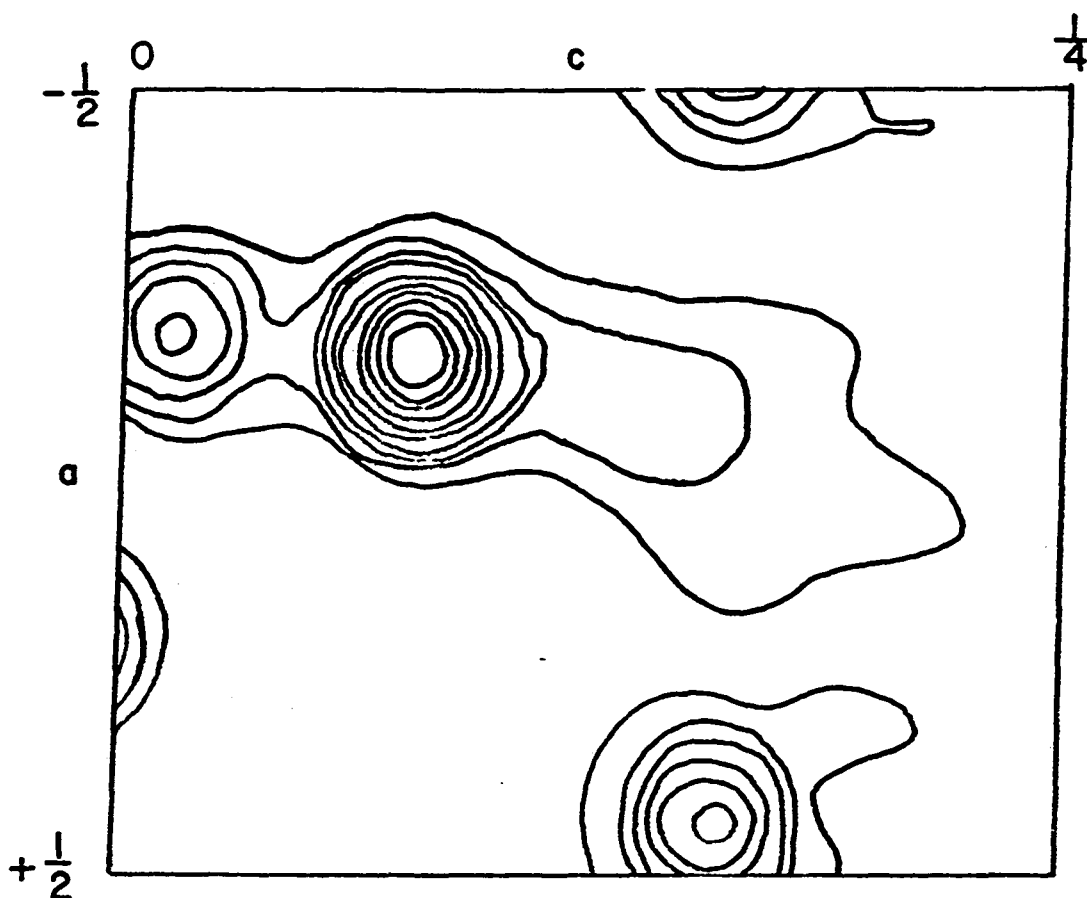


Figure 15. Fourier projection onto the (010) plane
for $\text{Cu}_2\text{Cl}_4(\text{CH}_3\text{CN})_2$

4. Refinement

The least squares refinement portion of the structural determination was carried out on the MURA IBM 704 using Busing and Levy's least squares program. The weighting scheme defined by Equation 4 was used for the $\{0k\ell\}$ Weissenberg data. Unobserved reflections were omitted from the refinement. The same weighting scheme was used for the $\{h0\ell\}$ precession data. Unobserved reflections were included in the refinement process because of the small number of reflections for which intensity measurements were made.

Both zones were refined separately with isotropic temperature factors only. Values of $R_1 = 0.118$ and 0.128 were obtained for the [100] and the [010] zones respectively. The z-parameters obtained from the two zones are not in very good agreement, although only for the first chlorine atom (Cl_1) is the difference greater than three times the larger standard deviation. The standard deviations of the z-parameters obtained from the [010] zone for the nitrogen and carbon atoms are extremely high due to the partial overlap of these atoms (see Figure 15). This probably accounts for the large temperature factors for the two carbon atoms in this zone. The final results are given in Table 10.

A weighted average of the z-parameters from the two zones was used for computation of interatomic distances, bond angles, and the least squares plane computations. The

Table 10. Parameters, temperature factors, standard deviations and R factors for $\text{Cu}_2\text{Cl}_4(\text{CH}_3\text{CN})_2$ ^a

Atom	[010] zone			[100] zone		
	x	z	B	y	z	B
Cu	.8386 (0011)	.0778 (0004)	3.89 (17)	.0766 (0006)	.0788 (0002)	4.48 (16)
Cl ₁	.1885 (0020)	-.0155 (0006)	3.96 (24)	.1720 (0010)	-.0135 (0004)	3.29 (17)
Cl ₂	.4380 (0022)	.1580 (0005)	3.72 (22)	-.0143 (0010)	.1585 (0004)	3.66 (19)
N	.8700 (0093)	.1204 (0035)	2.62 (95)	.3018 (0034)	.1235 (0016)	4.71 (74)
C ₁	.9465 (0189)	.1534 (0048)	4.62 (132)	.4396 (0033)	.1493 (0014)	3.06 (60)
C ₂	.0023 (0186)	.1783 (0044)	11.18 (280)	.5994 (0040)	.1760 (0017)	3.97 (76)
			[010] zone		[100] zone	
		R ₁	.128		.118	
		R ₂	.112		.141	

^aStandard deviations are in parentheses.

standard deviation of the copper-chlorine distances is approximately 0.01^oÅ, while the standard deviations of the distances involving nitrogen or carbon atoms are in the range of 0.03 to 0.04^oÅ. The standard deviations of the bond angles involving only copper and chlorine atoms are

Table 11. Interatomic distances and bond angles for
 $\text{Cu}_2\text{Cl}_4(\text{CH}_3\text{CN})_2^a$

Bond	Distance	Bond	Distance
Cu-Cl ₁	2.31 ^o Å	N-C ₁	1.17 ^o Å
Cu-Cl ₁	2.30 ^o Å	C ₁ -C ₂	1.45 ^o Å
Cu-Cl ₂	2.27 ^o Å	Cu-Cu	3.39 ^o Å
Cu-N	1.96 ^o Å	Cu ['] -Cl ₂	2.79 ^o Å
		Cu ['] -Cl ₁	3.08 ^o Å
<u>Angle</u>	<u>Value</u>	<u>Angle</u>	<u>Value</u>
Cu-Cl ₁ -Cu [']	94 ^o	Cl ₂ ['] -Cu-Cl ₂	98 ^o
Cl ₁ -Cu-Cl ₁	86 ^o	Cl ₂ ['] -Cu-N	90 ^o
Cl ₁ -Cu-Cl ₂	92 ^o	Cu ['] -Cl ₂ ['] -Cu	98 ^o
Cl ₁ -Cu-N	90 ^o	Cl ₁ ['] -Cu-N	92 ^o
Cl ₂ -Cu-N	92 ^o	Cl ₂ ['] -Cu-Cl ₂	83 ^o
Cu-N-C ₁	165 ^o	Cl ₁ ['] -Cu-Cl ₁	90 ^o
N-C ₁ -C ₂	170 ^o	Cl ₁ ['] -Cu-Cl ₁	84 ^o
Cl ₂ ['] -Cu-Cl ₁	89 ^o	Cu ['] -Cl ₁ -Cu	90 ^o
Cl ₂ ['] -Cu-Cl ₁	95 ^o	Cu ['] -Cl ₁ -Cu	96 ^o

^aAn atom displaced one unit cell in the x-direction is denoted by '.

Table 12. Least squares plane^a for $\text{Cu}_2\text{Cl}_4(\text{CH}_3\text{CN})_2$

	A	B	C	$\Sigma d_i /n$	Σd_i^2	$\sqrt{\Sigma d_i^2/n}$
Case 1 ^b	.2615	-.1264	.1903	.0591	.0500	.0645
Case 2 ^c	.2859	-.1264	.2083	.0481	.0275	.0587

Distance from plane

<u>Atom</u>	<u>Case 1^b</u>	<u>Case 2^c</u>
Cu	.0803A	.1011A
Cl ₁	-.0799A	-.0384A
Cl ₂	-.0427A	-.0447A
N	-.0836A	-.0080A
C ₁	.0567A	.1659A
C ₂	.0111A	.1621A

^aThe molecule was fit to the plane $Ax + By + Cz = 0$.

^bAll atoms were included.

^cCarbon atoms were not included.

approximately 0.3 to 0.4 degrees, while for the bond angles involving carbon and nitrogen atoms the standard deviations are several degrees. In particular, the standard deviation is about 4 degrees for the Cu-N-C₁ bond angle and about 6 degrees for the N-C₁-C₂. The interatomic distances and bond angles are given in Table 11.

Table 13. Comparison of observed and calculated structure factors for $\{0k\}$ data for $\text{Cu}_2\text{Cl}_4(\text{CH}_3\text{CN})_2$

k	l	F _{obs}	F _{calc}	k	l	F _{obs}	F _{calc}	k	l	F _{obs}	F _{calc}
2	0	316	357	4	3	291	-310	2	6	77	-66
4	0	73	-49	5	3	69	-66	3	6	62	-60
6	0	25	-20	7	3	93	-74	4	6	118	123
8	0	100	-83	8	3	52	-58	5	6	54	-63
10	0	24	23	9	3	59	-67	6	6	215	244
1	1	323	561	10	3	40	-26	7	6	32	29
2	1	131	-88	0	4	269	-308	8	6	47	47
4	1	168	-122	1	4	168	-156	1	7	143	-151
5	1	13	-13	2	4	322	-327	2	7	124	123
6	1	60	-57	3	4	330	-366	3	7	29	-31
7	1	42	-27	4	4	128	-99	4	7	46	48
8	1	55	-59	5	4	182	-182	5	7	206	247
9	1	56	-44	6	4	108	109	6	7	46	44
10	1	39	-24	7	4	31	30	7	7	127	163
0	2	236	356	9	4	36	19	8	7	30	37
1	2	199	-216	10	4	18	-22	9	7	17	8
2	2	182	-133	1	5	151	-146	0	8	67	-71
3	2	216	-288	2	5	175	-196	1	8	228	225
4	2	172	-149	3	5	196	-171	2	8	231	-249
5	2	138	-118	4	5	242	-245	3	8	178	198
7	2	40	49	5	5	225	249	4	8	32	29
8	2	88	-88	6	5	80	-88	5	8	57	56
9	2	85	75	7	5	117	108	6	8	154	146
10	2	9	-14	8	5	19	15	7	8	47	49
1	3	112	63	9	5	9	-18	1	9	151	-112
2	3	191	-211	0	6	185	134	2	9	322	377
3	3	375	-399	1	6	186	164	3	9	195	-186

Table 13. (Continued)

k	l	F _{obs}	F _{calc}	k	l	F _{obs}	F _{calc}	k	l	F _{obs}	F _{calc}
4	9	141	137	2	13	34	21	2	17	21	-21
5	9	25	-40	3	13	37	34	3	17	17	-17
6	9	74	65	4	13	88	-80	4	17	118	-133
8	9	17	-12	7	13	25	-12	6	17	7	-17
9	9	19	-39	8	13	45	43	0	18	36	-40
1	10	168	145	0	14	186	187	1	18	21	32
2	10	167	-150	1	14	65	60	3	18	25	-26
3	10	174	174	2	14	72	75	4	18	33	41
4	10	117	-113	3	12	79	-85	5	18	50	-54
5	10	24	24	4	14	23	-21	6	18	69	51
8	10	50	-45	5	14	55	-63	1	19	5	-18
9	10	42	-41	6	14	29	-27	2	19	28	32
1	11	194	179	7	14	66	67	3	19	32	29
2	11	204	204	8	14	37	-33	4	19	52	-60
3	11	45	-56	1	15	6	11	5	19	66	63
4	11	24	-20	3	15	59	-59	0	20	44	-49
7	11	42	-47	4	15	82	-95	1	21	61	-52
8	11	34	-26	5	15	54	-60	2	21	90	85
9	11	47	-33	7	15	31	-32	3	21	14	-17
0	12	317	365	0	16	66	-55	4	21	26	20
1	12	142	136	2	16	109	-98	0	22	57	-49
2	12	197	194	3	16	107	-134	1	22	60	52
3	12	64	74	4	16	53	-52	2	22	27	-27
5	12	21	-26	5	16	97	-96	3	22	28	19
6	12	19	-23	6	16	17	-12	1	23	14	-10
8	12	30	-21	7	16	47	43	2	23	42	46
1	13	238	272	1	17	68	-68	1	20	49	59
								3	20	29	30

Scale factor = 9.20

Table 14. Comparison of observed and calculated structure factors for $\{h0\}$ data for $\text{Cu}_2\text{Cl}_4(\text{CH}_3\text{CN})_2$

h	l	F _{obs}	F _{calc}	h	l	F _{obs}	F _{calc}	h	l	F _{obs}	F _{calc}
1	0	250	222	4	12	38	-35	-1	6	236	-250
2	0	62	-66	0	14	132	140	-2	6	98	109
3	0	248	-209	1	14	117	118	-3	6	65	64
4	0	48	-42	2	14	57	64	-4	6	83	70
1	2	415	449	3	14	77	-92	-1	8	78	77
2	2	117	122	4	14	18	-21	-2	8	<15	4
3	2	172	-150	0	16	56	-41	-3	8	85	87
4	1	40	-34	1	16	165	175	-4	8	44	-30
0	4	246	-226	2	16	47	48	-1	10	155	156
1	4	342	338	3	16	17	0	-2	10	<16	-1
2	4	46	44	0	18	43	-40	-3	10	40	-36
3	4	50	53	1	18	17	36	-4	10	<16	-8
4	4	58	-63	2	18	54	66	-1	12	<14	-2
0	6	90	65	3	18	16	33	-2	12	<16	8
1	6	66	-74	0	20	43	-51	-3	12	92	-84
2	6	113	128	1	20	43	-51	-4	12	<16	8
3	6	33	47	2	20	38	53	-1	14	33	-35
4	6	<17	-4	3	20	<13	10	-2	14	139	-135
0	8	58	-71	0	22	45	-52	-3	14	17	-13
1	8	134	-134	1	22	<16	-8	-4	14	<15	-4
2	8	<15	2	2	22	<15	-16	-1	16	65	-74
3	8	32	-31	0	24	28	14	-2	16	120	-114
4	8	52	53	1	24	<15	-3	-3	16	<17	5
0	10	13	-9	0	26	25	25	-4	16	42	33
1	10	44	47	-1	2	96	-84	-1	18	130	-138
2	10	163	-173	-2	2	598	-480	-2	18	<17	3
3	10	<17	-17	-3	2	87	-91	-3	18	<16	14
4	10	<16	-3	-4	2	<17	-8	-1	20	42	-50
0	12	270	251	-1	4	358	-325	-2	20	<17	12
1	12	45	52	-2	4	239	-230	-3	20	66	47
2	12	44	-53	-3	4	<16	-16	-1	22	35	28
3	12	74	-71	-4	4	121	106	-2	22	<16	12
								-1	24	<15	4

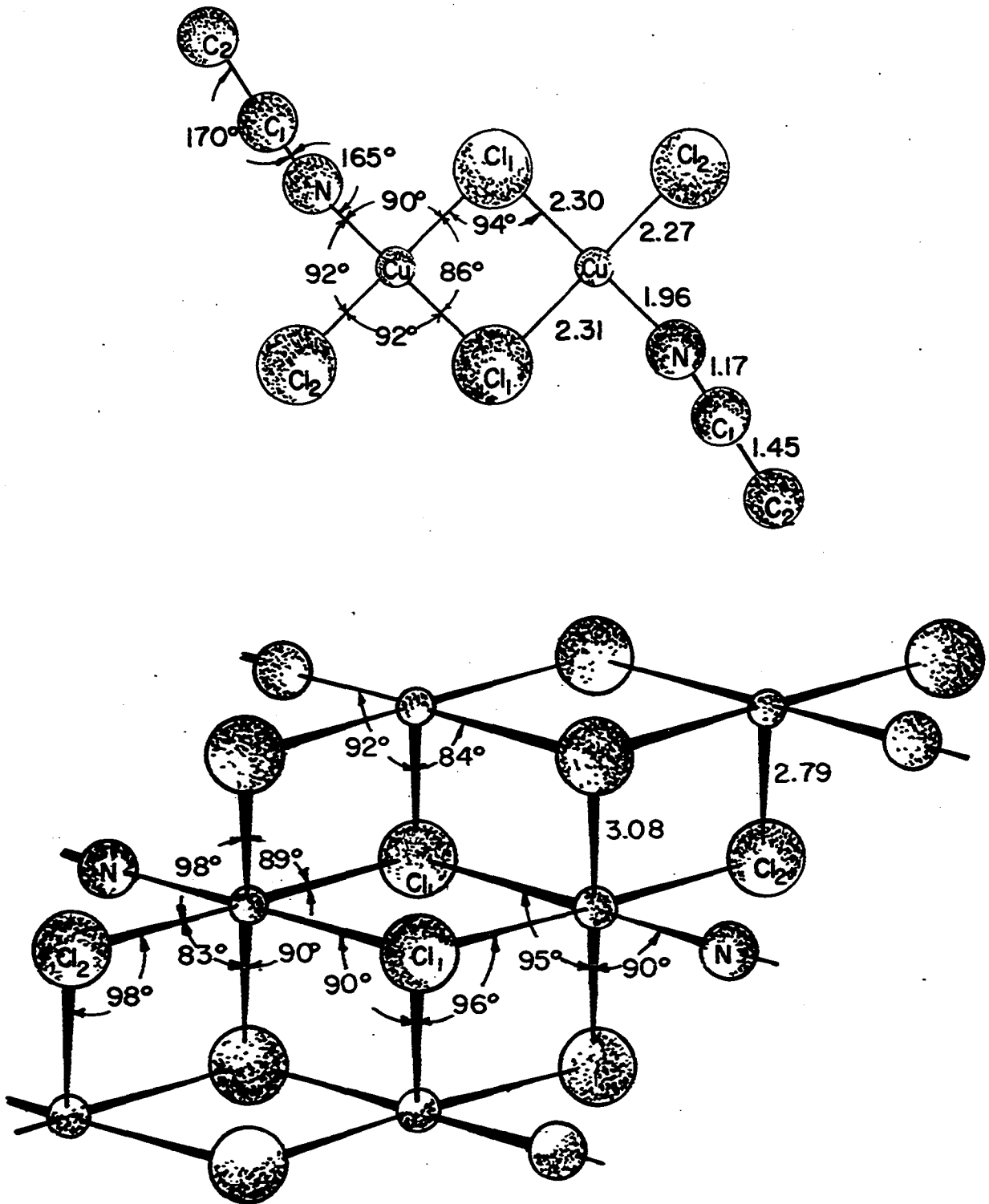
Scale factor = 6.87

5. Discussion of structure

This compound presents an interesting variation of the dimer which exists in the compounds KCuCl_3 , NH_4CuCl_3 , and $\text{LiCuCl}_3 \cdot 2\text{H}_2\text{O}$. In these latter three compounds, the negatively charged dimer Cu_2Cl_6^- occurs, while the neutral dimer $\text{Cu}_2\text{Cl}_4(\text{CH}_3\text{CN})_2$ is found in this compound. The dimer is again planar, with the two acetonitrile groups occurring trans across the molecule. The structure of the dimer is illustrated in Figure 16, along with the stacking of the molecule.

Each copper atom fulfills its four-fold coordination by bonding to three chlorine atoms and one nitrogen atom with all atoms located in the plane of the dimer. The distances to the two bridging chlorines (chlorine Cl_1 and its centrosymmetrical equivalent in Figure 16) are 2.30 and 2.31 Å. The distance of 2.27 Å to the terminal chlorine atom (Cl_2) is slightly shorter than the distances to the bridging chlorines. The Cu-N bond length of 1.96 Å is in good agreement with the value of 1.973 Å found for the Cu-N bond length in $\text{Cu}_3\text{Cl}_6(\text{CH}_3\text{CN})_2$. The C-N and C-C bond lengths of 1.17 and 1.45 Å are in reasonable agreement with those determined in $\text{Cu}_3\text{Cl}_6(\text{CH}_3\text{CN})_2$ of 1.134 and 1.480 Å. It is necessary to view the bond lengths for this compound with considerable reservations because of the unfortunate partial overlap of the carbon and nitrogen atoms in the projection onto (010) which

Figure 16. Illustration of the $\text{Cu}_2\text{Cl}_4(\text{CH}_3\text{CN})_2$ molecule and its stacking in the crystalline state



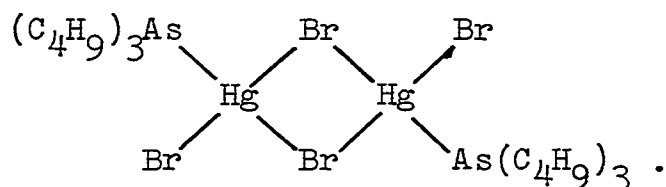
made the assignment of accurate x-parameters impossible for these atoms.

The angle between the bridging chlorines is 86° , in close agreement with the similar angle in the dimers in KCuCl_3 , NH_4CuCl_3 , and $\text{LiCuCl}_3 \cdot 2\text{H}_2\text{O}$. The $\text{Cl}_1\text{-Cu-Cl}_2$ and $\text{Cl}_2\text{-Cu-N}$ angles are 92° , while the $\text{Cl}_1\text{-Cu-N}$ angle is 90° . The Cu-N-C_1 angle is 165° with a standard deviation of about 4° , while the $\text{N-C}_1\text{-C}_2$ angle is 170° with a standard deviation of about 6° . Thus the acetonitrile molecule is linear to within the accuracy of the structural determination. However, the Cu-N-C_1 angle is not linear, as would be expected if pure sp hybrid orbitals were formed for the bonding orbitals of the nitrogen atom and thus it is necessary to include partial sp^2 character to this orbital. The observed nonlinearity of this bond can probably be accounted for by considering the packing of the molecules in the crystal. The dimers are stacked above each other along the a-axis in a manner analogous to that in KCuCl_3 and NH_4CuCl_3 . The interdimer Cu-Cl_1 and Cu-Cl_2 bond distances are 3.08 and 2.79^oA respectively. This latter distance is quite short in comparison with the interdimer distances in KCuCl_3 and NH_4CuCl_3 .

The results of the least squares plane computation are given in Table 12. Two separate calculations were made, one in which only the copper, chlorine, and nitrogen atoms were

included in the plane, and the second in which all atoms were included in the plane. With standard deviations for the copper and chlorine atoms of less than $.01\overset{\circ}{\text{A}}$, and standard deviations for the nitrogen and carbon atoms of around $.03\overset{\circ}{\text{A}}$, it is readily seen that the dimer deviates considerably from a truly planar configuration.

It is interesting to compare this structure to some of the arsine complexes of HgCl_2 and PdCl_2 . The structure of the compound $[(\text{C}_4\text{H}_9)_3\text{As}]_2\text{Hg}_2\text{Br}_4$ was studied by Evans *et al.* (56), and they showed that it contained planar bridged dimers of the type



This is directly analogous to the dimer found in $\text{Cu}_2\text{Cl}_4(\text{CH}_3\text{CN})_2$, with the acetonitrile groups being replaced by the arsine group. An investigation by Wells (57) of the structure of the compound $[(\text{CH}_3)_3\text{As}]_2\text{Pd}_2\text{Br}_4$ revealed that this structure was again planar, with the same molecular structure as the mercuric compound. Evans *et al.* (56) also studied the compound with the formula $[(\text{C}_4\text{H}_9)_3\text{As}]_2\text{Hg}_3\text{Br}_6$, and showed that it contained a mixture of the dimers and discrete HgBr_2 molecules. This is in direct contrast to the

compound $\text{Cu}_3\text{Cl}_6(\text{CH}_3\text{CN})_2$ (see the following section of the thesis), which contains a planar trimer.

E. Structure of $\text{Cu}_3\text{Cl}_6(\text{CH}_3\text{CN})_2$

1. Preparation and properties

During the course of the preparation of the compound $\text{CuCl}_2 \cdot \text{CH}_3\text{CN}$, a solution of acetonitrile saturated with anhydrous cupric chloride at the boiling point was allowed to cool. The deep red crystals which were formed had a powder pattern distinctly different from the powder patterns of $\text{CuCl}_2 \cdot \text{CH}_3\text{CN}$ and CuCl_2 . A literature search revealed no reference to any other complex between cupric chloride and acetonitrile.

These crystals show many of the properties exhibited by the other red cupric chloride complexes, such as pleochroism, hygroscopic nature, and the tendency of the crystals to twin. The density of the crystals was determined to be 2.42 g/cc by the flotation in a mixture of methylene bromide and ethylene bromide.

2. X-ray data

Examination of oscillation, precession and Weissenberg photographs established that the Laue symmetry was C_{2h} and that the crystal class was monoclinic. The systematic extinctions were:

$\{h0l\}$	$l \neq 2n$
$\{0k0\}$	$k \neq 2n$
$\{hkl\}$	none.

Thus it was probable that the space group was $P 2_1/c$.

Lattice constants were determined using a General Electric XRD-5 equipped with a single crystal orienter. The lattice constants are $\underline{a} = 6.78 \pm .01\overset{\circ}{\text{A}}$, $\underline{b} = 6.13 \pm .01\overset{\circ}{\text{A}}$, $\underline{c} = 16.51 \pm .02\overset{\circ}{\text{A}}$, and $\beta = 105.68 \pm .05^\circ$. The a-axis was chosen coincident with the needle axis.

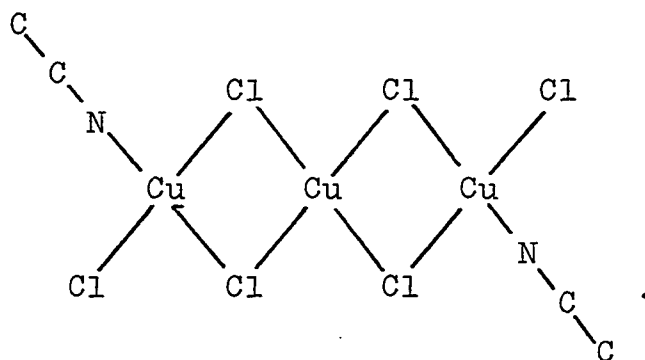
Intensity data for the reflections in the [010] zone were taken on a precession camera with Mo K_α radiation using the timed exposure technique. The LP corrections were estimated using the standard graphical method (51). In this manner, the intensities of 161 reflections were measured.

Three-dimensional intensity data were taken on the Weissenberg camera with Mo K_α radiation using the multiple exposure technique. The zero through fifth layers were recorded in this manner. The LP corrections were made on the MURA IBM 704 using the intensity correction program described on page 13. In order to obtain intensity data for those reflections which could not be observed using a Weissenberg camera, a second crystal was mounted on the single crystal orienter of the General Electric XRD-5. The standard θ - 2θ scan technique was used, with the background measurements obtained by offsetting ω . A total of 1490 re-

flections was examined and approximately 1060 were observed.

3. Structural determination

The first task in the structure determination was to ascertain the actual composition of the compound. Since the compound was formed at a higher temperature than $\text{CuCl}_2 \cdot \text{CH}_3\text{CN}$, it had to be less highly solvated than $\text{CuCl}_2 \cdot \text{CH}_3\text{CN}$. However, the observed density of 2.32 g/cc was much less than the density of 3.47 g/cc for anhydrous cupric chloride. Thus this new compound could not be another crystal form of anhydrous cupric chloride. The next most plausible choice consistent with the observed density was the empirical formula in a centrosymmetric space group is



The type of approach used to solve this structure had been used previously by Vand and Bell (58) in studying long chain aliphatic acids. In Figure 17 a $\{h0l\}$ precession photograph is reproduced. This gives a direct view of the reciprocal lattice, with each lattice point weighted

approximately with the intensity of the reflection corresponding to that point. It is noticed immediately that the strong reflections repeat themselves periodically throughout the reciprocal lattice. This regularity in intensity distribution is indicative of a regularity in the spatial distribution among the atoms in the unit cell. The problem of the solution of the crystal structure thus reduced largely to the problem of discovering this regularity in spatial distribution of the atoms.

The first step was to assume that the actual reciprocal lattice could be replaced by a super lattice. This super lattice was defined such that the strong reflections of the reciprocal lattice lay at or near the lattice points of the super lattice. The super lattice was transformed to real space and the sub cell in real space to which it corresponds was found. This is illustrated in Figure 18.

With six copper atoms in the unit cell of the proposed structure and with four-fold general positions in the space group $P 2_1/c$, it was necessary to assume that two of the copper atoms were located in special positions. The most logical assumption was that these two copper atoms were located at the centrosymmetric special set $(0, 0, 0)$ and $(0, \frac{1}{2}, \frac{1}{2})$. Thus, if one molecule of $\text{Cu}_3\text{Cl}_6(\text{CH}_3\text{CN})_2$ is centered at $(0, 0, 0)$, the second will be centered at $(0, \frac{1}{2}, \frac{1}{2})$. In the projection onto (010) , both molecules

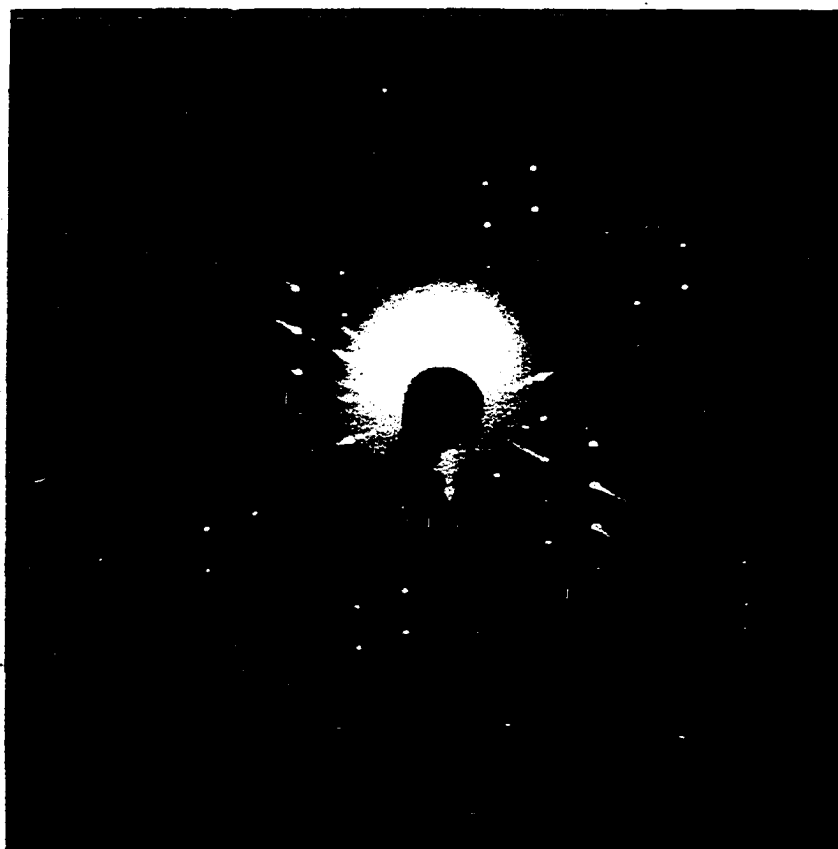
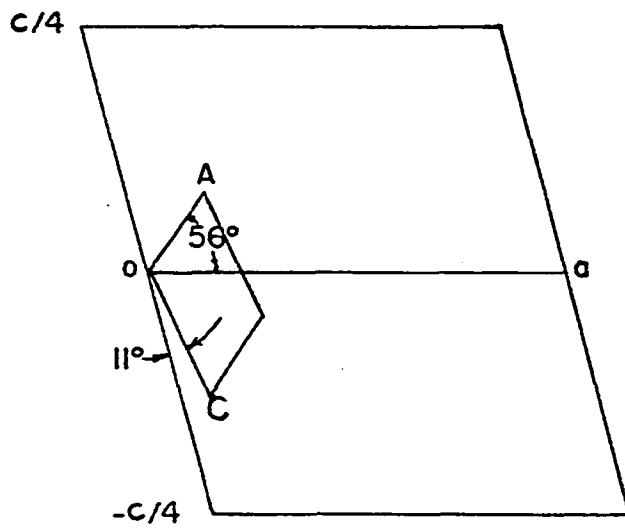
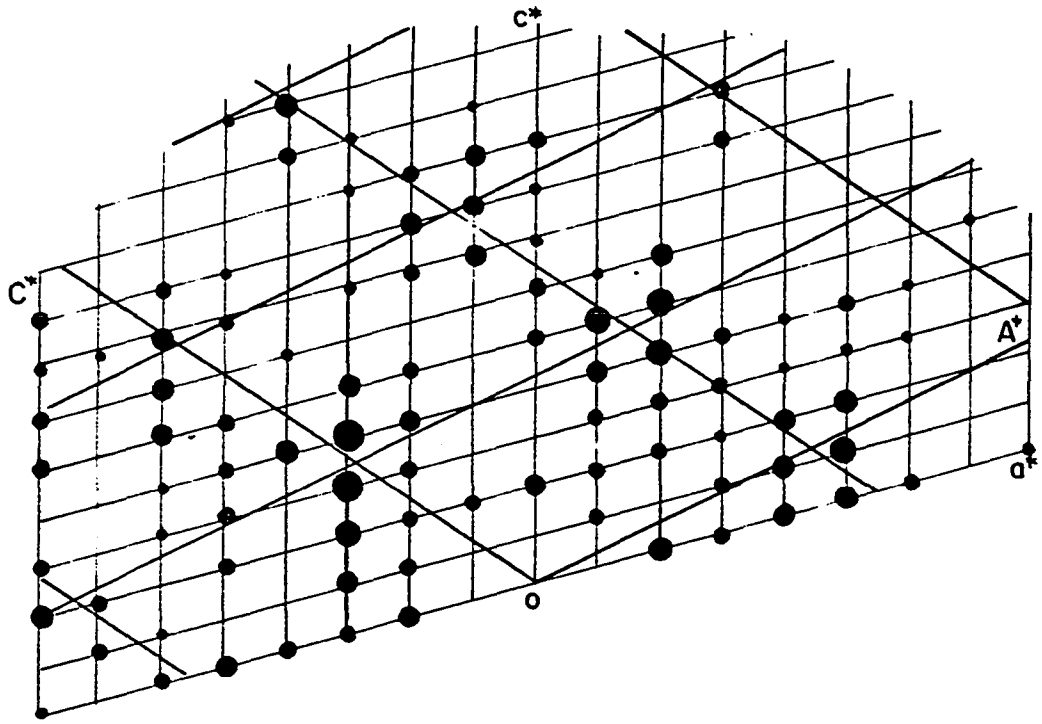


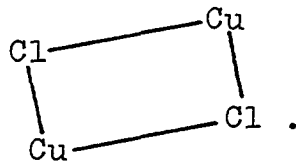
Figure 17. $\{h0l\}$ precession photograph of $\text{Cu}_3\text{Cl}_6(\text{CH}_3\text{CN})_2$

Figure 18. Weighted reciprocal lattice, super lattice,
and sub cell for the [010] zone of
 $\text{Cu}_3\text{Cl}_6(\text{CH}_3\text{CN})_2$



will have the same orientation.

Examination of the proposed structure suggested that the $\text{Cu}-(\text{Cl})_2\text{-Cu}$ chain was probably the repeated structure which corresponds to the sub cell. With one of the copper atoms in the unit cell being located at $(0, 0, 0)$, it was necessary that the sub cell be of the form



The structure factor for $\{h0l\}$ reflections in the space group $P 2_1/c$ is

$$F(h0l) = \sum_i f_i (\cos 2\pi h x_i \cos 2\pi l z_i - \sin 2\pi h x_i \sin 2\pi l z_i) \quad (\text{Eq. 15})$$

where f_i is the atomic scattering factor of the i^{th} atom and x_i and z_i are the coordinates of the i^{th} atom with respect to the unit cell axes. It was assumed that the copper and chlorine atoms were replaced by four identical scattering centers in the sub cell described above. For reflections lying at or near the corners of the super lattice, the structure factor is

$$F'(HOL) = \sum_J f'_J (\cos 2\pi H X_J \cos 2\pi L Z_J - \sin 2\pi H X_J \sin 2\pi L Z_J) \quad (\text{Eq. 16})$$

where H and L are the Miller indices of the super lattice, X_J and Z_J are the coordinates of the J^{th} atom in the sub cell with respect to the sub cell axes, and f'_J is the scattering factor for the J^{th} atom. The only atoms in the sub cell, however, are the atoms at the corners of the sub cell, so that the summation reduces to a single term, that with $X = Z = 0$. The sine term, moreover, is zero, and the cosine term is unity under these conditions. Thus the expression for the structure factor becomes

$$F'(HOL) = f' \quad (\text{Eq. 17})$$

where f' is the scattering factor of the scattering centers located at the corners of the sub cell. This is always greater than zero, and the important conclusion is reached that the sign of the structure factor for reflections located at or near the lattice points of the super lattice is always positive.

With this information, a Fourier projection onto (010) was computed using an IBM 650 from 27 of the stronger reflections in this zone. The result is shown in Figure 18. All of the copper, chlorine and nitrogen atoms were located

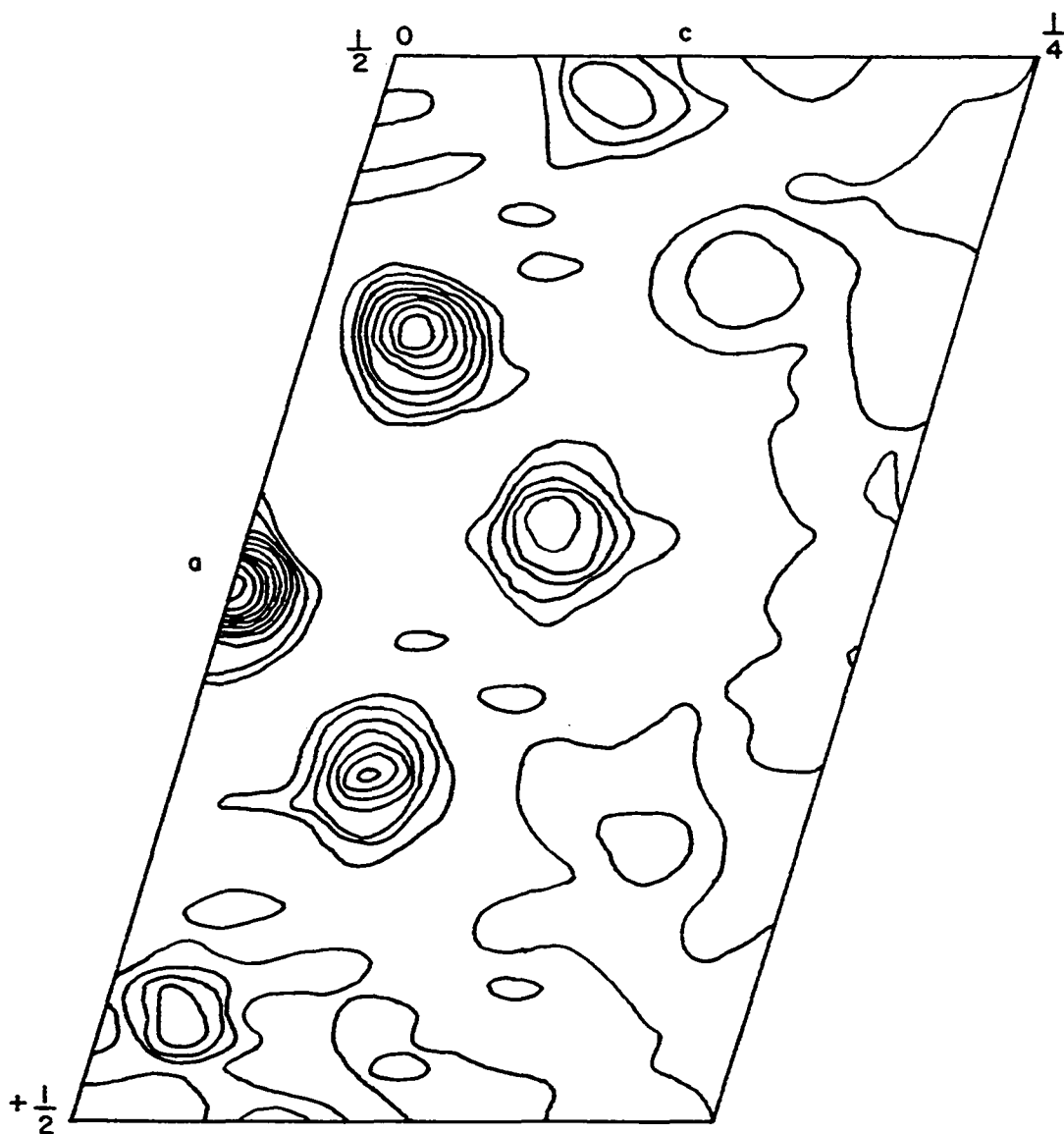


Figure 19. Fourier projection onto the (010) plane for $\text{Cu}_3\text{Cl}_6(\text{CH}_3\text{CN})_2$

The computations were made with only the 27 strongest reflections included.

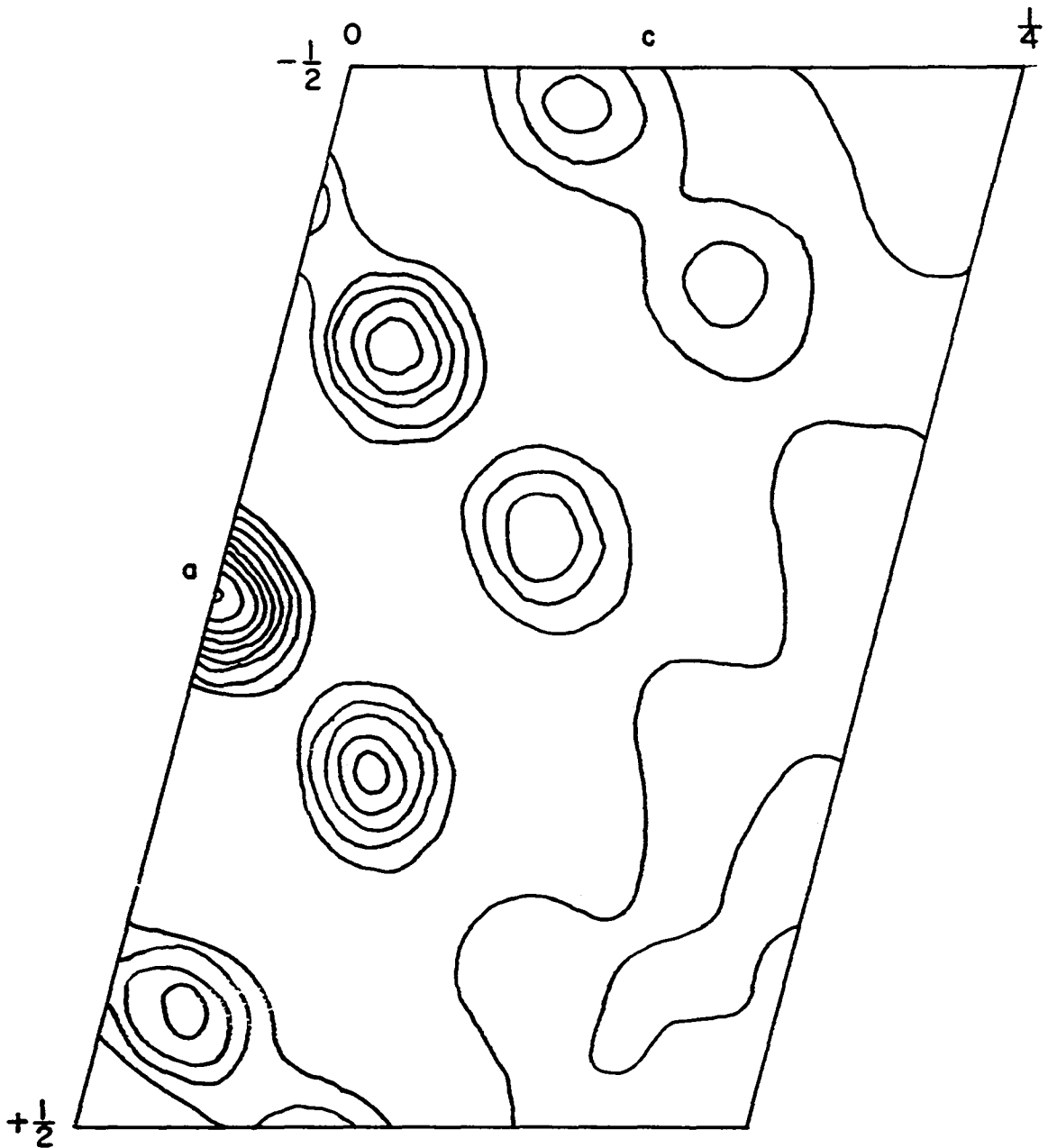


Figure 20. Patterson projection onto the (010) plane
for $\text{Cu}_3\text{Cl}_6(\text{CH}_3\text{CN})_2$

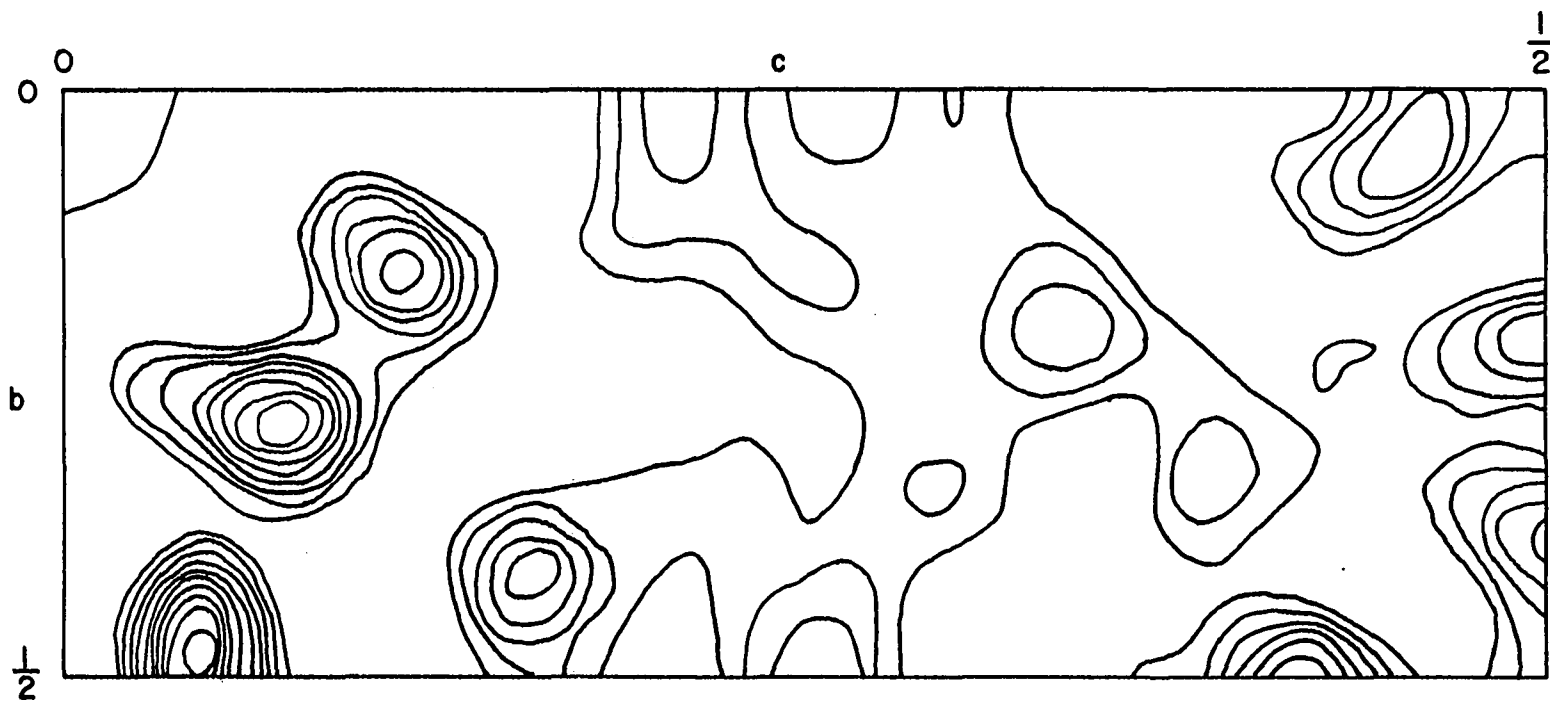


Figure 21. Patterson projection onto the (100) plane for $\text{Cu}_3\text{Cl}_6(\text{CH}_3\text{CN})_2$
The origin peak has not been drawn in.

from this Fourier projection and the positions of the two carbon atoms were located by alternately calculating structure factors and Fourier projections.

Simultaneous with the above procedure, a Patterson projection onto (010) was computed on an IBM 650 using the TDF-2 program. This is illustrated in Figure 20. The Patterson peak at $(U, W) = (-9.5/40, 3.5/80)$ was identified as a superposition of many Cu-Cu vectors and the two peaks at $(U, W) = (6.5/40, 6.0/80)$ and $(-2.5/40, 9.5/80)$ were identified as superpositions of many Cu-Cl vectors. Other large Patterson peaks were identified as combinations of these three basic vectors. The two vectors identified as Cu-Cl vectors had the same magnitude and direction as the two sides of the sub cell postulated previously and thus confirmed the identification of the sub cell and its contents.

The one problem left in the structural determination was the determination of the y-parameter of each of the atoms. A Patterson projection onto (100) was computed on an IBM 650 using the TDF-2 program. This is illustrated in Figure 21. The peak at $(V, W) = (19.5/40, 3.5/80)$ was identified as a superposition of many Cu-Cu vectors and the two peaks at $(V, W) = (11.5/40, 6.0/80)$ and $(6.5/40, 9.5/80)$ were identified as superposition of many Cu-Cl vectors. Again other large Patterson peaks could be identified as a

combination of these three basic vectors.

It was also observed that the length of the b-axis in this compound was the same as the length of the a-axis in $\text{LiCuCl}_3 \cdot 2\text{H}_2\text{O}$ (1). In this latter compound, the a-axis was the axis along which the Cu_2Cl_6^- dimers were stacked. This then suggested that the stacking of the $\text{Cu}_3\text{Cl}_6(\text{CH}_3\text{CN})_2$ trimers was similar to that of the dimers in $\text{LiCuCl}_3 \cdot 2\text{H}_2\text{O}$, and not similar to the dimers in KCuCl_3 . With this information it was quite easy to assign the y-coordinates to the copper, chlorine and nitrogen atoms. The y-parameters of the two carbon atoms were determined by the computation of structure factors of the other known atoms and then computing successive Fourier projections onto (100).

4. Refinement

The structure was refined on the MURA IBM 704 using Busing and Levy's least squares program. For the intensity data obtained with the Weissenberg technique, the weighting scheme given in Equation 5 was used where the constant I_1 was chosen as $2 I_{\min}$, the constant I_2 was chosen as the median value of I_0 for each particular layer, and values of the constant K which were used are indicated below:

<u>Layer</u>	<u>K</u>
$0k^l$.050
$1k^l$.050

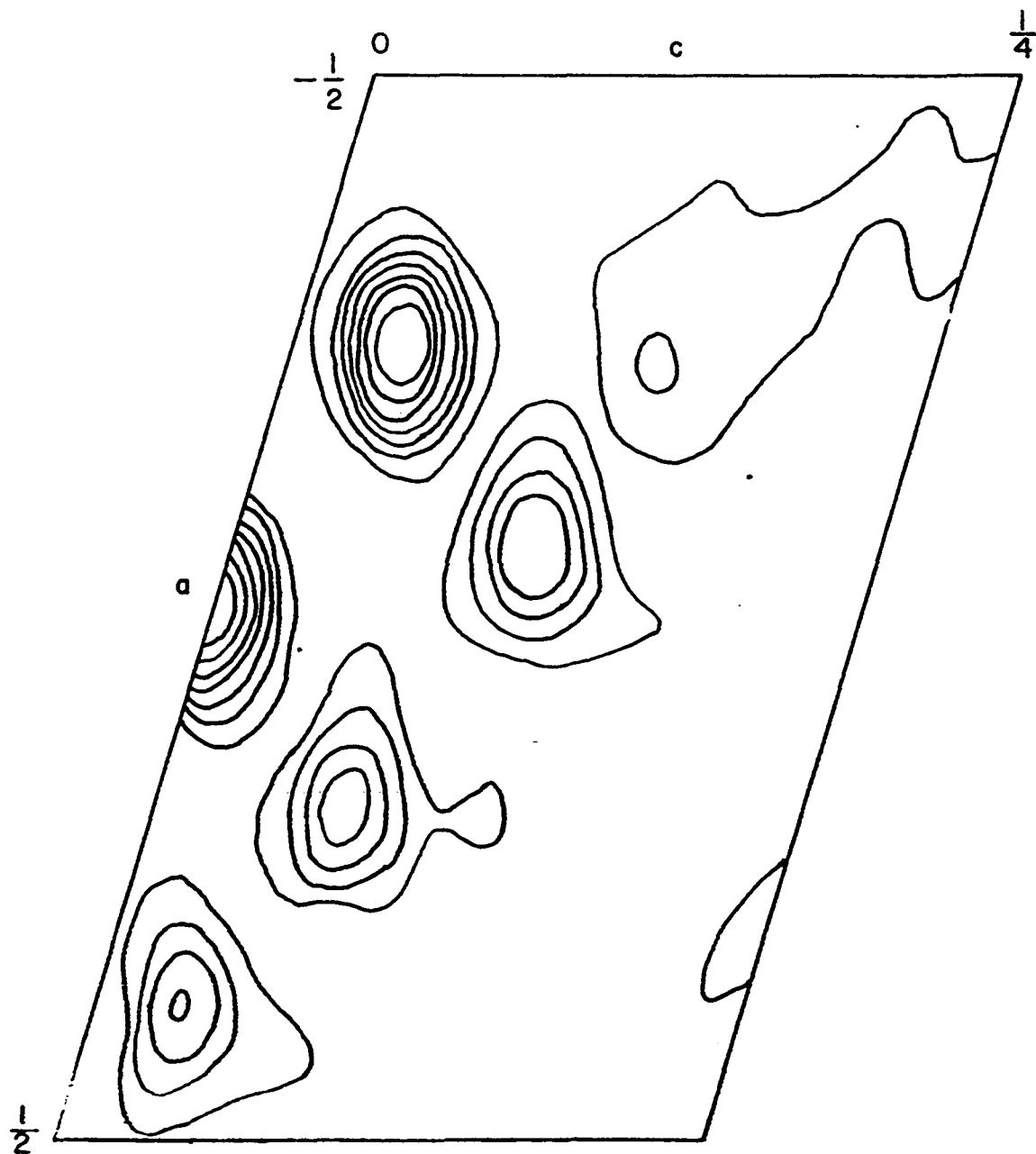


Figure 22. Final Fourier projection onto the (010) plane for $\text{Cu}_3\text{Cl}_6(\text{CH}_3\text{CN})_2$

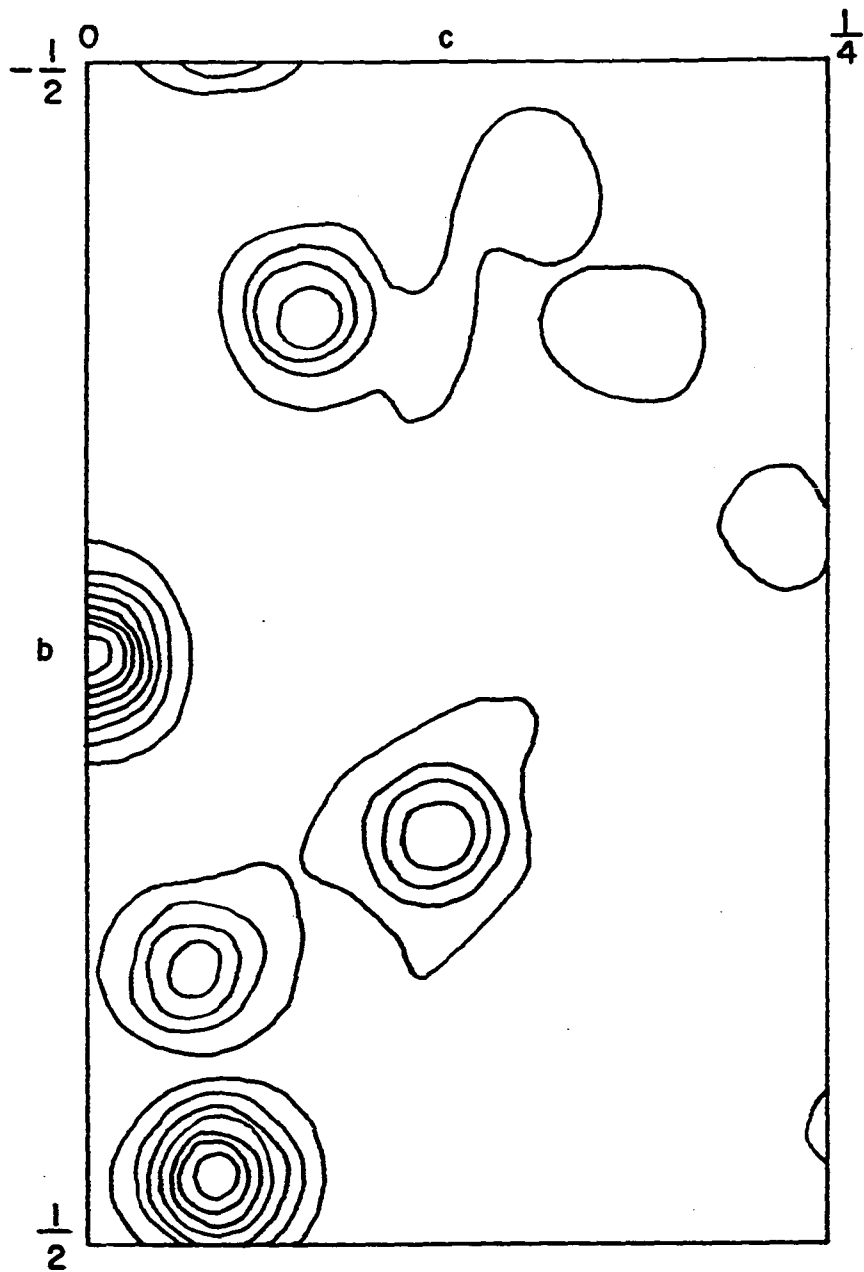


Figure 23. Fourier projection onto the (100) plane
for $\text{Cu}_3\text{Cl}_6(\text{CH}_3\text{CN})_2$

2kl	.055
3kl	.055
4kl	.060
5kl	.060

For the intensity data obtained using the single crystal orienter-scintillation counter technique, σ was computed using Equations 6 and 7.

All data were scaled approximately to absolute scale prior to the start of the least squares refinement by comparison with the $\{h0l\}$ precession intensity data. During initial isotropic refinement the scale factor for the $\{kl\}$ reflections changed by a factor of two. Examination of the film data revealed that this layer had been misindexed. This was corrected, and the isotropic refinement proceeded rapidly to a value of $R_1 = .120$ for observed reflections only. Anisotropic refinement was started at this point and, after three cycles in which the anisotropic temperature factors were varied, a value of $R_1 = .074$ was obtained for observed reflections only. The reflections $0\cdot0\cdot2$, $\bar{3}\cdot0\cdot6$, and $\bar{3}\cdot0\cdot8$ were omitted from the refinement because it was thought that their intensities might have been seriously reduced by extinction.

The final parameters and anisotropic temperature factors, along with their standard deviations, are listed in Table 15 and the bond distances and bond angles are listed

Table 15. Final parameters, temperature factors, standard deviations, and R factors for $\text{Cu}_3\text{Cl}_6(\text{CH}_3\text{CN})_2^a$

Atom	x	y	z	B_{11}	B_{22}	B_{33}	B_{12}	B_{13}	B_{23}
Cu_1	0 (0)	0 (0)	0 (0)	.0168 (0010)	.0142 (0005)	.00192 (00007)	.00711 (00054)	.00270 (00021)	.00060 (00015)
Cu_2	.7581 (0003)	.4434 (0002)	.04262 (00010)	.0106 (0007)	.0116 (0003)	.00218 (00005)	.00323 (00035)	.00231 (00014)	-.00022 (00010)
Cl_1	.1726 (0007)	-.2855 (0005)	.07324 (00018)	.0152 (0014)	.0133 (0006)	.00222 (00010)	.00442 (00071)	.00257 (00028)	.00087 (00020)
Cl_2	.9384 (0007)	.1556 (0005)	.11657 (00018)	.0153 (0014)	.0140 (0006)	.00205 (00009)	.00316 (00070)	.00259 (00028)	-.00003 (00020)
Cl_3	.3865 (0007)	-.7343 (0005)	.03442 (00020)	.0132 (0014)	.0122 (0006)	.00288 (00012)	.00260 (00068)	.00272 (00031)	.00053 (00021)
N	.7484 (0025)	.6008 (0021)	.1457 (0007)	.0134 (0050)	.0224 (0031)	.0026 (0004)	.0009 (0031)	.0029 (0012)	-.0014 (0009)
C_1	.7041 (0031)	.7303 (0019)	.1867 (0009)	.0221 (0060)	.0098 (0025)	.0030 (0005)	.0024 (0030)	.0034 (0013)	-.0007 (0009)
C_2	.6392 (0033)	.9007 (0024)	.2377 (0011)	.0257 (0072)	.0183 (0032)	.0047 (0008)	.0022 (0037)	.0062 (0019)	-.0051 (0013)

$R_1 = 0.126$ for all reflections

$R_1 = 0.074$ for observed reflections only

$R_3 = 0.161$

^aStandard deviations are given in the parentheses.

Table 16. Interatomic distances and bond angles for $\text{Cu}_3\text{Cl}_6(\text{CH}_3\text{CN})_2^a$

Bond	Distance	Bond	Distance
Cu_1-Cl_1	$2.264 \pm .003\overset{\circ}{\text{A}}$	$\text{N}-\text{C}_1$	$1.134 \pm .017\overset{\circ}{\text{A}}$
Cu_1-Cl_2	$2.285 \pm .003\overset{\circ}{\text{A}}$	C_1-C_2	$1.480 \pm .018\overset{\circ}{\text{A}}$
Cu_2-Cl_1	$2.303 \pm .004\overset{\circ}{\text{A}}$	Cu_1-Cu_2	$3.346 \pm .002\overset{\circ}{\text{A}}$
Cu_2-Cl_2	$2.300 \pm .004\overset{\circ}{\text{A}}$	Cu_1-Cl_3	$3.006 \pm .004\overset{\circ}{\text{A}}$
Cu_2-Cl_3	$2.255 \pm .003\overset{\circ}{\text{A}}$	Cl_1-Cu_2	$3.185 \pm .005\overset{\circ}{\text{A}}$
Cu_2-N	$1.973 \pm .012\overset{\circ}{\text{A}}$	Cu_2-Cl_3	$2.714 \pm .005\overset{\circ}{\text{A}}$
<u>Angle</u>	<u>Value</u>	<u>Angle</u>	<u>Value</u>
$\text{Cl}_1-\text{Cu}_1-\text{Cl}_2$	$86.7 \pm .1^\circ$	$\text{Cl}_2-\text{Cu}_1-\text{Cl}_3$	$92.1 \pm .1^\circ$
$\text{Cl}_1-\text{Cu}_2-\text{Cl}_2$	$90.3 \pm .1^\circ$	$\text{Cu}_1-\text{Cl}_1-\text{Cu}_2$	$90.7 \pm .1^\circ$
$\text{Cl}_2-\text{Cu}_2-\text{Cl}_1$	$93.3 \pm .1^\circ$	$\text{Cu}_2-\text{Cl}_1-\text{Cu}_2$	$91.0 \pm .1^\circ$
$\text{Cl}_1-\text{Cu}_2-\text{Cl}_3$	$91.1 \pm .1^\circ$	$\text{N}'-\text{Cu}_2-\text{Cl}_1$	$80.9 \pm .4^\circ$
$\text{Cl}_2-\text{Cu}_2-\text{N}$	$93.1 \pm .4^\circ$	$\text{Cl}_3-\text{Cu}_2-\text{Cl}_1$	$84.7 \pm .1^\circ$
$\text{Cu}_1-\text{Cl}_1-\text{Cu}_2$	$94.2 \pm .1^\circ$	$\text{Cl}_2-\text{Cu}_2-\text{Cl}_1$	$89.8 \pm .1^\circ$
$\text{Cu}_1-\text{Cl}_2-\text{Cu}_2$	$93.7 \pm .1^\circ$	$\text{Cl}_1-\text{Cu}_2-\text{Cl}_3$	$100.6 \pm .1^\circ$
$\text{Cu}_2-\text{N}-\text{C}_1$	$158.8 \pm 1.3^\circ$	$\text{Cl}_2-\text{Cu}_2-\text{Cl}_3$	$94.1 \pm .1^\circ$
$\text{N}-\text{C}_1-\text{C}_2$	$177.9 \pm 1.9^\circ$	$\text{Cl}_3-\text{Cu}_2-\text{Cl}_3$	$91.9 \pm .1^\circ$
$\text{Cl}_3-\text{Cu}_2-\text{N}$	$89.4 \pm .4^\circ$	$\text{N}'-\text{Cu}_2-\text{Cl}_3$	$89.6 \pm .5^\circ$
$\text{Cl}_1-\text{Cu}_1-\text{Cl}_3$	$91.1 \pm .1^\circ$	$\text{Cu}_2-\text{Cl}_3-\text{Cu}_2$	$88.1 \pm .1^\circ$

^aAn atom displaced one unit cell in the y-direction is denoted by '.

Table 17. Least squares plane^a for $\text{Cu}_3\text{Cl}_6(\text{CH}_3\text{CN})_2$

	A	B	C	$\Sigma d_i / n$	Σd_i^2	$\sqrt{\Sigma d_i^2 / n}$
Case 1 ^b	.8655	.4895	.1059	.0623	.1243	.0910
Case 2 ^c	.8592	.4933	.1357	.0684	.0781	.0842
Case 3 ^d	.8474	.4997	.1794	.0433	.0227	.0502
Case 4 ^e	.8443	.5026	.1861	.0442	.0302	.0502

Distance from plane

<u>Atom</u>	<u>Case 1^b</u>	<u>Case 2^c</u>	<u>Case 3^d</u>	<u>Case 4^e</u>
	o	o	o	o
Cu ₁	.0000A	.0000A	.0000A	.0000A
	o	o	o	o
Cu ₂	.1819A	.1397A	.0714A	.0529A
	o	o	o	o
Cl ₁	-.0033A	.0194A	.0491A	.0490A
	o	o	o	o
Cl ₂	.1487A	.0838A	-.0141A	-.0324A
	o	o	o	o
Cl ₃	-.0101A	-.0266A	-.0604A	-.0778A
	o	o	o	o
N	-.0087A	-.1068A	-.2590A	-.2929A
	o	o	o	o
C ₁	-.1474A	-.1710A	-.3624A	-.4045A
	o	o	o	o
C ₂	-.0672A	-.2232A	-.4645A	-.5173A

^aThe molecule was fit to the plane $Ax + By + Cz = 0$.

^bAll atoms were included.

^cCarbon atoms were not included.

^dCarbon and nitrogen atoms were not included.

^eCarbon and nitrogen atoms were not included, and the copper atoms were included with double weight.

Table 18. Comparison of observed and calculated structure factors for the $\{h0l\}$ data for $\text{Cu}_3\text{Cl}_6(\text{CH}_3\text{CN})_2$

h	l	F _{obs}	F _{calc}	h	l	F _{obs}	F _{calc}	h	l	F _{obs}	F _{calc}
2	0	333	-341	4	6	78	93	0	14	122	-134
3	0	217	213	5	6	170	177	1	14	20	-8
4	0	282	311	6	6	96	-78	2	14	26	47
5	0	315	302	7	6	19	-18	3	12	21	-20
6	0	120	-117	0	8	15	-20	4	12	20	-19
7	0	54	-40	1	8	492	509	5	12	42	-45
8	0	95	101	2	8	647	659	0	16	63	34
9	0	50	-51	3	8	131	-124	1	16	26	-17
2	2	13	-27	4	8	68	-67	2	16	21	7
3	2	112	-100	5	8	97	110	3	16	98	86
4	2	447	505	6	8	20	-16	0	18	64	29
5	2	576	630	7	8	18	-24	1	18	21	0
6	2	20	-25	0	10	172	-198	2	18	27	10
7	2	67	-61	1	10	462	461	3	18	176	176
8	2	68	72	2	10	611	664	0	20	27	17
0	4	310	296	3	10	57	41	1	20	42	-44
1	4	240	-233	4	10	29	-41	2	20	15	-30
2	4	83	76	5	10	51	48	0	22	29	46
3	4	105	-94	6	10	140	154	-2	2	218	-212
4	4	219	219	7	10	83	91	-3	2	221	224
5	4	475	491	0	12	211	-228	-4	2	43	-5
6	4	96	-78	1	12	150	135	-5	2	19	-34
7	4	19	-18	2	12	342	326	-6	2	98	-93
0	6	13	33	3	12	20	5	-7	2	66	95
1	6	177	174	4	12	21	-19	-8	2	198	198
2	6	180	177	5	12	20	18	-9	2	40	-34
3	6	240	-221	6	12	161	169	-1	4	159	-134

Table 18. (Continued)

h	l	F _{obs}	F _{calc}	h	l	F _{obs}	F _{calc}	h	l	F _{obs}	F _{calc}
-2	4	197	-161	-1	10	16	27	-1	16	458	416
-3	4	542	601	-2	10	196	180	-2	16	307	289
-4	4	59	50	-3	10	317	302	-3	16	20	-56
-5	4	110	-102	-4	10	34	-27	-4	16	33	34
-6	4	20	46	-5	10	195	-172	-5	16	101	93
-7	4	182	216	-6	10	176	180	-6	16	234	206
-8	4	273	302	-7	10	20	23	-7	16	56	55
-9	4	15	4	-8	10	96	-98	-8	16	88	-91
-1	6	127	-117	-9	10	13	-6	-1	18	294	280
-2	6	217	219	-1	12	118	116	-2	18	261	222
-3	6	878	985	-2	12	64	63	-3	18	144	-145
-4	6	302	313	-3	12	42	-35	-4	18	21	-3
-5	6	126	-132	-4	12	97	-98	-5	18	78	62
-6	6	94	103	-5	12	30	46	-6	18	19	-3
-7	6	172	206	-6	12	370	376	-7	18	49	-32
-8	6	205	208	-7	12	54	51	-1	20	96	82
-9	6	15	-7	-8	12	95	-94	-2	20	21	3
-1	8	14	-27	-9	12	59	76	-3	20	105	-112
-2	8	349	331	-1	14	320	332	-4	20	120	105
-3	8	872	914	-2	14	236	222	-5	20	54	61
-4	8	196	174	-3	14	123	-126	-6	20	84	-87
-5	8	222	-199	-4	14	27	46	-1	22	53	-48
-6	8	101	109	-5	14	216	193	-2	22	21	-18
-7	8	41	39	-6	14	409	339	-3	22	18	12
-8	8	20	36	-7	14	132	114	-4	22	167	160
-9	8	27	-35	-8	14	60	-59	-5	22	103	107

Scale factor = 10.0

Figure 24. Comparison of observed and calculated structure factors for $\text{Cu}_3\text{Cl}_6(\text{CH}_3\text{CN})_2$

The reflections are grouped into sections of constant h and l . The first column is the running index k ; the second column is $10|F_o|$; the third column is $10F_c$. An asterisk following the running index denotes an unobserved reflection.

Table with multiple columns and rows containing numerical data and alphanumeric labels (e.g., O.K., K.0, K.1, K.2, etc.). The data appears to be organized in vertical columns, with some rows serving as headers for the columns.

Figure 24. (Continued)

A large table with 15 columns containing numerical data, likely representing a grid of values for a statistical or scientific analysis. The data is organized into columns, with some columns having headers like '1 50 51', '2 85 97', etc. The numbers range from 0 to over 1000.

in Table 16. Since the molecule is essentially planar, the molecule was fit to the plane $Ax + By + Cz = 0$ using the Least Squares Plane program written by J. M. Stewart. The results are listed in Table 17. A list of the final three-dimensional structure factors is given in Figure 24 and a list of the structure factors for the $\{h0l\}$ precession data is given in Table 18.

5. Discussion

This compound contains a new complex of cupric chloride, the complex forming a trimer with the formula of $\text{Cu}_3\text{Cl}_6(\text{CH}_3\text{CN})_2$. The trimer is planar, with each copper atom surrounded by four ligands in a square-planar configuration. The two acetonitrile groups are located trans across the molecule.

The trimer contains a center of symmetry, with the central copper atom (labeled Cu_1 in Figure 25) located on this center of symmetry. This central copper atom is bonded to four chlorine atoms (Cl_1 and Cl_2 and their centrosymmetrical equivalents) at distances of 2.264 and 2.285^oÅ. The other crystallographic independent copper atom (Cu_2) is bonded to three chlorine atoms (Cl_1 , Cl_2 and Cl_3) and one nitrogen atom at distances of 2.303, 2.300, 2.255, and 1.973^oÅ. The Cu_2 - Cl_3 bond distance is considerably shorter than the other two Cu-Cl bond distances, as is expected when

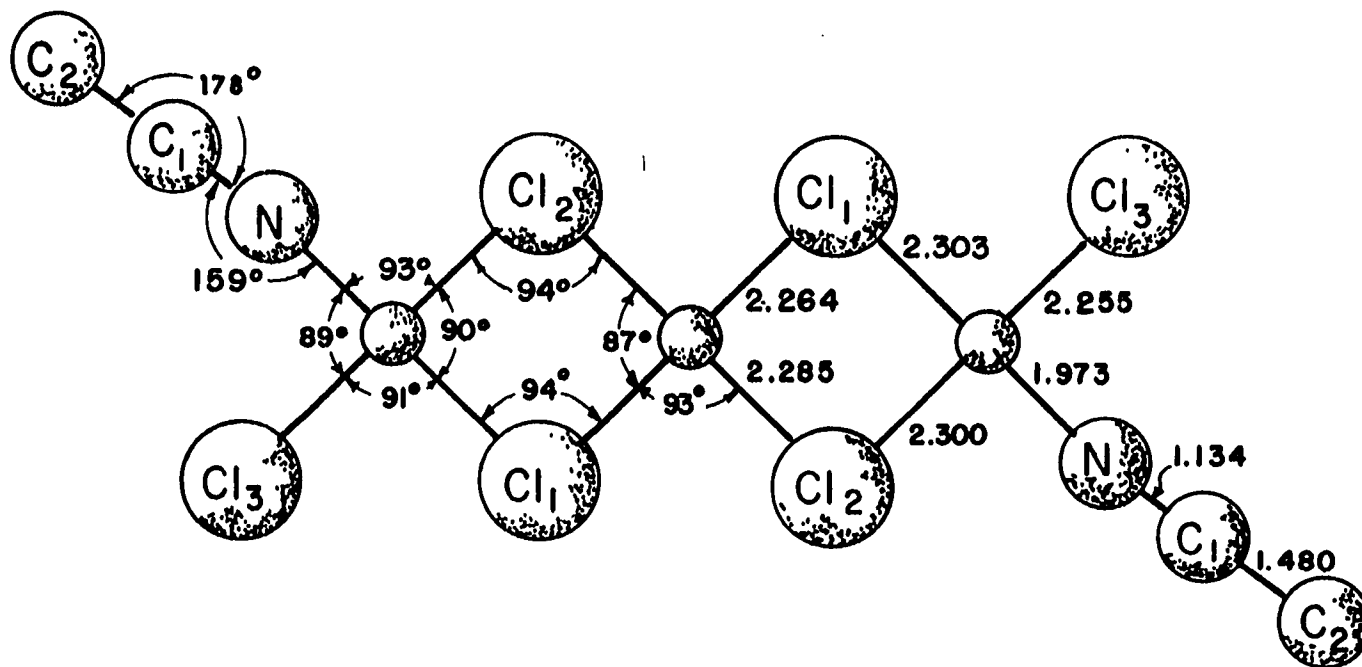


Figure 25. Illustration of the $\text{Cu}_3\text{Cl}_6(\text{CH}_3\text{CN})_2$ molecule

the bond lengths of terminal and bridging chlorine atoms are compared. The N-C₁ and C₁-C₂ bond lengths are 1.13 and 1.48Å respectively. These are in good agreement with the values of 1.15 and 1.46Å reported in two determinations of the structure of acetonitrile (59, 60), the values of 1.126 and 1.426Å reported in B₉H₁₃(CH₃CN) (61) and the values of 1.137 and 1.446Å reported in B₁₀H₁₂(CH₃CN)₂ (62).

The N-C₁-C₂ bond angle of 178° shows that the acetonitrile group is linear. The Cu₂-N-C₁ bond angle of 159° shows that this angle deviates a considerable amount from a linear arrangement. It thus appears that the nitrogen atom does not use pure sp hybrid orbitals, but that the orbitals also have partial sp² character. This partial sp² character could be obtained by forming a double bond between the carbon and nitrogen and leaving an electron pair on the nitrogen atom. A similar situation exists in Fe₂S₂(CH₂CH₃)₂NO, where the Fe-N-O bond angle is 168° (63). It is probable that packing efficiency of the Cu₃Cl₆(CH₃CN)₂ molecules also influences the Cu-N-C₁ bond angle.

The molecules stack above each other along the b-axis in much the same manner that the dimers in LiCuCl₃·2H₂O are stacked. (Compare the b-axis length of 6.13Å with the a-axis length of 6.08Å in LiCuCl₃·2H₂O.) The stacking is illustrated in Figure 23. Each trimer is joined by four long Cu-Cl bonds to the trimer directly above it along the

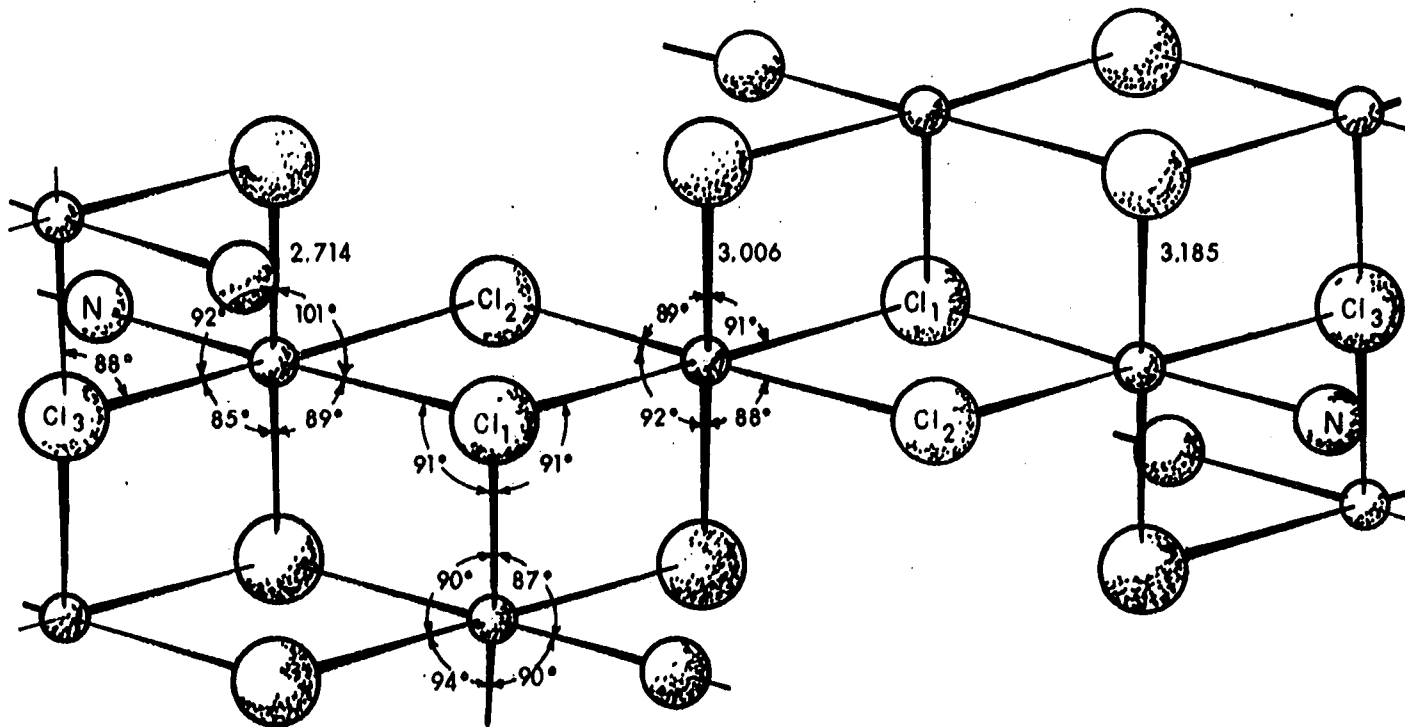


Figure 26. Stacking of the trimers in $\text{Cu}_3\text{Cl}_6(\text{CH}_3\text{CN})_2$

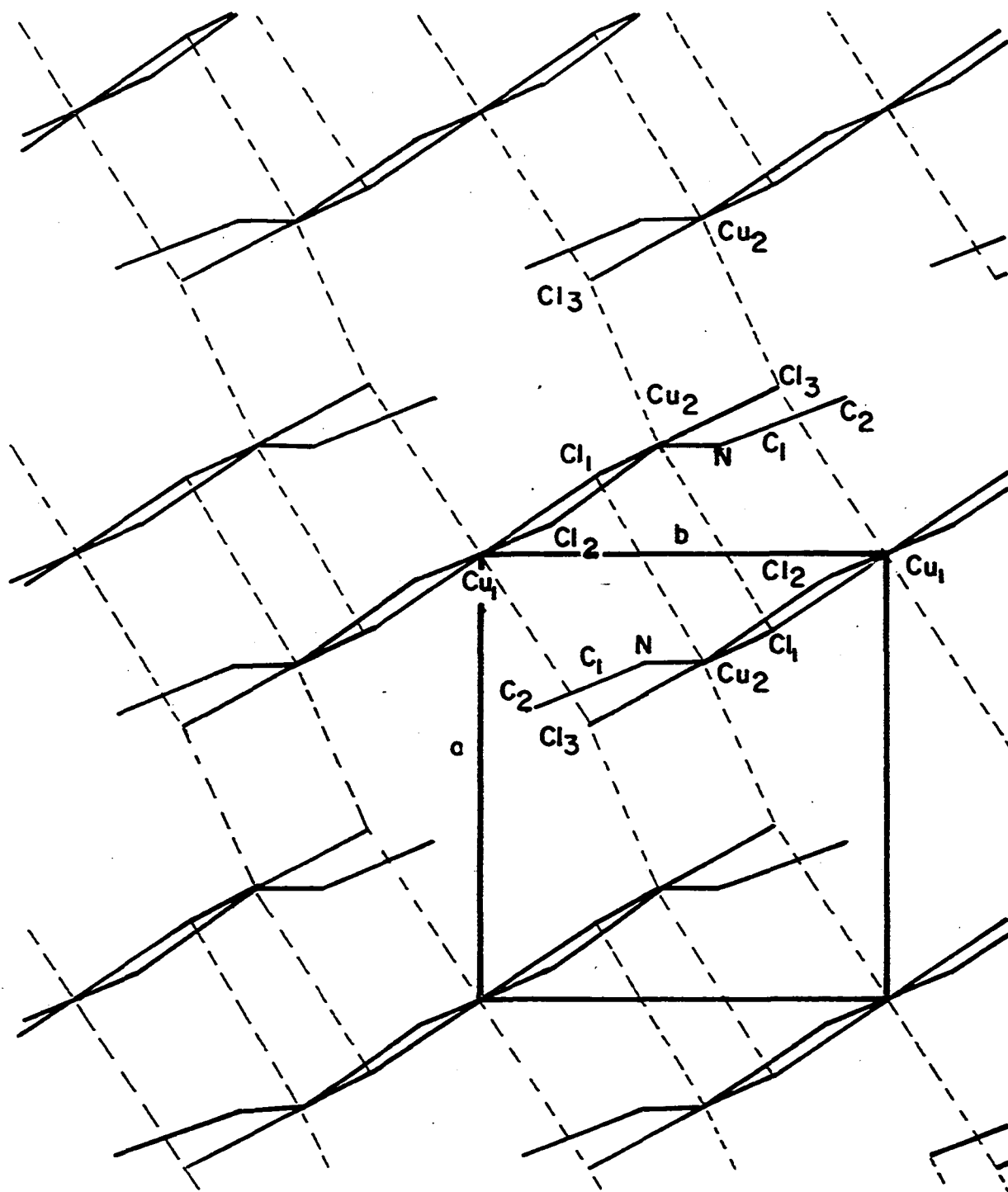


Figure 27. View of the structure of $\text{Cu}_3\text{Cl}_6(\text{CH}_3\text{CN})_2$ from the (001) direction

b-axis. The lengths of these bonds are $3.006\overset{\circ}{\text{A}}$ for the $\text{Cu}_1\text{-Cl}_3$ bonds and $3.185\overset{\circ}{\text{A}}$ for the $\text{Cu}_2\text{-Cl}_1$ bonds. Thus the central copper atom (Cu_1) completes its distorted octahedral coordination by forming two long Cu-Cl bonds, one to the trimer located above it along the b-axis, and one to the trimer located below it. The other copper atom (Cu_2) bonds to only one chlorine atom in this manner and completes its coordination by bonding to a chlorine atom (Cl_3) in a trimer that is located one unit cell up along the b-axis and one unit cell back along the a-axis. This is illustrated in Figure 27. Thus the chains of trimers stacked along the b-axis are tied together by Cu-Cl bonds into sheets which lie in the ab-plane. This bond distance, $\text{Cu}_2\text{-Cl}_3$, is $2.714\overset{\circ}{\text{A}}$.

The formation of sheets in this manner explains why the a-axis is the needle axis in this compound. In $\text{LiCuCl}_3 \cdot 2\text{H}_2\text{O}$, the needle axis is the axis along which the Cu_2Cl_6^- ions are stacked. Thus the b-axis would be expected to be the needle axis in $\text{Cu}_3\text{Cl}_6(\text{CH}_3\text{CN})_2$ since this is the corresponding axis. Examination of Figure 27 reveals, however, that the trimers are tied together in a very neat fashion along the a-axis.

The results of the least squares plane computation are given in Table 17. Four separate computations were made, one which included all atoms in the molecule, one which omitted the carbon atoms, another which omitted the entire

acetonitrile molecule and the last one in which the copper atoms were given double weight as well as omitting the acetonitrile group. This latter computation was made because the positions of the chlorine atoms obtained from the least squares refinement had about twice the standard deviation as the positions of the copper atoms. Since the standard deviations of the copper and chlorine atoms are about $.0015\overset{\circ}{\text{A}}$ and $.003\overset{\circ}{\text{A}}$ respectively, and the standard deviations of the lighter nitrogen and carbon atoms are close to $.01\overset{\circ}{\text{A}}$, it is seen that the atoms in the molecule deviate from a truly planar configuration. Also, the acetonitrile group is tilted significantly out of the plane. The terminal carbon atom (C_2) lies almost $.5\overset{\circ}{\text{A}}$ below the plane defined by the copper and chlorine atoms. The maximum deviation of the copper and chlorine atoms themselves is less than $.08\overset{\circ}{\text{A}}$, which is quite small compared with the overall length of the molecule of about $10\overset{\circ}{\text{A}}$.

F. Structure of $\text{Cu}_5\text{Cl}_{10}(\text{C}_3\text{H}_7\text{OH})$

1. Preparation and properties

The solubility of cupric chloride in anhydrous alcohols was studied by Lloyd et al. (64), who reported that no complex was formed between cupric chloride and n-propyl alcohol. Because of the interest in obtaining large single crystals of anhydrous cupric chloride for a neutron diffraction

investigation of the magnetic ordering, an attempt was made to utilize n-propyl alcohol as a solvent for recrystallization. The compound obtained exhibited a powder diffraction pattern distinctly different from that of anhydrous cupric chloride.

When a saturated solution of anhydrous cupric chloride in n-propyl alcohol was slowly evaporated at room temperature (by placing in a desiccator over magnesium perchlorate), thin, reddish-orange needles of the compound were obtained. These crystals were extremely hygroscopic and exhibited the usual pleochroic behavior when examined under the polarizing microscope. The density of the crystals was determined to be 2.32 g/cc by flotation in a mixture of methylene bromide and ethylene bromide.

2. X-ray data

Examination of oscillation, precession and Weissenberg photographs established that the Laue symmetry was C_{2h} and that the crystal class was monoclinic. The systematic extinctions,

$$\begin{array}{ll} \{h0l\} & h + l \neq 2n \\ \{0k0\} & k \neq 2n \\ \{hkl\} & \text{none,} \end{array}$$

implied that the crystals belonged to the space group $P 2_1/n$. Lattice constants, determined on a General Electric

XRD-5, are $a = 10.17 \pm .01\overset{\circ}{\text{Å}}$, $b = 6.04 \pm .01\overset{\circ}{\text{Å}}$, $c = 18.30 \pm .02\overset{\circ}{\text{Å}}$, and $\beta = 94.57 \pm .05^\circ$.

Three-dimensional intensity data were obtained on a General Electric XRD-5 equipped with a single crystal orienter and a scintillation counter. The intensity of approximately 2140 reflections was measured using the stationary crystal, stationary counter technique. The three Eulerian angles φ , χ , and θ were calculated on the Cyclone computer using the SCO-3 program written by D. E. Williams. The intensity of a standard reflection was measured periodically, and all data were scaled to time zero by multiplying by the factor $I_{\text{std}}(0)/I_{\text{std}}(t)$, where $I_{\text{std}}(0)$ was the intensity of the standard reflection initially, and $I_{\text{std}}(t)$ was the intensity of the standard reflection at the time t .

For a given value of 2θ and χ , it was observed that the variation in background measurements with φ was almost within the limits set by the statistical counting error. For a given value of 2θ and φ , it was observed that the background increased as χ was increased from 0° to approximately 45° , and remained essentially constant as χ was increased from 45° to 90° . Thus two background tables were prepared; one to give the variation of the background with 2θ at $\chi = 0^\circ$, and the second to give the variation of the background with 2θ at $\chi = 90^\circ$. In the data processing program written for the IBM 704, the value of the background for a given value

of 2θ and χ , denoted by $B(2\theta, \chi)$, was obtained in the following manner:

$$B(2\theta, \chi) = B(2\theta, 90^\circ) \quad (\text{Eq. 18})$$

for $\chi > 45^\circ$, and

$$B(2\theta, \chi) = B(2\theta, 0^\circ) + \frac{\chi}{45} [B(2\theta, 90^\circ) - B(2\theta, 0^\circ)] \quad (\text{Eq. 19})$$

for $\chi < 45^\circ$. LP and streak corrections were also made in the data processing program.

3. Structure determination

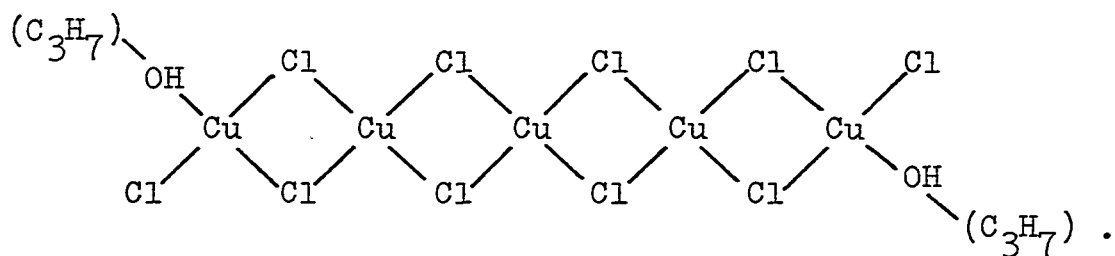
The first problem encountered was to determine the actual composition of this compound. Comparison of the density of these crystals with the density of anhydrous cupric chloride, which is 3.47 g/cc (5), and the chemical analysis indicated that the compound was probably not free of solvent, in contrast to what was reported by Lloyd et al. The above authors did not report the results of any chemical analysis, and probably assumed that the compound was solvent free largely on the strength of the reddish-orange coloration, which is in sharp contrast to the bluish-green coloration of the dialcoholates. Density considerations indicated that the empirical formulas of $\text{CuCl}_2 \cdot \text{C}_3\text{H}_7\text{OH}$ and

$\text{Cu}_5\text{Cl}_{10}(\text{C}_3\text{H}_7\text{OH})_2$ were also possible. Although the first of these two formulas seemed more likely in light of the compound $\text{CuCl}_2 \cdot \text{CH}_3\text{CN}$, the chemical analysis and molecular volume calculations indicated that the formula $\text{Cu}_5\text{Cl}_{10}(\text{C}_3\text{H}_7\text{OH})_2$ was the correct formula.

Table 19. Chemical analysis

Compound	%Cu	%Cl	Density	Unit cell volume
CuCl_2	47.3%	52.7%	2.39 g/cc	785\AA^3
$\text{Cu}_5\text{Cl}_{10}(\text{C}_3\text{H}_7\text{OH})_2$	40.1%	45.3%	2.35 g/cc	1150\AA^3
$\text{CuCl}_2 \cdot \text{C}_3\text{H}_7\text{OH}$	32.8%	36.4%	2.32 g/cc	1520\AA^3
Observed	40.5%	43.1%	2.34 g/cc	1120\AA^3

It seemed reasonable to assume that the molecular structure of the compound would be a planar chain of the type



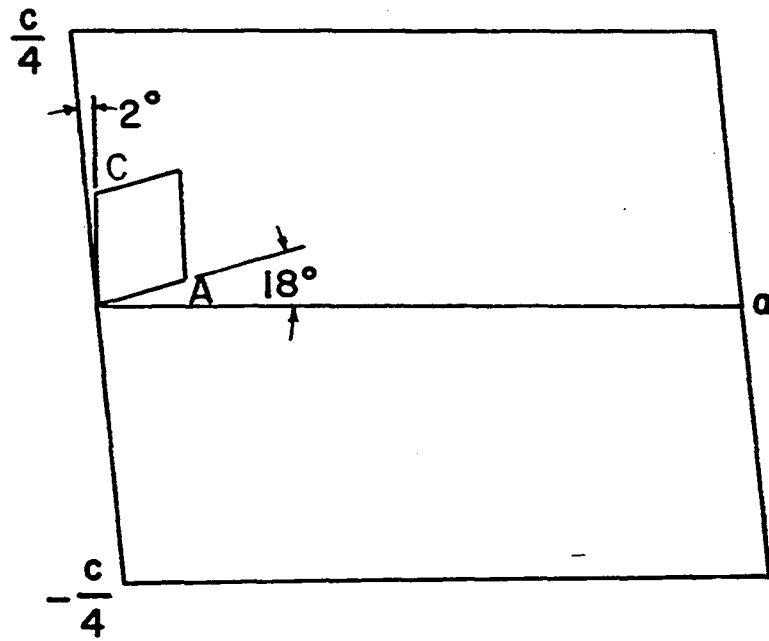
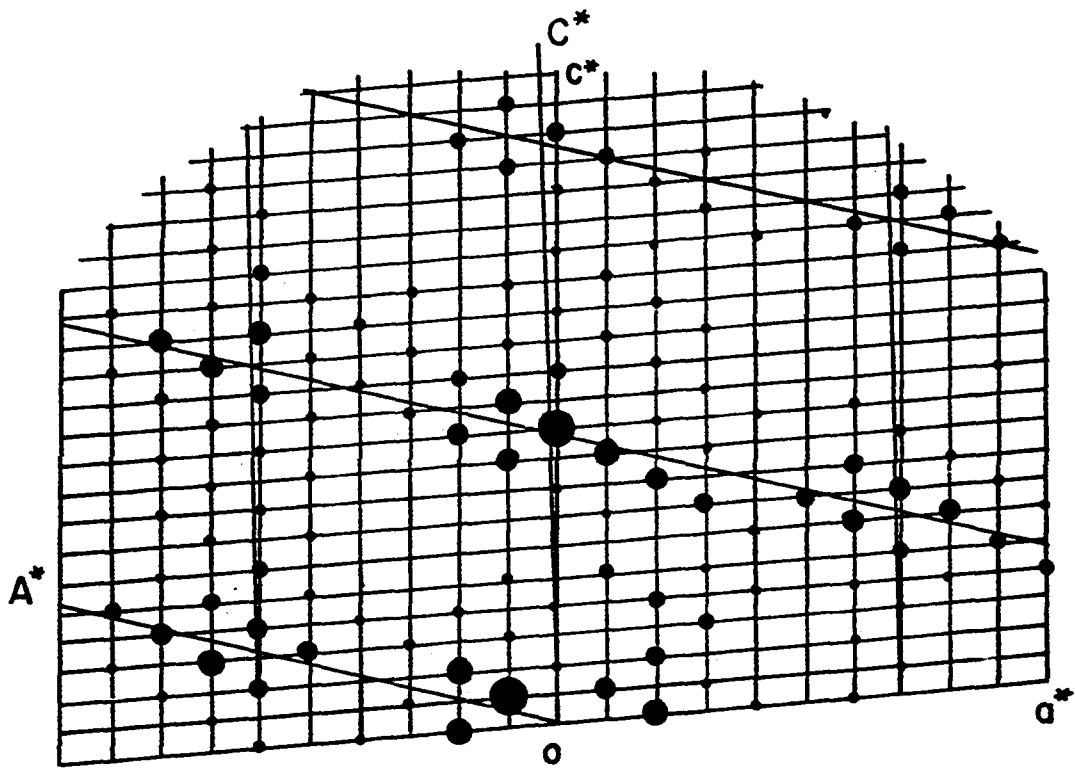
The same basic technique was used to attack the structural

problem as was used in solving the structure of $\text{Cu}_3\text{Cl}_6(\text{CH}_3\text{CN})_2$. A weighted reciprocal lattice was prepared of the reflections in the [010] zone and it was observed that the strong reflections again fell at or near the lattice points of a super lattice. This super lattice was transformed back into real space to obtain the corresponding sub cell.

With ten copper atoms in the unit cell, it was necessary to place two copper atoms in special positions and the centrosymmetrical special positions $(0, 0, 0)$ and $(\frac{1}{2}, \frac{1}{2}, \frac{1}{2})$ were chosen. It was again assumed that the sides of the sub cell corresponded to Cu-Cl bonds in the proposed structure. The same arguments as set forth in discussing the structural determination of $\text{Cu}_3\text{Cl}_6(\text{CH}_3\text{CN})_2$ were used to determine that the signs of the structure factors of the strong reflections lying at or near the lattice points of the super lattice must have positive signs.

A Fourier projection onto (010) was computed on an IBM 650 using 30 of the stronger reflections in this zone. All of the copper and chlorine atoms were resolved in this projection. The atomic coordinates of these atoms were used to compute structure factors for all reflections in this zone. A second Fourier projection onto (010) was computed using the results of this structure factor calculation. From this projection the atomic coordinates for the oxygen atom were

Figure 28. Weighted reciprocal lattice, super lattice,
and sub cell for the [010] zone of
 $\text{Cu}_5\text{Cl}_{10}(\text{C}_3\text{H}_7\text{OH})_2$



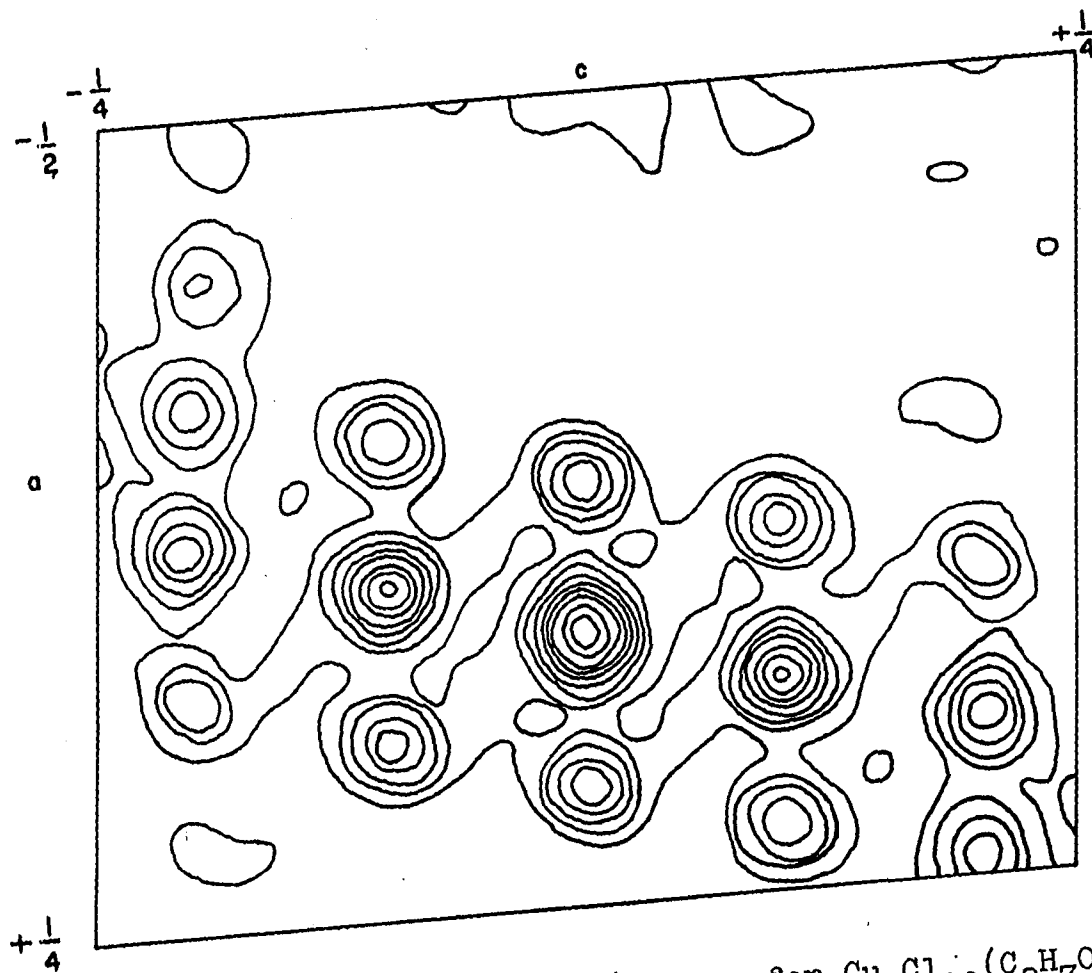


Figure 29. Fourier projection onto the (010) plane for $\text{Cu}_5\text{Cl}_{10}(\text{C}_3\text{H}_7\text{OH})_2$. The computations were made with only the 30 strongest reflections included.

obtained along with more accurate coordinates for the copper and chlorine atoms.

Patterson projections onto (010) and (100) were computed on an IBM 650 using the TDF-2 program. The Patterson peaks at $(U, W) = (5.5/40, 0/80), (6/40, 8/80), (9/40, 16/80), (3/40, 8/80),$ and $(1.5/40, 16/80)$ were interpreted as a superposition of many Cu-Cl vectors and the peaks at $(U, W) = (2/40, 8/80)$ and $(4.5/40, 20.4/80)$ were interpreted as superposition of many Cu-Cu and Cl-Cl vectors. In the Patterson projection onto (100), the peaks at $(V, W) = (12/40, 0/80), (7/40, 8/80), (16/40, 16/80), (1/40, 24/80), (13/40, 40/80)$ and $(7/40, 32/80)$ were interpreted as superpositions of many Cu-Cl vectors and the peaks at $(V, W) = (20/40, 8/80), (5/40, 16/80), (14/40, 24/80)$ and $(20/40, 32/80)$ were interpreted as a superposition of many Cu-Cu and Cl-Cl vectors.

These assignments substantiated the x- and z-parameters obtained from the weighted reciprocal lattice approach and allowed the assignment y-parameters for the copper, chlorine and oxygen atoms. It was noted that the length of the b-axis was almost identical to the length of the b-axis in $\text{Cu}_3\text{Cl}_6(\text{CH}_3\text{CN})_2$. It was assumed that the stacking of the molecules along the b-axis was the same as in $\text{Cu}_3\text{Cl}_6(\text{CH}_3\text{CN})_2$ and this helped in assigning the y-parameters.

It is interesting to note the similarity between the

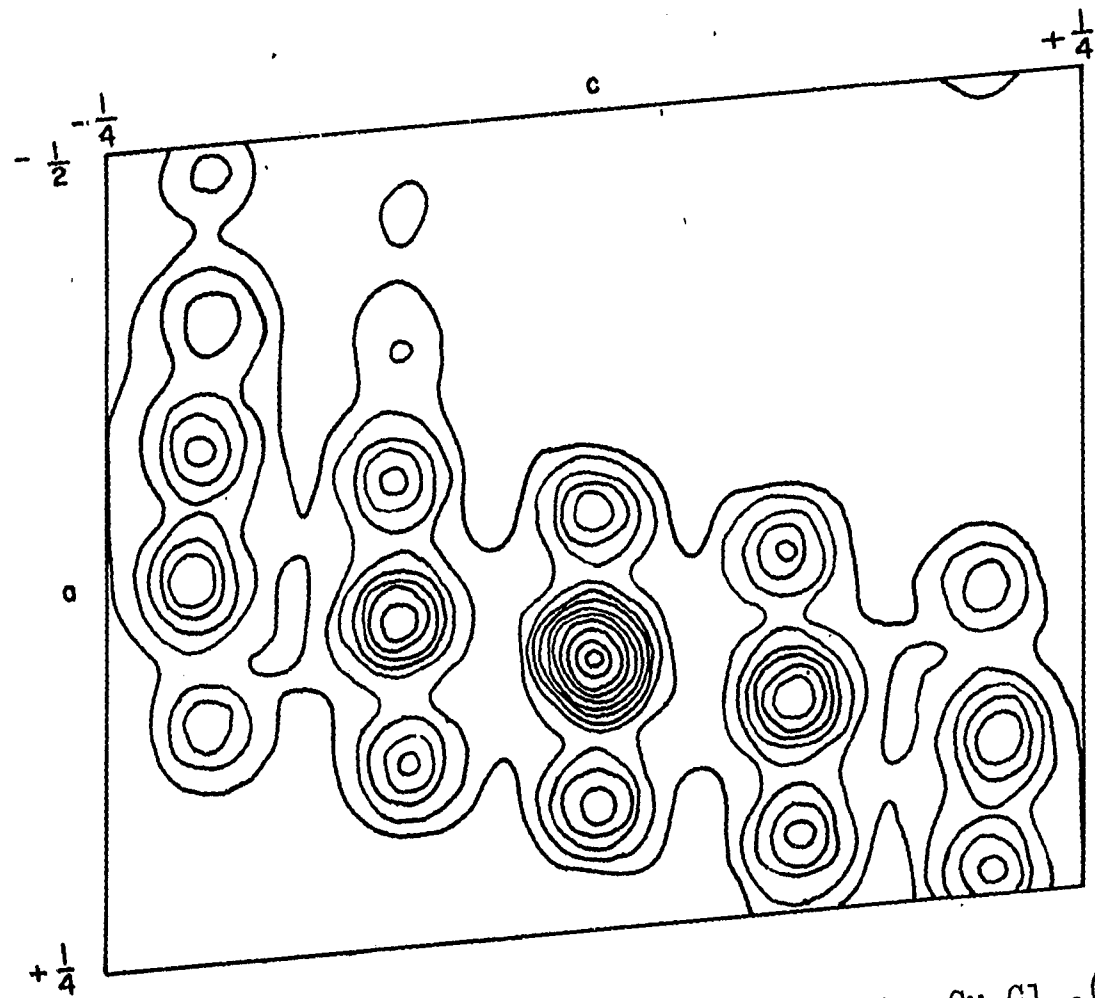


Figure 30. Patterson projection onto the (010) plane for $\text{Cu}_5\text{Cl}_{10}(\text{C}_3\text{H}_7\text{OH})_2$

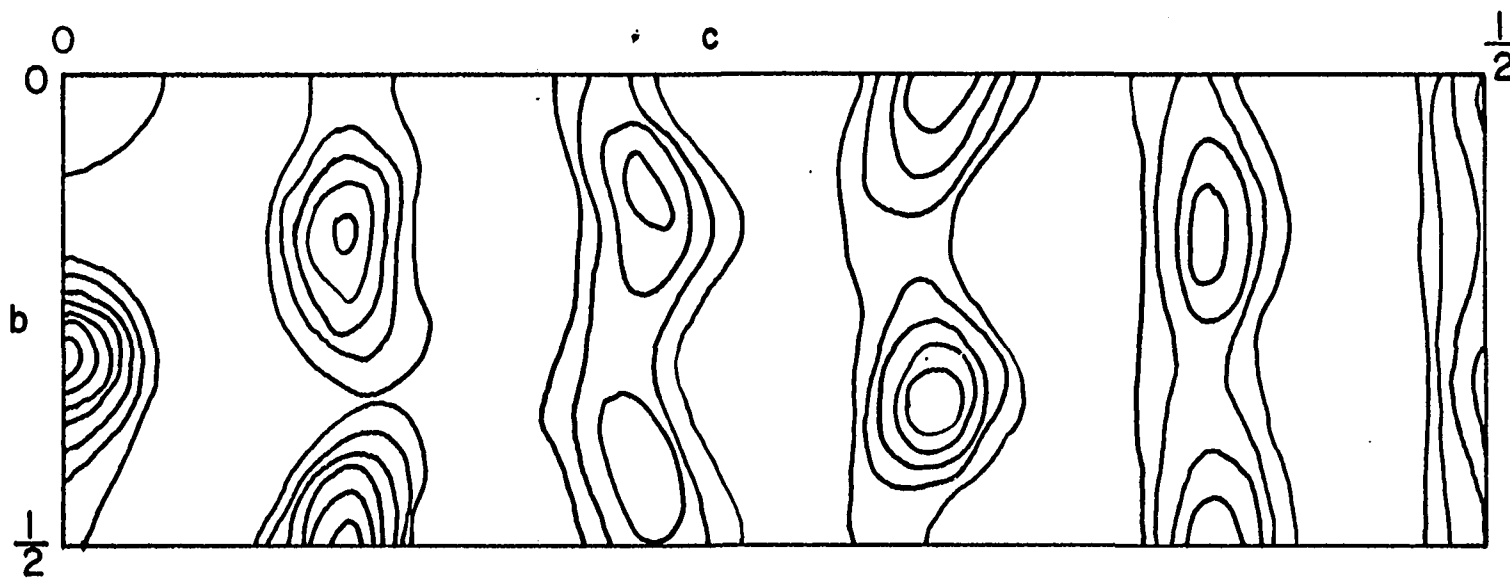


Figure 31. Patterson projection onto the (100) plane for $\text{Cu}_5\text{Cl}_{10}(\text{C}_3\text{H}_7\text{OH})_2$
 The origin peak has not been drawn in.

Patterson projection onto (010) and the Fourier projection onto (010) computed using only the strong reflections. This is to be expected since the strong reflections dominate the Patterson function where their contribution goes as F^2 , while in the Fourier function these strong reflections all enter with positive structure factors.

Attempts to locate the carbon atoms using only the $\{h0l\}$ and $\{0kl\}$ intensity data were largely unsuccessful. Approximate x- and z-parameters were obtained from successive Fourier projections onto (010), but even so the atoms were not clearly defined. It proved to be impossible to achieve even this much refinement with the Fourier projection onto (100), since there was overlap among atoms in this projection due to the long a-axis. It was decided to go directly to three-dimensional data and attempt to locate the carbon atoms through the use of the three-dimensional Fourier technique.

4. Refinement

The least squares refinement of the structure was carried out on the MURA IBM 704 using Busing and Levy's least squares refinement program and the three-dimensional \overline{F} ouriers and difference \overline{F} ouriers were computed on the same computer using Sly and Shoemaker's MIFR1 Fourier program. For the least squares refinement, $\sigma(F)$ was obtained from

$\sigma(I)$ by the finite difference method as discussed in the section on weighting schemes, and a reflection was called unobserved if the observed structure factor was less than $\sigma(F)$. In the computation of $\sigma(I)$, both $\%G$ and $\%B$ were chosen equal to .10. That is, it was felt that the reliability of both the intensity measurements and the background computations were accurate to within ten per cent.

The positions of the copper, chlorine, and oxygen atoms were refined using the complete three-dimensional intensity data. A three-dimensional difference Fourier was computed from the final structure factors obtained in the least squares process. Three positive peaks were observed in this difference Fourier which corresponded to a reasonable configuration of the propyl alcohol group. No other such peaks were observed on the difference Fourier.

Attempts to refine the positional parameters and temperature factors of the carbon atoms using the complete three-dimensional data all ended in failure. The positional parameters did not converge on any specific locations and one or more of the temperatures always increased beyond a reasonable value. Three-dimensional difference Fouriers gave no conclusive indication of any parameter shifts which would improve the structure.

At this point, a re-examination of the three-dimensional data was made. This revealed that the total count for the

Table 20. Final parameters, temperature factors, standard deviations, and R factors for $\text{Cu}_5\text{Cl}_{10}(\text{C}_3\text{H}_7\text{OH})_2^a$

Atom	x	y	z	B_{11}	B_{22}	B_{33}	B_{12}	B_{13}	B_{23}
Cu_1	.0 (0)	.0 (0)	.0 (0)	.00572 (00059)	.0140 (0040)	.00181 (00016)	-.0016 (0013)	.00062 (00021)	-.0003 (0006)
Cu_2	.05721 (00039)	.4333 (0011)	.10711 (00020)	.00761 (00047)	.0164 (0030)	.00157 (00011)	-.0002 (0011)	-.00005 (00016)	-.0009 (0005)
Cu_3	.10731 (00034)	.8892 (0011)	.20455 (00019)	.00441 (00038)	.0141 (0027)	.00173 (00011)	-.0005 (0010)	.00066 (00014)	-.0011 (0005)
Cl_1	.13291 (00078)	.2951 (0022)	.00364 (00039)	.00732 (00088)	.0192 (0066)	.00183 (00023)	.0006 (0021)	.00078 (00032)	-.0018 (0010)
Cl_2	-.09236 (00077)	.1540 (0022)	.09827 (00039)	.00793 (00088)	.0106 (0046)	.00179 (00023)	-.0078 (0022)	.00028 (00032)	-.0012 (0009)
Cl_3	-.03805 (00075)	.5997 (0025)	.20101 (00042)	.00569 (00083)	.0272 (0070)	.00234 (00024)	.0003 (0021)	.00144 (00032)	-.0021 (0011)
Cl_4	.18884 (00075)	.7443 (0021)	.10309 (00038)	.00624 (00088)	.0133 (0051)	.00175 (00023)	-.0062 (0020)	-.00015 (00031)	-.0009 (0009)
Cl_5	.22789 (00083)	.2053 (0023)	.19354 (00043)	.00768 (00084)	.0170 (0059)	.00218 (00023)	.0004 (0022)	-.00224 (00031)	-.0009 (0010)

^aStandard deviations are given in the parentheses.

Table 20. (Continued)

Atom	x	y	z	B ₁₁	B ₂₂	B ₃₃	B ₁₂	B ₁₃	B ₂₃
O ^b	.4340 (0020)	.5432 (0057)	.2181 (0011)	.00678	.0194	.00210	.0	.00030	.0
C ₁ ^b	.5837 (0052)	.4989 (0121)	.1831 (0029)	.01851	.0530	.00574	.0	.00082	.0
C ₂ ^b	.5821 (0059)	.5819 (0171)	.1068 (0034)	.02319	.0664	.00719	.0	.00103	.0
C ₃ ^b	.5631 (0053)	.8452 (0167)	.0936 (0030)	.02046	.0586	.00635	.0	.00091	.0

R₁ = 0.156 for all reflections

R₁ = 0.149 for observed reflections only

R₃ = 0.140

^bAnisotropic thermal parameters were not varied.

Table 21. Interatomic distances and bond angles for
 $\text{Cu}_5\text{Cl}_{10}(\text{C}_3\text{H}_7\text{OH})_2^a$

Bond	Distance	Bond	Distance
$\text{Cu}_1\text{-Cl}_1$	$2.235 \pm .011\text{A}$	O-C_1	$1.36 \pm .06\text{A}$
$\text{Cu}_1\text{-Cl}_2$	$2.291 \pm .008\text{A}$	$\text{C}_1\text{-C}_2$	$1.48 \pm .08\text{A}$
$\text{Cu}_2\text{-Cl}_1$	$2.260 \pm .009\text{A}$	$\text{C}_2\text{-C}_3$	$1.62 \pm .09\text{A}$
$\text{Cu}_2\text{-Cl}_2$	$2.268 \pm .012\text{A}$	$\text{Cu}_1\text{-Cu}_2$	$3.294 \pm .006\text{A}$
$\text{Cu}_2\text{-Cl}_3$	$2.273 \pm .010\text{A}$	$\text{Cu}_2\text{-Cu}_3$	$3.298 \pm .006\text{A}$
$\text{Cu}_2\text{-Cl}_4$	$2.311 \pm .013\text{A}$	$\overset{\circ}{\text{Cu}}_1\text{-Cl}_4$	$3.009 \pm .009\text{A}$
$\text{Cu}_3\text{-Cl}_3$	$2.287 \pm .014\text{A}$	$\overset{\circ}{\text{Cu}}_2\text{-Cl}_1$	$3.148 \pm .011\text{A}$
$\text{Cu}_3\text{-Cl}_4$	$2.268 \pm .009\text{A}$	$\overset{\circ}{\text{Cu}}_2\text{-Cl}_5$	$2.641 \pm .010\text{A}$
$\text{Cu}_3\text{-Cl}_5$	$2.286 \pm .010\text{A}$	$\overset{\circ}{\text{Cu}}_3\text{-Cl}_2$	$3.136 \pm .011\text{A}$
$\text{Cu}_3\text{-O}$	$1.933 \pm .024\text{A}$	$\overset{\circ}{\text{Cu}}_3\text{-Cl}_5$	$2.650 \pm .010\text{A}$
<u>Angle</u>	<u>Value</u>	<u>Angle</u>	<u>Value</u>
$\text{Cu}_1\text{-Cl}_1\text{-Cu}_2$	$94.3 \pm .3^\circ$	$\text{Cl}_3\text{-Cu}_2\text{-Cl}_4$	$87.0 \pm .4^\circ$
$\text{Cu}_1\text{-Cl}_2\text{-Cu}_2$	$92.5 \pm .3^\circ$	$\text{Cl}_3\text{-Cu}_3\text{-Cl}_4$	$87.7 \pm .4^\circ$
$\text{Cl}_1\text{-Cu}_1\text{-Cl}_2$	$86.4 \pm .3^\circ$	$\text{Cl}_3\text{-Cu}_3\text{-O}$	$94.3 \pm .9^\circ$
$\text{Cl}_1\text{-Cu}_2\text{-Cl}_2$	$86.4 \pm .4^\circ$	$\text{Cl}_4\text{-Cu}_3\text{-Cl}_5$	$90.9 \pm .4^\circ$
$\text{Cu}_2\text{-Cl}_3\text{-Cl}_3$	$92.6 \pm .3^\circ$	$\text{Cl}_5\text{-Cu}_3\text{-O}$	$85.8 \pm .9^\circ$

^aAn atom displaced one unit cell in the y-direction is denoted by ' and an atom located in an adjacent chain is denoted by " .

Table 21. (Continued)

Angle	Value	Angle	Value
$\text{Cu}_2\text{-Cl}_4\text{-Cu}_3$	$92.1 \pm .3^\circ$	$\text{Cu}_3\text{-O-C}_1$	$131.8 \pm 3.8^\circ$
$\text{Cl}_1\text{-Cu}_2\text{-Cl}_4$	$92.1 \pm .4^\circ$	$\text{O-C}_1\text{-C}_2$	$115.5 \pm 5.1^\circ$
$\text{Cl}_2\text{-Cu}_2\text{-Cl}_3$	$93.4 \pm .4^\circ$	$\text{C}_1\text{-C}_2\text{-C}_3$	$117.7 \pm 6.5^\circ$
$\text{Cl}_1\text{-Cu}_1\text{-Cl}_4$	$92.1 \pm .3^\circ$	$\text{Cu}_2\text{-Cl}_1$	$93.3 \pm .3^\circ$
$\text{Cl}_2\text{-Cu}_1\text{-Cl}_4$	$89.8 \pm .3^\circ$	$\text{Cu}_2\text{-Cl}_1\text{-Cu}_2$	$96.6 \pm .4^\circ$
$\text{Cl}_1\text{-Cu}_1\text{-Cl}_4$	$87.9 \pm .3^\circ$	$\text{Cl}_2\text{-Cu}_3\text{-Cl}_3$	$89.3 \pm .4^\circ$
$\text{Cl}_2\text{-Cu}_1\text{-Cl}_4$	$90.2 \pm .3^\circ$	$\text{Cl}_2\text{-Cu}_3\text{-Cl}_4$	$87.1 \pm .3^\circ$
$\text{Cu}_1\text{-Cl}_4\text{-Cu}_3$	$93.4 \pm .4^\circ$	$\text{Cl}_2\text{-Cu}_3\text{-O}$	$85.1 \pm .8^\circ$
$\text{Cu}_1\text{-Cl}_4\text{-Cu}_2$	$95.4 \pm .3^\circ$	$\text{Cl}_2\text{-Cu}_3\text{-Cl}_5$	$81.1 \pm .4^\circ$
$\text{Cl}_1\text{-Cu}_2\text{-Cl}_5$	$93.3 \pm .4^\circ$	$\text{Cu}_3\text{-Cl}_2\text{-Cu}_1$	$89.7 \pm .3^\circ$
$\text{Cl}_2\text{-Cu}_2\text{-Cl}_5$	$93.4 \pm .4^\circ$	$\text{Cu}_3\text{-Cl}_2\text{-Cu}_2$	$86.4 \pm .3^\circ$
$\text{Cl}_3\text{-Cu}_2\text{-Cl}_5$	$94.4 \pm .4^\circ$	$\text{Cl}_5\text{-Cu}_3\text{-Cl}_3$	$94.0 \pm .4^\circ$
$\text{Cl}_4\text{-Cu}_2\text{-Cl}_5$	$95.1 \pm .4^\circ$	$\text{Cl}_5\text{-Cu}_3\text{-Cl}_4$	$99.4 \pm .4^\circ$
$\text{Cu}_2\text{-Cl}_5\text{-Cu}_3$	$99.0 \pm .3^\circ$	$\text{Cl}_5\text{-Cu}_3\text{-Cl}_5$	$88.3 \pm .7^\circ$
$\text{Cl}_1\text{-Cu}_2\text{-Cl}_1$	$83.4 \pm .4^\circ$	$\text{Cl}_5\text{-Cu}_3\text{-O}$	$95.7 \pm .2^\circ$
$\text{Cl}_1\text{-Cu}_2\text{-Cl}_2$	$88.2 \pm .4^\circ$	$\text{Cu}_3\text{-Cl}_5\text{-O}$	$100.8 \pm .5^\circ$
$\text{Cl}_1\text{-Cu}_2\text{-Cl}_3$	$88.8 \pm .4^\circ$	$\text{Cu}_3\text{-Cl}_5\text{-Cu}_3$	$127.0 \pm .4^\circ$
$\text{Cl}_1\text{-Cu}_2\text{-Cl}_4$	$83.3 \pm .4^\circ$	$\text{Cu}_3\text{-Cl}_5\text{-Cl}_4$	$139.7 \pm .5^\circ$

Table 22. Least squares plane^a for $\text{Cu}_5\text{Cl}_{10}(\text{C}_3\text{H}_7\text{OH})_2$

A	B	C	$\Sigma d_i /n$	Σd_i^2	$\sqrt{\Sigma d_i^2/n}$
-.09836	.07641	-.09448	.07587	.15257	.09473
<u>Distance from plane</u> $\overset{\circ}{}$			<u>Distance from plane</u> $\overset{\circ}{}$		
Cu_1	.0000A		Cl_3	-.0181A	
Cu_2	-.1692A		Cl_4	-.0524A	
Cu_3	-.1292A		Cl_5	.1442A	
Cl_1	-.0154A		O	.0641A	
Cl_2	.0522A		C_1^b	-.3583A	

^aThe molecule was fit to the plane $Ax + By + Cz = 0$.

^bThe carbon atom was omitted from the least squares plane computation.

0.1.5 reflection had been erroneously recorded. Also, comparison of the observed structure factors with available film data revealed that many reflections which were unobserved on the films had large observed structure factors, and vice versa. This was evidently due to the method used in computation of the background counts for each reflection and thus could not be remedied without retaking the entire three-dimensional intensity data. Refinement was attempted using only those data for which film data were available and

reflections for which there was disagreement between the film and counter data were given zero weight during the refinement. Isotropic refinement of these 890 reflections then gave $R_1 = .175$ for all reflections and $R_1 = .163$ for observed reflections only. The temperature factors for the carbon atoms settled down at a value of approximately 8.0 for all three atoms, and the positional parameters of the carbon atoms gave reasonable bond lengths. At this point it was decided to refine the heavier copper and chlorine atoms anisotropically. Three cycles of refinement gave a final value of $R_1 = .156$ for all reflections and $R_1 = .149$ for observed reflections only. The final parameters are listed in Table 20 and the bond lengths and bond angles are listed in Table 21.

5. Discussion

This compound contains discrete $\text{Cu}_5\text{Cl}_{10}(\text{C}_3\text{H}_7\text{OH})_2$ units, with all the copper, chlorine and oxygen atoms in the molecule lying essentially in a plane. Each copper atom is bonded to four ligands in a square-planar configuration. The n-propyl alcohol groups are bonded to the terminal copper atoms through the oxygen and are located trans across the molecule. The molecule is illustrated in Figure 34.

Each pentamer is located at a center of symmetry in the crystal and has approximate C_{2h} symmetry. The central

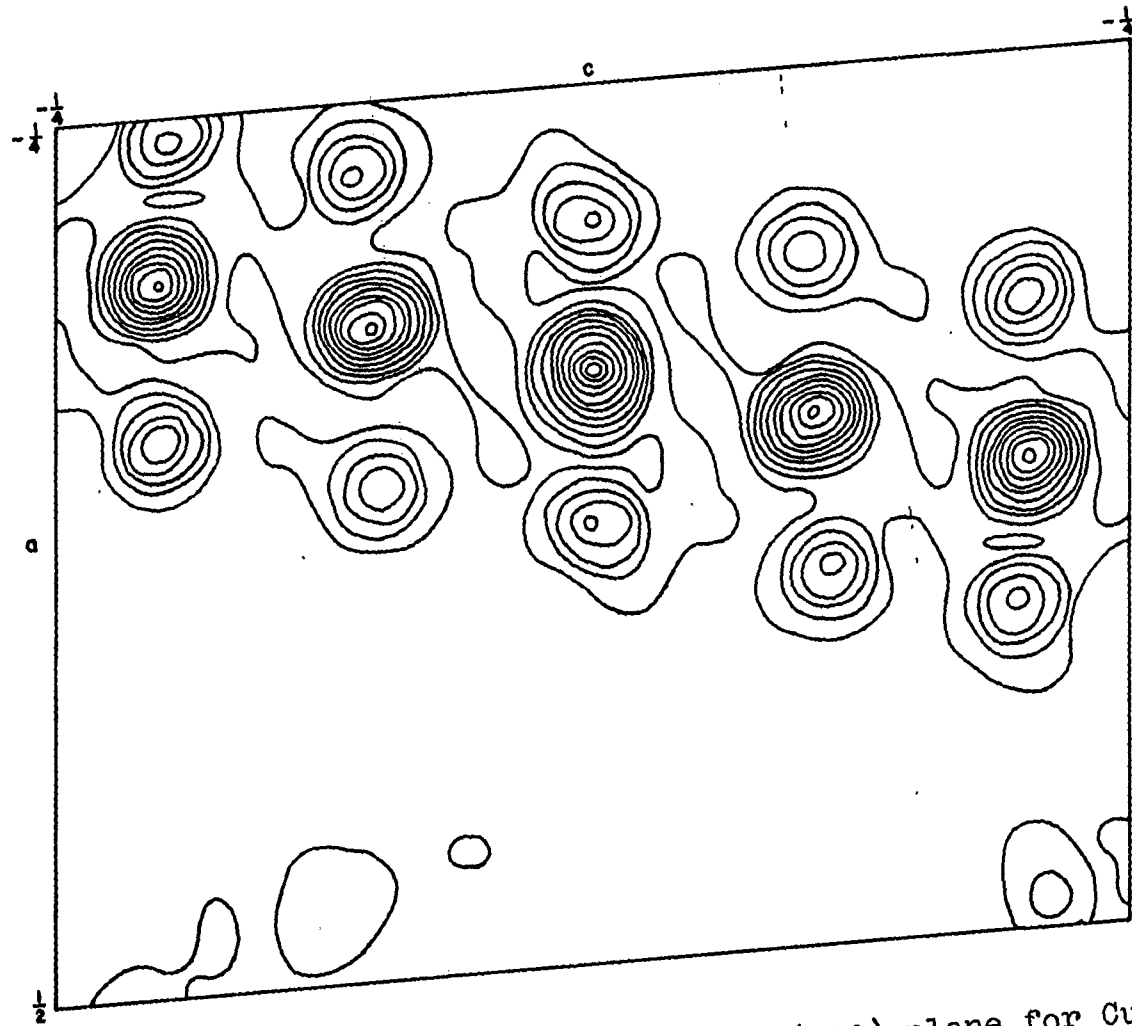


Figure 32. Final Fourier projection onto the (010) plane for $\text{Cu}_5\text{Cl}_{10}(\text{C}_3\text{H}_7\text{OH})_2$

Figure 33. Comparison of observed and calculated structure factors for $\text{Cu}_5\text{Cl}_{10}(\text{C}_3\text{H}_7\text{OH})_2$

The reflections are grouped together into sections of constant h and l (or h and k). The first column is the running index k (or l); the second column is $10|F_o|$; the third column is $10F_c$. An asterisk following the running index denotes a reflection which was not included in the least squares refinement. The value of $10|F_o|$ for the 0,1,5 reflection should be 108.0

0. K. 0	0. K.10	-1 142 134	11* 18 10	2 26 -27	10 30 -16	2 164 165	-10 33 -65	5 22 27	13 17 -3	0 37 -38
2 26 27	0*373 433	-1 492 473	-11 50 34	-2 26 -24	-10 38 -45	-2 44 49	11 36 42	-5 76 72	-13 127-137	1 18 10
4* 9 -22	1 24 24	-3 82 -84	-13 49 50	-3 104 100	-11 24 19	-3 105 103	-11 36 23	6 35 45	14 25 36	-1* 33 0
6* 9 -38	2 26 13	5 81 76	15* 7 38	4 260 253	12 114 112	4 46 37	-12 33 30	7 101-112	15 17 -21	-2 40 25
0. K. 1	3 15 -12	-5 70 67	-15 57 -45	-4* 34 21	-12 36 37	-4 39 -27	13 28 -34	-7 49 -55	-15 23 16	3* 30 15
4 18 -17	7 36 -34	17 56 55	5 117-115	13 47 -39	5 47 -43	-13 35 -13	8 58 58	16 44 40	-3 53 -10	-2 40 14
5* 0 -21	5* 0 -12	-7 12 -10	-17* 37 15	-5 122-129	-13* 28 -17	-5 38 -18	14 17 -17	-8* 8 19	-16 32 -25	4* 0 -44
1* 0 -21	9 292 311	15 25 25	6 36 -28	14 31 8	6 38 -33	-14 31 1	9 107 117	17 46 -43	-4 33 -14	-4 33 -14
2 25 27	7* 0 1	-9 147 159	-19* 22 -2	-6 185 191	-14* 23 -6	-6 45 62	15 21 4	-9 123 135	-17* 0 1	5 44 41
3* 0 -10	11 32 28	-7 12 28	7 25 36	15 36 35	7 34 29	16 13 24	10 133 140	18 65 67	-5 44 34	-5 44 34
4 92 82	0. K.11	-11 255 262	6. 0. L	-7 142-152	-15 24 15	-7 127 127	17* 10 12	-10 130 130	-18 24 28	6 41 31
5 18 24	13 52 -55	8 0 -23	16 46 -48	8 40 36	-16 107 107	-8 112 112	9. 1. L	-11 43 29	-19 26 21	7 26 18
6 21 -33	1 20 22	-13 68 -73	0 71 -80	-8 17 -26	-16 107 107	-8 112 112	9. 1. L	-11 43 29	-19 26 21	7 26 18
7 60 63	2 52 57	15 51 52	2 30 31	9* 0 -4	7 15 -3	9 32 9	0 110 117	12 22 -10	5. 2. L	8 19 11
0. K. 2	3 21 10	-15 27 36	-2 144 145	-9 48 51	-17 93 -89	-9 42 34	-1 58 -45	13 31 -25	0 36 37	-8 30 18
4 67 66	4 67 66	17 16 46	4 35 -38	10* 0 26	18 33 26	-10 54 -47	-1 59 -60	-13 61 -61	1 14 13	-9 31 9
5 26 25	5 26 25	-17 22 -5	-4 204 213	-10* 4 10	-18 34 23	-10 41 -33	2 32 -30	14 24 -6	1 14 13	-9 31 9
0 44 -50	6* 0 -12	19 108 115	6 192 193	11* 2 -7	19 18 15	11 62 60	-2 14 -0	-14 28 -18	-1 43 33	10 34 -34
1 20 15	7 27 26	-19 92 93	-6 90 -99	-11 37 -37	-19* 9 -10	-11 38 -10	3* 9 5	15* 10 -6	2 36 -38	-10 28 -10
2 26 26	0. K.12	2. 0. L	8 89 87	12 18 26	4. 1. L	-12 35 29	-3 22 20	-15 44 50	-2 51 45	11 20 21
3 29 -37	0 42 -48	0 261 224	-10 46 -62	-13 53 57	0* 3 -12	-13 28 12	-4 40 16	-16 16 4	-3 171 166	12* 7 15
4 112 104	1 32 -32	2 165-149	-12 114 109	14 122 124	1 27 25	14 26 11	5 17 -2	17 31 -37	4 31 29	13 16 5
5 43 43	2 29 -25	-2 227 189	12* 6 -6	-14 48 43	-1* 0 11	-14* 9 -13	-5 17 -15	-17 22 -23	-4 171-175	14 32 -27
7 50 -52	3 38 -38	4 76 75	14 19 15	15 45 -35	2 43 -42	15 22 -23	6 12 14	18 24 39	5 50 44	15 26 6
0. K. 3	4 77 78	-4 57 -45	-14 97 89	-15 70 -61	-2 14 6	-15 21 6	-6* 6 -1	-18 16 20	-5 62 56	16 39 32
1 70 81	5* 0 -1	6 54 -53	-16 94 88	16 41 -40	3 27* 276	16 26 -26	7 21 -3	19 65 63	6 133-131	17 25 18
2* 26 41	4 58 48	-6 19 15	-16 59 44	-16 64 57	3* 0 -4	-16 43 46	-19 50 53	-19 50 53	-6 133-131	18 19 -1
3 154 167	7 32 -34	-8 19 27	-18 41 37	-17 57 -57	-4 155 150	17* 0 15	8 26 13	7 134 143	7 134 143	8. 2. L
4 68 76	0. K.13	10 44 58	7. 0. L	18* 0 -5	-5 31 34	18 21 19	9 34 -28	0 286 272	-8 35 -26	0 22 -5
5* 0 -1	1 45 48	12 69 -88	1 31 44	-18 37 -17	-6 96 105	-18 52 42	-10 79 80	1 48 58	9 26 -14	1 25 16
6 58 61	2 24 -24	-12 73 71	1 60 -58	-19 39 41	-8 62 -61	-19 27 5	-10 75 86	-1 269 251	-9 26 30	-1 24 -14
7 17 14	3 73 74	14 62 62	-14 78 -19	2. 1. L	8 62 -61	7. 1. L	11 15 11	2 62 -60	-10 23 5	2 25 11
0. K. 4	4 43 41	-9 28 19	-3 249 263	-9 44 -33	-9 44 -33	7. 1. L	-11 50 -56	-2 97 -98	-10 51 52	-2 35 8
0 37 -25	6 60 43	-16* 5 6	5 112 104	0 62 61	10* 22 -4	0 61 58	-12 16 -7	-3 106 103	-11 60 52	-3 57 0
1 60 -59	7* 0 7	-18 14 16	-7 67 -52	2 88 -80	-12 20 12	-2 77 78	14 13 2	5* 0 14	13 18 28	5 32 7
2 20 24	0. K.14	3. 0. L	9 60 -62	-2 60 -55	-13 26 -9	-2 35 -12	-14 11 9	-6* 0 7	-13 99 96	-5 26 -5
3 190-198	1 32 -28	2 25 18	1 36 -21	11 26 18	-3 41 -25	-15 47 46	-3 37 37	-15 13 -14	-6 47 56	-14 101-105
4 26 21	3 69 -63	-1 54 -33	-11 34 -28	4 240-235	-16 37 29	4 38 -34	7 105 109	15 30 25	7 34 56	7 34 56
5 13 26	4* 7 -7	3 78 86	13 11 2	4 53 50	-17 108 107	-4 39 30	1. 2. L	-7* 0 3	-15 40 30	-7 34 56
6 36 41	5* 0 23	-3* 54 3	-13 167 176	5 30 14	18* 5 -21	5 38 -29	0 140 130	-8 17 -30	-16 56 -52	8 13 2
7 26 18	6 22 29	7* 0 12	-5* 9 -0	-15 46 36	6 39 38	6 25 17	1 109 96	9 165 164	17 60 57	9 14 -21
0. K. 5	0. K.15	7* 86 94	17 75 80	-6 251-252	-19 36 -25	-6 38 -20	-1 38 -13	-9 56 51	10 23 4	10 23 4
1* 0 130	0. K.15	9 28 -42	19 32 -27	-7 206 211	5. 1. L	7 72 71	-2 51 -53	-10 170 174	-16 19 -14	11* 4 16
2* 8 0	1 67 71	-9* 0 11	-19 40 29	8 18 -29	8 19 6	8 19 6	3 19 13	11 37 28	19 23 -17	11 25 -13
3 64 67	2 13 1	11 51 -53	8. 0. L	-8 70 -72	0 24 -30	-8 91 90	-3* 25 12	-11 160 158	-19 30 26	-12 22 11
4 39 -28	3 46 46	-11 62 68	0 13 15	10 18 11	2 165 169	10 68 56	5* 0 -17	13 25 -26	6. 2. L	-13 34 32
5 22 -32	4 31 -38	13 41 47	0 13 15	10 18 11	2 165 169	10 68 56	5* 0 -17	13 25 -26	6. 2. L	-13 34 32
6* 0 -7	5* 0 -12	-13 44 -43	2 40 -35	-2 40 35	-12 48 56	-12 48 37	6* 0 -6	14 18 6	1 40 -40	-15 36 6
7 26 -24	6* 0 -9	-15 27 17	4 33 18	11 17 2	3 228 231	11 36 32	6* 0 -6	14 18 6	1 40 -40	-15 36 6
0* 48 -7	0. K.16	-17* 8 3	-6 41 -9	12 54 -51	4 88 88	12 28 21	7 32 49	15 32 32	2 24 30	16 23 -1
1 69 66	0* 0 8	19 30 -34	8 43 -49	-12 36 -29	-4 25 -21	-12 29 -8	-7* 0 4	-15 27 -14	-2 36 -12	-16 34 -12
2* 0 7	4 33 41	-19 28 23	-10 58 25	13 152 161	5 15 9	13 18 13	8 26 -33	16 48 -49	3 28 33	9. 2. L
3 214 230	0* 0 8	19 30 -34	8 43 -49	-12 36 -29	-4 25 -21	-12 29 -8	-7* 0 4	-15 27 -14	-2 36 -12	-16 34 -12
4 33 41	1 38 30	-19 28 23	-10 58 25	13 152 161	5 15 9	13 18 13	8 26 -33	16 48 -49	3 28 33	9. 2. L
5* 0 -15	2 6 1	-10 32 8	-13 29 -16	-5 37 27	-13 23 23	-8 61 61	-16 41 38	-3 45 -40	9. 2. L	9. 2. L
6 29 29	3 113 120	12 23 24	14 56 -68	6 34 -31	14 24 -21	9 21 20	17 48 44	4 29 21	4 29 21	4 29 21
7 16 -17	4 25 28	4. 0. L	-12 34 17	-14 34 29	-6 108 109	-14 21 15	-9* 48 72	-17 19 7	-4 105 108	0 17 -6
0. K. 7	5* 0 -8	0 28 -33	14 26 23	15 27 -2	7 33 -30	15 25 -26	10 121 135	18 24 13	5 76 -75	1* 0 -10
1* 10 2	6* 0 8	2* 0 -18	-14 153 157	-15 74 76	-7 166 168	-15 17 -5	-10 34 29	-18* 7 -10	-5 69 -69	-1* 0 -3
2 15 -25	0. K.17	-4 22 -18	-16 28 -14	-16 114 -117	-8 147 149	-16 27 8	-11* 52 2	-19 31 32	-6* 38 6	-2 22 15
3 130 145	1 26 -30	6 74 80	-18 23 15	-17 20 -28	9* 26 5	17 29 29	12* 25 -3	7 27 9	3 25 21	3 25 21
4 53 -55	2 17 -16	-6* 4 -26	18* 21 -1	-18* 49 -32	-10 61 -57	-18 44 42	-13 40 -35	0 75 72	-8 35 29	-4 86 36
5* 0 15	3 63 59	8* 7 7	9. 0. L	19 19 17	11 32 -21	19 34 -24	-14 42 37	-1 211 213	-9 76 -21	-5 34 30
6 38 -40	4 14 -20	-8* 0 8	1 19 37	-19 24 -28	-11 33 -2	12 95 88	8. 1. L	-15 13 3	2* 0 -14	10 29 -11
7 10 16	5 18 14	10 49 -48	3 18 -4	-3 36 13	3. 1. L	-12 42 37	-15 19 23	-2 227 226	-10 30 13	-6 34 -47
0. K. 8	6* 0 -12	-10* 0 -6	-3 36 13	3. 1. L	-12 42 37	-15 19 23	-2 227 226	-10 30 13	-6 34 -47	-6 34 -47
0 38 40	0. K.18	-12 28 26	5 99 116	13 134 138	0 63 -63	16* 0 -20	3* 0 4	11 38 -36	7 41 -47	7 41 -47
1 41 -51	0 40 49	14* 10 -9	-5 112 122	-10 48 56	-13 33 -5	1 74 15	-16 11 -8	-3 226-225	-11 40 31	-7 29 0
2 16 30	1 26 -34	16 51 52	-7 24 -19	-1* 34 4	-14 28 -11	2 27 -3	-17* 10 1	-4 102 106	-12 28 19	-8 51 12
3 16 14	2 27 25	-16 14 3	9* 0 -4	2 169 151	15 21 -3	-2 32 14	18 21 3	5 28 -27	13 14 22	9* 0 -8
4 76 76	3* 9 4	18* 0 -8	-9 26 38	-2 50 51	-15 33 18	3 35 -39	-18 22 24	-5* 81 3	-13 59 -56	-9 19 -2
5* 0 -11	4 33 31	-18 13 9	11 33 37	3 152-147	16 16 -14	-3 35 -16	19 14 17	6 98 89	14 20 17	10 15 0
6* 7 17	5* 0 -12	-11 23 -C	-3 38 -31	-16 79 76	4 23 -14	-19 24 29	-6 25 -28	-14 55 55	-10* 1 4	-10* 1 4
7 44 50	6* 0 8	13* 0 1	4 232 232	-4 44 -46	-17 64 58	5 17 13	2. 2. L	-7* 0 -1	-15 36 -30	-11 16 -7
0. K. 9	0. K.19	1* 7 -7	15 51 52	5 79 90	18 18 12	-5 34 26	0 265 241	-8 28 34	-16 27 5	-12 17 15
1 16 -25	1* 0 -5	3* 0 7	17 31 -27	6 72 -75	19 15 5	-6 33 2	1 182 166	9 152 153	17 36 20	13 2* 27
2* 8 -3	2 15 17	-3 105 115	-17 16 -17	-6 210 222	-19 19 -9	7 23 5	-1 131 123	-9 32 25	-17 19 16	-13 31 40
3 19 -11	3 14 -3	5 18 7	7 13 -19	-7 167-170	8 36 38	6. 1. L	-7 35 -20	2 13 -25	10 40 31	18 26 -27
4 56 -57	4* 11 -21	-5 54 -44	-7 167-170	8 36 38	6. 1. L	-7 35 -20	2 13 -25	10 40 31	18 26 -27	14 46 -47
5* 0 4	5 13 -9	7 134 130	8 36 38	6. 1. L	8 36 38	6. 1. L				

copper atom (Cu_1) is bonded to four chlorine atoms (Cl_1 and Cl_2) at distances of 2.235Å and 2.291Å. The Cu_1 - Cl_1 bond length is considerably shorter than what would be expected for this type of bond. Four chlorine atoms (Cl_1 , Cl_2 , Cl_3 and Cl_4) bond to the second crystallographically independent copper atom at distances of 2.260Å, 2.268Å, 2.273Å and 2.311Å respectively while the third crystallographically independent copper atom is bonded to three chlorine atoms (Cl_3 , Cl_4 and Cl_5) and one oxygen atom at 2.287Å, 2.268Å, 2.287Å and 1.933Å. The bond lengths within the propyl alcohol group are 1.36Å for the C-O bond length and 1.49Å and 1.62Å for the two C-C bond lengths. Considering the large standard deviation of these bond lengths, they are in reasonable agreement with the bond lengths normally found. The Cu_3 -O-C₁ bond angle is 132° , with the carbon atom lying 0.36Å out of the plane of the molecule (see Table 22). It is of interest to compare this with $\text{CuCl}_2 \cdot 2\text{H}_2\text{O}$ where it has been found (65) that both hydrogen atoms of the water molecule lie in the plane with the Cu-O direction bisecting the H-O-H angle.

The molecules stack above each other along the b-axis in exactly the same manner as the molecules in $\text{Cu}_3\text{Cl}_6(\text{CH}_3\text{CN})_2$. Each pentamer is joined by eight long copper-chlorine bonds to the one directly above (or below) it along the b-axis. The Cu_1 - Cl_4 bond length is 3.009Å,

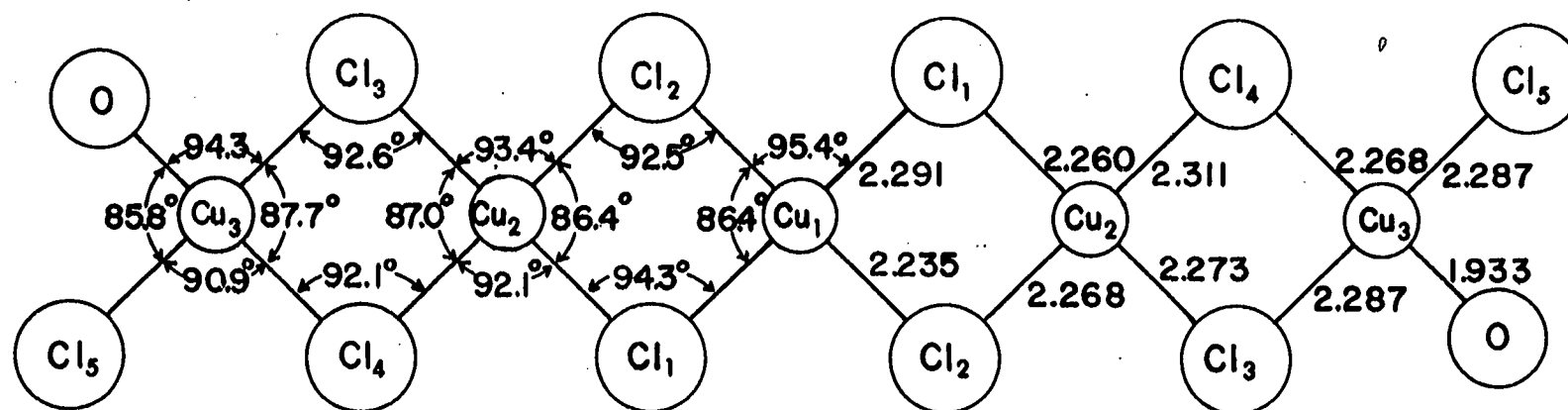


Figure 34. Illustration of the $\text{Cu}_5\text{Cl}_{10}(\text{C}_3\text{H}_7\text{OH})_2$ molecule

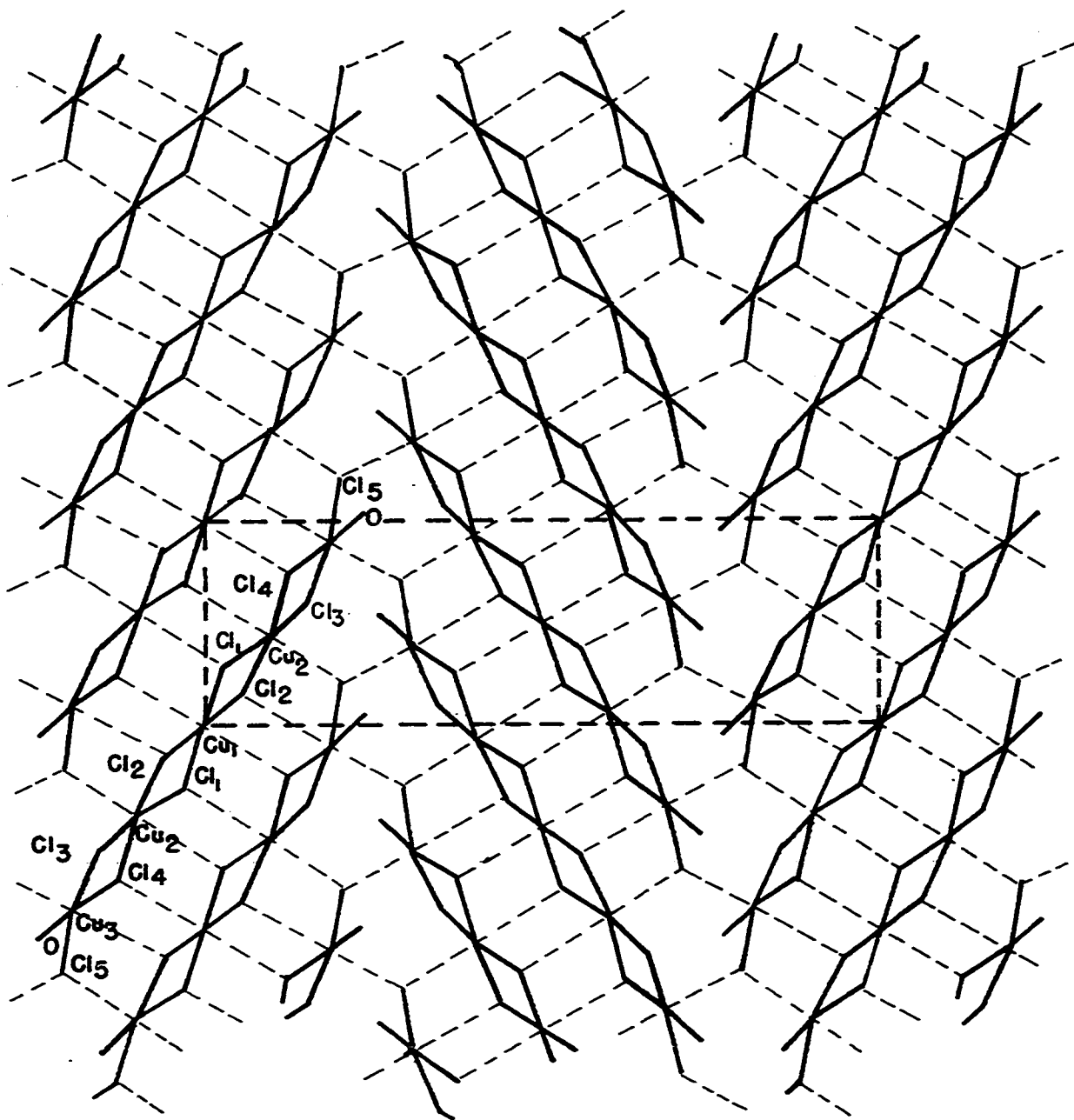


Figure 35. View of the structure of $\text{Cu}_5\text{Cl}_{10}(\text{C}_3\text{H}_7\text{OH})_2$ from a direction perpendicular to the $(10\bar{1})$ direction

the $\text{Cu}_2\text{-Cl}_1$ bond length is $3.148\overset{\circ}{\text{A}}$, the $\text{Cu}_3\text{-Cl}_2$ bond length is $3.136\overset{\circ}{\text{A}}$ and the $\text{Cu}_2\text{-Cl}_5$ bond length is $2.641\overset{\circ}{\text{A}}$. These chains of pentamers stacked along the b-axis are tied together into sheets lying in the $(10\bar{1})$ plane by $\text{Cu}_3\text{-Cl}_5$ bonds which are $2.650\overset{\circ}{\text{A}}$ long. This is illustrated in Figure 35.

III. MAGNETIC SUSCEPTIBILITY MEASUREMENTS

A. Introduction

The magnetic susceptibility measurements in the temperature range below 80°K were made with an apparatus consisting of essentially an Hartshorn mutual inductance bridge modified for use with a cryogenic system. The apparatus has been described elsewhere in detail (66, 67), so only a brief description will be given here.

The bridge portion of the apparatus consists of a 33 cycle source, primary and secondary inductance coils, high gain amplifier and oscilloscope. The coils are composed of two segments, with one set of primary and secondary coils located inside the cryostat, and another variable set located externally. The basic wiring diagram is given in Figure 36.

The cryostat system consists of an outer dewar for liquid nitrogen, an inner dewar for either liquid nitrogen or liquid helium, and a sample tube. The sample tube consists of a sample holder, thermocouple, and heater placed inside a Vycor tube. The sample tube is so constructed that it can be evacuated to isolate the sample from the low temperature bath. The primary and secondary coils are wound around this sample tube. The primary is of sufficient length to insure that the field at the sample is uniform.

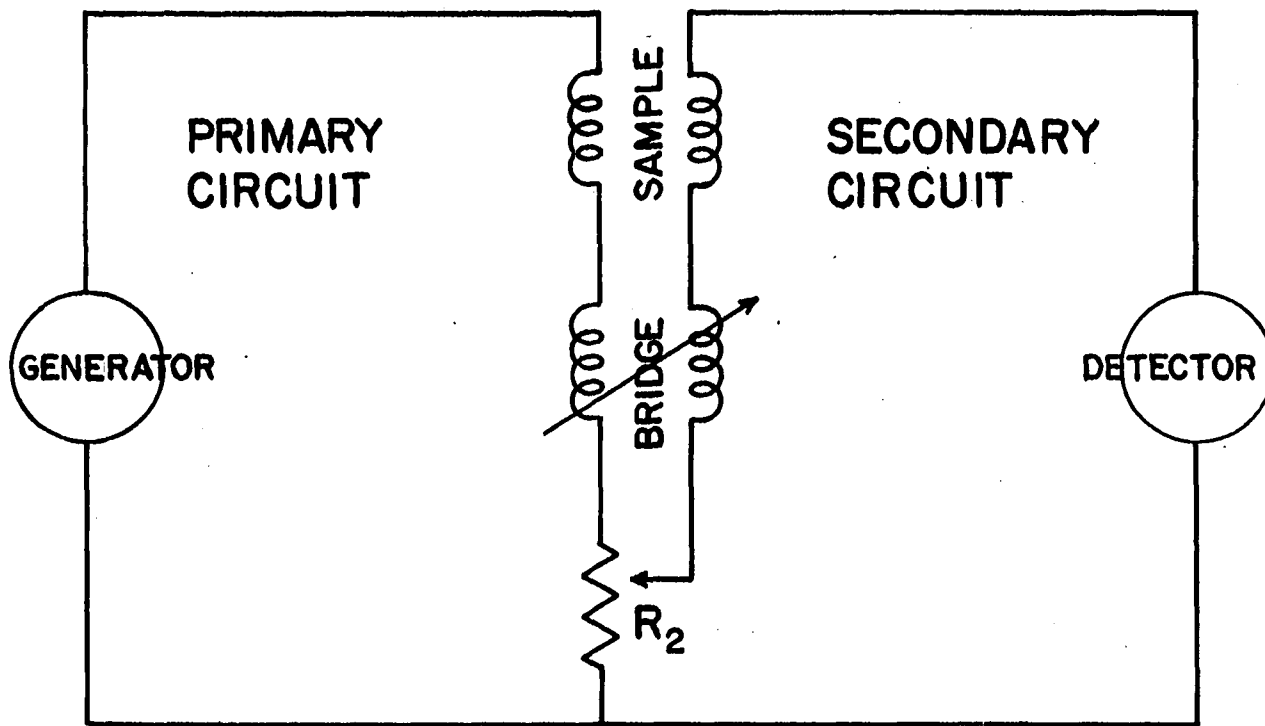


Figure 36. Wiring diagram for a Hartshorn type mutual inductance magnetic susceptibility apparatus

The secondary coil consists of three smaller coils, the outer two being wound antiparallel to the inner coil, giving a net mutual inductance of nearly zero between the primary and the secondary coils. The apparatus is so constructed that the sample tube can be raised, allowing the measurement of the mutual inductance with and without the presence of the sample inside the two coils. For temperatures from 4.2°K to room temperature, the temperature was measured with a gold-constantine thermocouple. For temperatures below 4.2°K, the temperature was measured by measuring the vapor pressure of the liquid helium. Temperatures down to about 1.4°K could be obtained by pumping on the liquid helium.

For the secondary portion of the bridge circuit illustrated in Figure 1,

$$i_p [j\omega(M_S + M_B) + \gamma_B r_B + \gamma_S r_S + R_2] + i_s [j\omega(L_S + L_B) + r_B + r_S + R_2] = 0 , \quad (\text{Eq. 20})$$

where the first term represents the voltage drop in the secondary circuit due to the primary current and the second term is the voltage drop due to the secondary current. In the above equation, i_p and i_s are the currents in the primary and second circuits respectively; j represents the square root of minus one (since the inductance is 90° out of phase

with the resistance); ω is the frequency of the alternating current, M and L are mutual and self inductances respectively, and γ_S and γ_B are geometrical constants defining the dependence of the secondary current on the primary current. The secondary circuit is brought into balance (as seen on the oscilloscope) by adjusting the variable inductance M_B and the variable resistance R_2 such that $M_S + M_B = 0$ and $\gamma_S R_S + \gamma_B R_B + R_2 = 0$. Under these conditions the current in the secondary circuit is zero.

The magnetic susceptibility is defined as $\chi = M/H$, where M is the magnetic moment of the sample and H is the applied field. If the magnetic moment is parallel to the field, it can be shown that

$$\Delta M = \beta \mu_0 n_s n_p \chi V = \gamma \chi V \quad (\text{Eq. 21})$$

where ΔM is the change in mutual inductance when the sample is removed from the sample coils, β is a geometrical constant depending on the shape of the coils, n_s and n_p and the number of turns on the secondary and primary coils respectively, and V is the volume of the sample. The susceptibility defined by this equation is a dimensionless quantity. While it would be possible to calculate the quantity γ , it is determined experimentally by calibration against a substance of known magnetic susceptibility. The molar susceptibility

χ_m , is related to χ by the relation $\chi_m = \chi V_m$, where V_m is the molar volume. Experimentally, ΔM and N , the number of moles of sample, are the measurable quantities. Since $V/N = V_m$,

$$\chi_m = \frac{\Delta M}{N\gamma} . \quad (\text{Eq. 22})$$

For the apparatus used, γ has been determined to be 4595.

For temperatures above 80°K, the standard Gouy method was used to measure the susceptibility. The apparatus was equipped with a dewar to enable the sample to be cooled to liquid nitrogen temperature. The temperature was measured by means of a previously calibrated thermocouple. The field strength of the electromagnet was obtained by measuring the frequency of the Li^7 nuclear magnetic resonance.

B. Magnetic Susceptibility of CuCl_2

The magnetic susceptibility of anhydrous cupric chloride was measured in the range 1.4°K to 290°K. The sample was prepared by reacting copper metal with chlorine gas in a hydrogen chloride atmosphere. The results of the measurements are shown in Figures 37 and 38.

At high temperatures, the susceptibility obeys the Curie-Weiss law with $\theta = 111^\circ\text{K}$ and $\mu_{\text{eff}} = 2.12$. This is in very good agreement with the results of Starr, Bitter, and

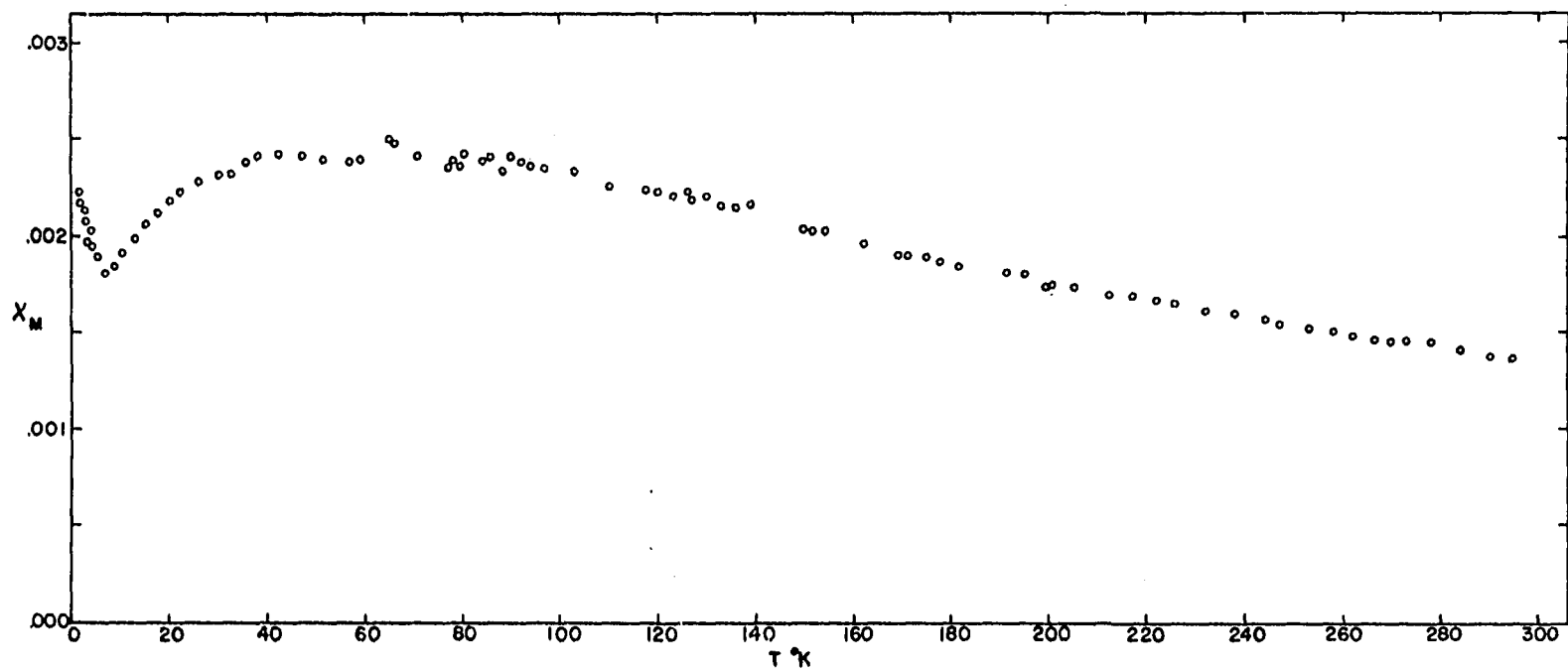


Figure 37. Plot of the molar magnetic susceptibility versus temperature for CuCl_2

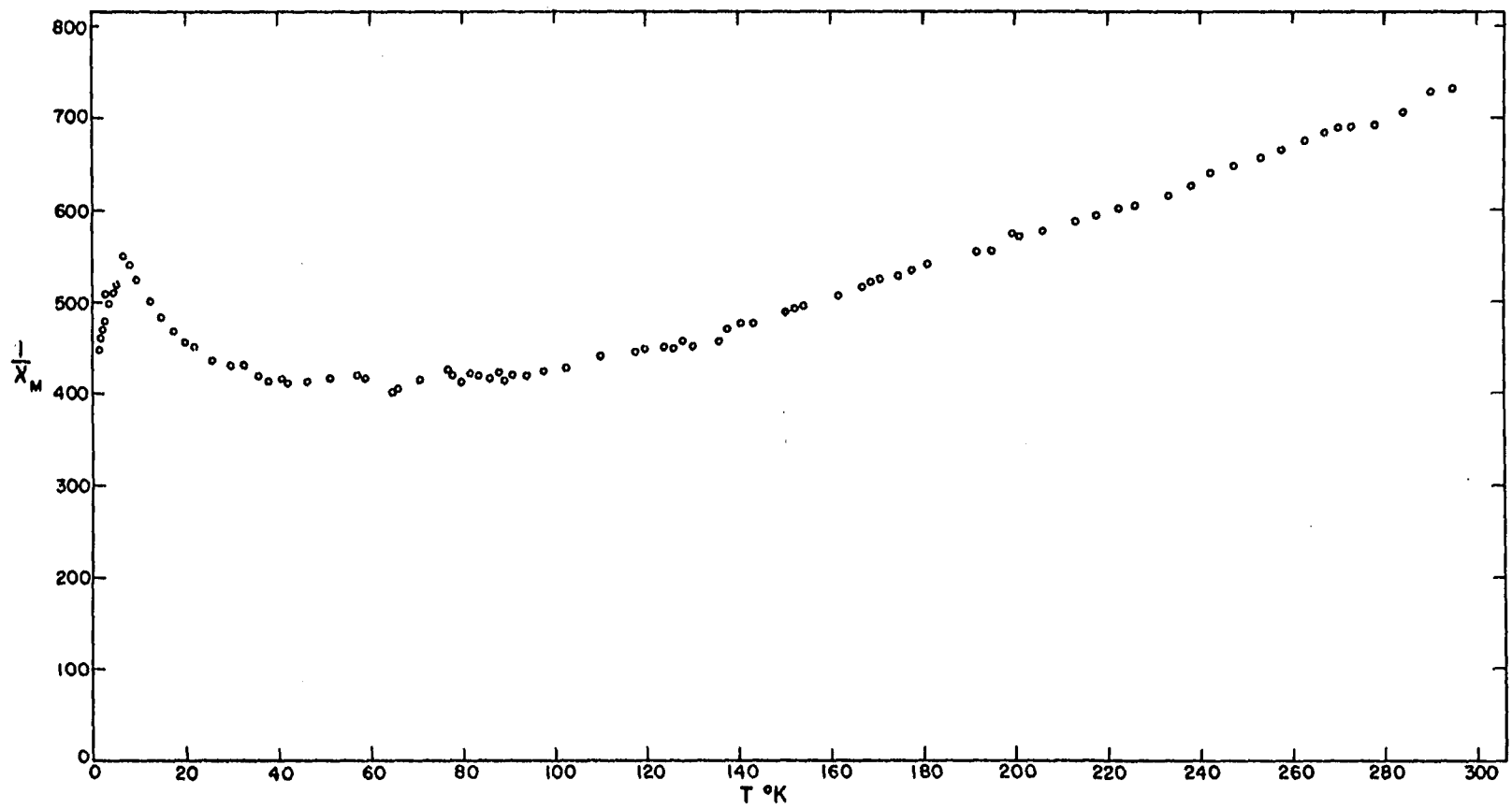


Figure 38. Plot of the reciprocal molar magnetic susceptibility versus temperature for CuCl_2

Kaufmann (25) who have reported values of $\theta = -109^{\circ}\text{K}$ and $\mu_{\text{eff}} = 2.08$. The maximum in the susceptibility occurs at approximately 65°K . This is also in very good agreement with previous work.

At low temperatures, the susceptibility deviates considerably from the normal behavior of an antiferromagnetic substance and the results differ considerably from the results of the previous studies by De Haas and Gorter (24) and by Starr, Bitter, and Kaufmann (25). Initial measurement on a sample prepared by dehydrating $\text{CuCl}_2 \cdot 2\text{H}_2\text{O}$ in a stream of hydrogen chloride gas at approximately 120°C gave a susceptibility curve which increased rapidly as the temperature decreased below 20°K , with a value of approximately .007 obtained at 1.4°K . In the region below 10°K , the susceptibility obeys a Curie-Weiss law with $\theta = -2.2^{\circ}$ and $\mu_{\text{eff}} = .44$. This effect is much smaller in the more carefully prepared sample, and thus it seems likely that it is due to an impurity in the sample. The impurities could have entered into the sample either in the preparation or handling of the sample, with the latter seeming more likely since analysis of the anhydrous cupric chloride indicated that iron could not be present in amounts greater than ten parts per million, while an impurity of approximately one part per thousand would be required to produce the observed effect.

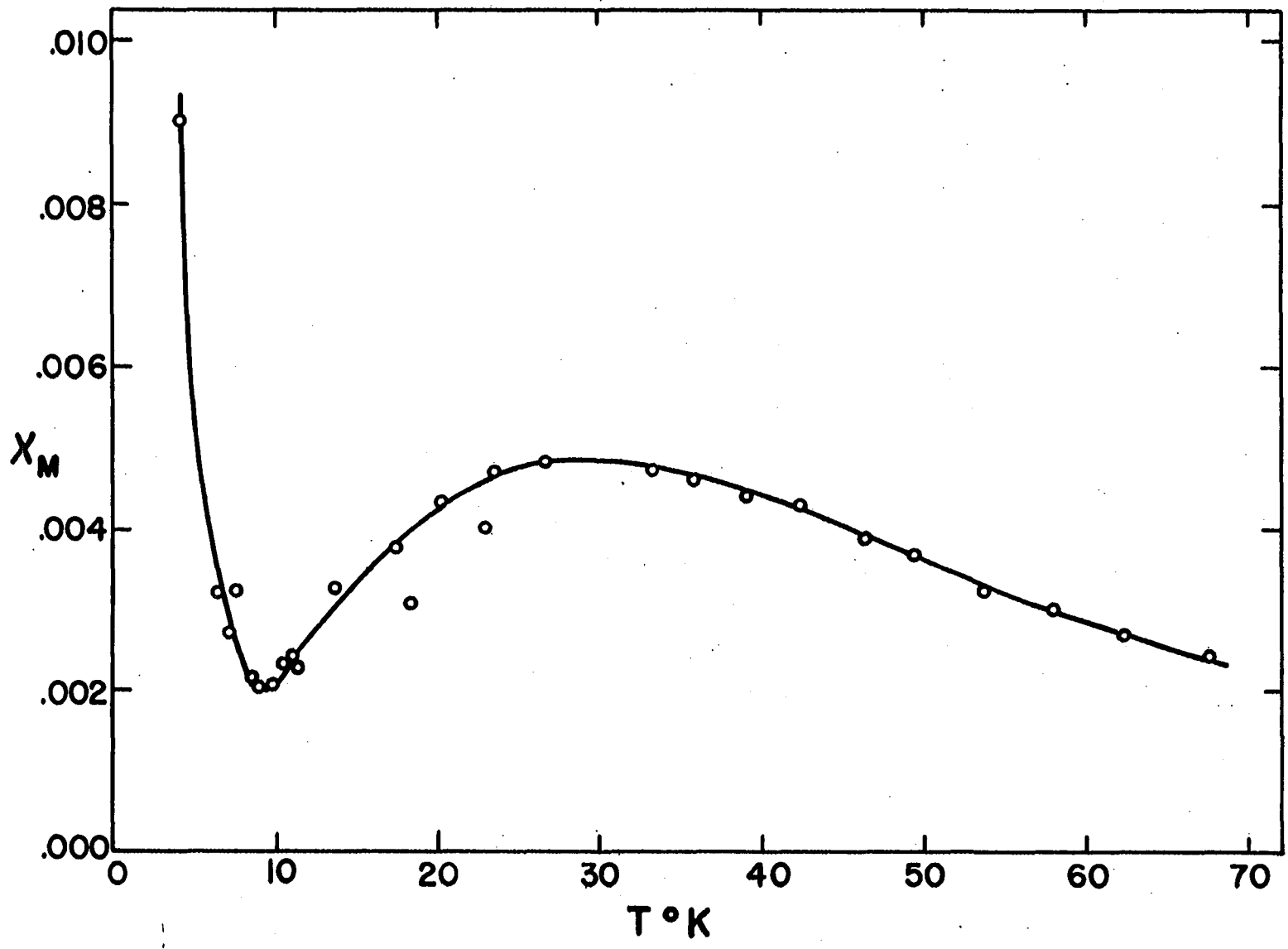
C. Magnetic Susceptibility of KCuCl_3

The magnetic susceptibility of KCuCl_3 was measured in the temperature range 1.4°K to 70°K . The sample was prepared by mixing an excess of equimolar quantities of KCl and $\text{CuCl}_2 \cdot 2\text{H}_2\text{O}$ in hydrochloric acid, filtering, and washing with glacial acetic acid to remove the excess hydrochloric acid. The results are shown in Figures 39 and 40.

The susceptibility curve exhibits a broad maximum at approximately 30°K and thus the compound becomes antiferromagnetic below this temperature. The paramagnetic region at higher temperatures was not investigated. It is evident from Figure 40 that the Curie temperature will be positive. This is of interest in light of the negative Curie temperature for $\text{LiCuCl}_3 \cdot 2\text{H}_2\text{O}$.

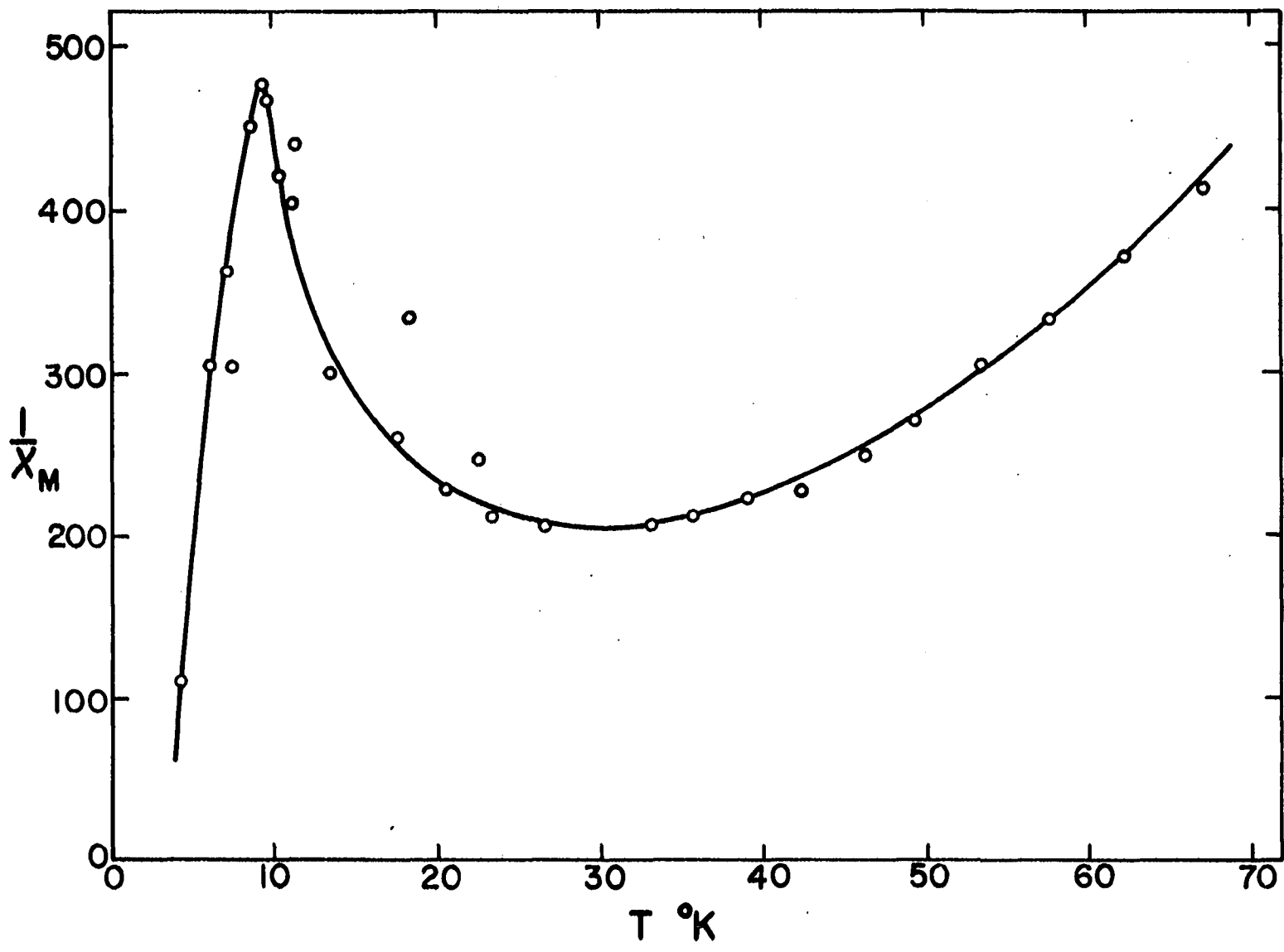
The same unusual behavior at very low temperatures was observed in this case as was observed for anhydrous cupric chloride, where it obeys a Curie-Weiss law with $\theta = 2.0^\circ\text{K}$ and $\mu_{\text{eff}} = 0.74$ below approximately 5°K . Again, it seems very likely that the anomalous behavior is due to an impurity, rather than some inherent property of the compound.

Figure 39. Plot of the molar magnetic susceptibility versus temperature
for KCuCl_3



150b

Figure 40. Plot of the reciprocal molar magnetic susceptibility versus temperature for KCuCl_3



151b

IV. THEORETICAL ASPECTS

A. Introduction

In this section a proposal will be set forth concerning the electronic structure of the cupric chloride complexes which were studied experimentally, and it will be shown how this electronic structure accounts for properties and bonding in these compounds. The discussion will be entirely qualitative, with no numerical calculations being made. However, all assumptions made regarding numerical quantities are reasonable, and so it is hoped that the results obtained are qualitatively correct and that they could point the way in which it would be possible to approach a quantitative attack on the type of problem involved.

The main experimental information available is the stereochemistry of the cupric complexes, their magnetic properties, and their optical properties. The stereochemistry of the problem will be used to assist in setting up the wave functions involved and these wave functions will be used to interpret the magnetic and optical properties. The molecular orbital (MO) method will be used with the usual linear combination of atomic orbital (LCAO) approach to construct the molecular orbitals. It will be assumed that the reader is familiar with the basic assumptions involved in this method. Considerable use of group theory

will be used to obtain the appropriate linear combinations of atomic orbitals. Derivation of the most important group theoretical results will be given in the appendices.

The molecular orbital type of approach was chosen for several reasons. It seems necessary to assume a delocalization of the unpaired electron from the copper atom unto the ligand atoms in order to explain NMR and EPR data (19, 68). This eliminates the possibility of using a simple crystal field or ligand field approach where the metal wave functions are assumed to be perturbed by the presence of the ligands, but where no delocalization of the metal orbitals is allowed. Also a simple valence bond approach does not succeed either, since upon formation of dsp^2 hybrid orbitals it is necessary for the unpaired electron to be localized in a metal p_z orbital. This does not allow for any interaction between the unpaired electrons on adjacent copper atoms in a chain type structure such as in $CuCl_2$ and thus it is not possible, without the inclusion of π -bonding, to explain the magnetic ordering in these compounds. Also, the molecular orbital approach has the advantage that it is easy to visualize the qualitative results, although it is difficult to obtain quantitatively accurate results. For those who would like to see a quantitative application of the molecular orbital method to a problem of a nature similar to this problem, the report of Richardson and Rundle (69) is

recommended.

B. Electronic Structure of the $\text{CuCl}_4^{=}$ Ion

The hypothetical square planar ion, $\text{CuCl}_4^{=}$, will be considered first. Although this ion has never been isolated in the crystalline state, it is the primary building block of the dimers, trimers, and other extended chains which exist in the red cupric chloride complexes. Thus, it seems likely that a study of this ion will provide us with some clues for understanding the bonding in the other, more complex, ions and molecules.

The ion $\text{CuCl}_4^{=}$ belongs to the symmetry group D_{4h} . Thus, it contains a four-fold axis, two classes of pairs of two-fold axes perpendicular to the four-fold axis, plus a center of symmetry with the associated operations obtained by the operation of the center of symmetry on the four-fold and two-fold axes, namely a four-fold inversion axis, and two classes of pairs of mirror planes parallel to the four-fold axis. The coordinate system is chosen such that the ion lies in the xy-plane, with two chlorine atoms at $\pm x$ along the x-axis and two chlorine atoms at $\pm y$ along the y-axis. Symmetry orbitals (SO) are formed for the metal atom and for the ligand atoms that transform in the same manner as the irreducible representations of the symmetry group D_{4h} . These orbitals are adapted to the symmetry of the group and

have the property that only orbitals which belong to the same irreducible representations can combine with each other. This greatly reduces the number of possible atomic orbitals which can combine in the LCAO method. For those who are not familiar with group theory, it may be convenient to think of the irreducible representation symbol which identifies the symmetry of each symmetry orbital as a tag to identify the wave function. The symmetry orbitals for the metal atoms are linear combinations of the free atom wave functions which transform in the same manner as the irreducible representations of the group D_{4h} . The symmetry adapted orbitals are listed in Table 28.

The molecular orbitals are formed from the metal orbitals and the ligand symmetry orbitals which have the same symmetry as the metal orbitals. Since the only sigma bonding ligand symmetry orbitals are the orbitals with E_u , B_{1g} , and A_g symmetry, only the metal orbitals with these symmetries need be considered. These are the s , p_x , p_y , $d_{x^2-y^2}$, and d_{z^2} orbitals.

The degeneracy of the p orbitals and the d orbitals on the metal atom will be split due to electrostatic interaction between the ligands and the electrons on the metal ion. This splitting is illustrated in Figure 41. The location of the A_{1g} orbital (the d_{z^2} orbital) will depend on the presence or absence of charge along the z -axis. In an

actual physical situation it would probably lie above the B_{2g} orbital, as is indicated in Figure 41, but in an isolated $CuCl_4^{=}$ ion, it probably would lie between the B_{2g} orbital and the E_g orbitals. See Fenske and Martin (70) for a discussion of this situation for platinum(II) complexes.

For each combination of metal and ligand symmetry orbitals there will be one bonding and one antibonding molecular orbital. The bonding molecular orbitals will have the form $\psi_i = c_1\varphi_i + c_2\sigma_i$, where φ_i and σ_i are the metal and ligand symmetry orbitals respectively, and c_1 and c_2 are parameters which would be obtained by a variational treatment if an actual numerical calculation were being made. The antibonding molecular orbital will have the form $\psi_i = c_2\psi_i - c_1\sigma_i$. When there are more than one metal symmetry orbital belonging to the same irreducible representation (such as the d_{z^2} and the s metal orbitals), it will be necessary to include one parameter, c_j , for each of the metal orbitals involved.

The shift in energy upon formation of the bonding and antibonding orbitals can only be estimated and postulated energy levels are given in Figure 41. Here it is assumed that only the 3d, 4s, and 4p metal orbitals are involved in the bonding and that no π -bonding occurs. Inclusion of other metal orbitals such as the 3p orbitals, and of π -bonding will not affect the final results obtained since both the

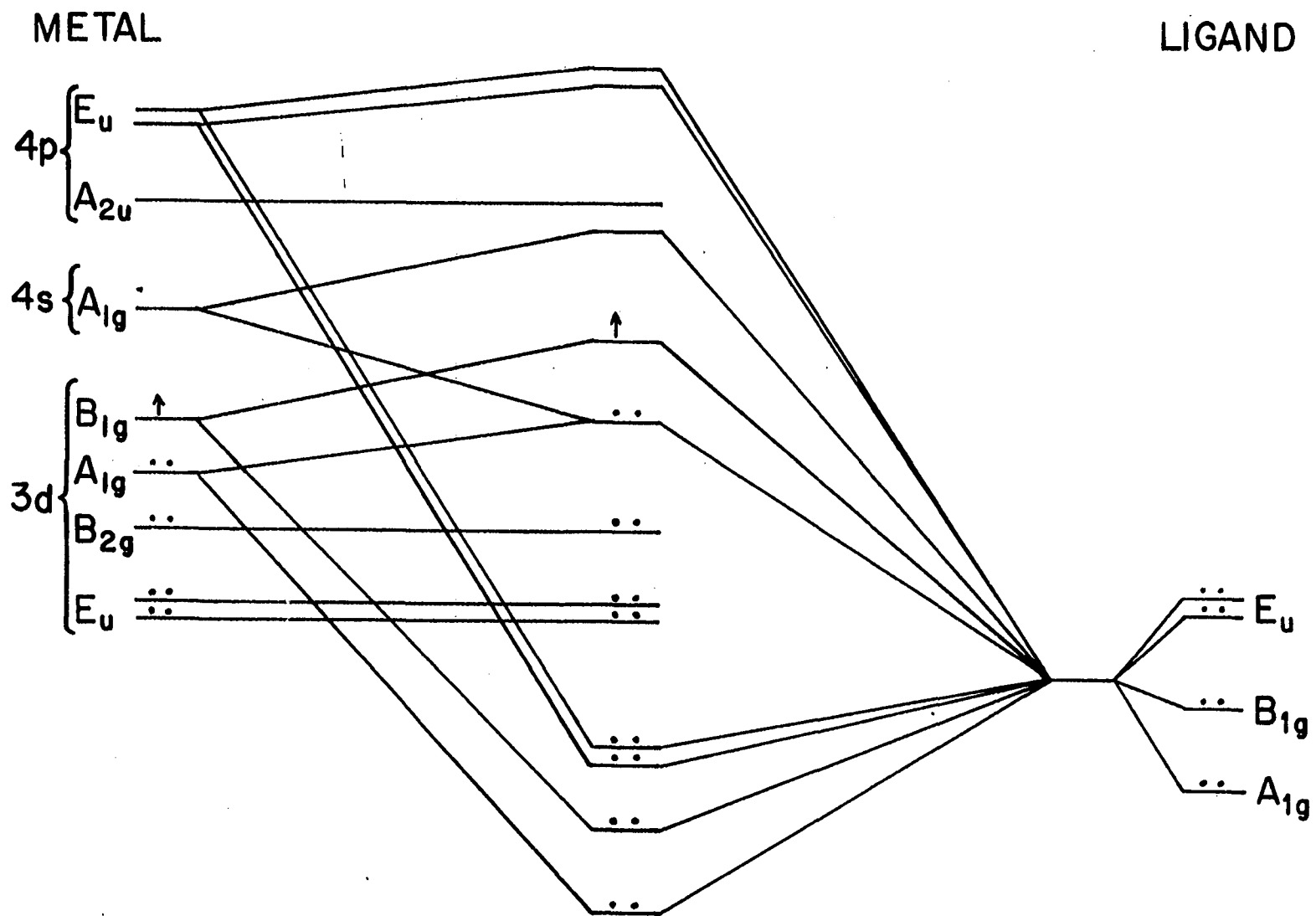


Figure 41. Scheme of the molecular orbital energy levels for the CuCl_4^{2-} ion

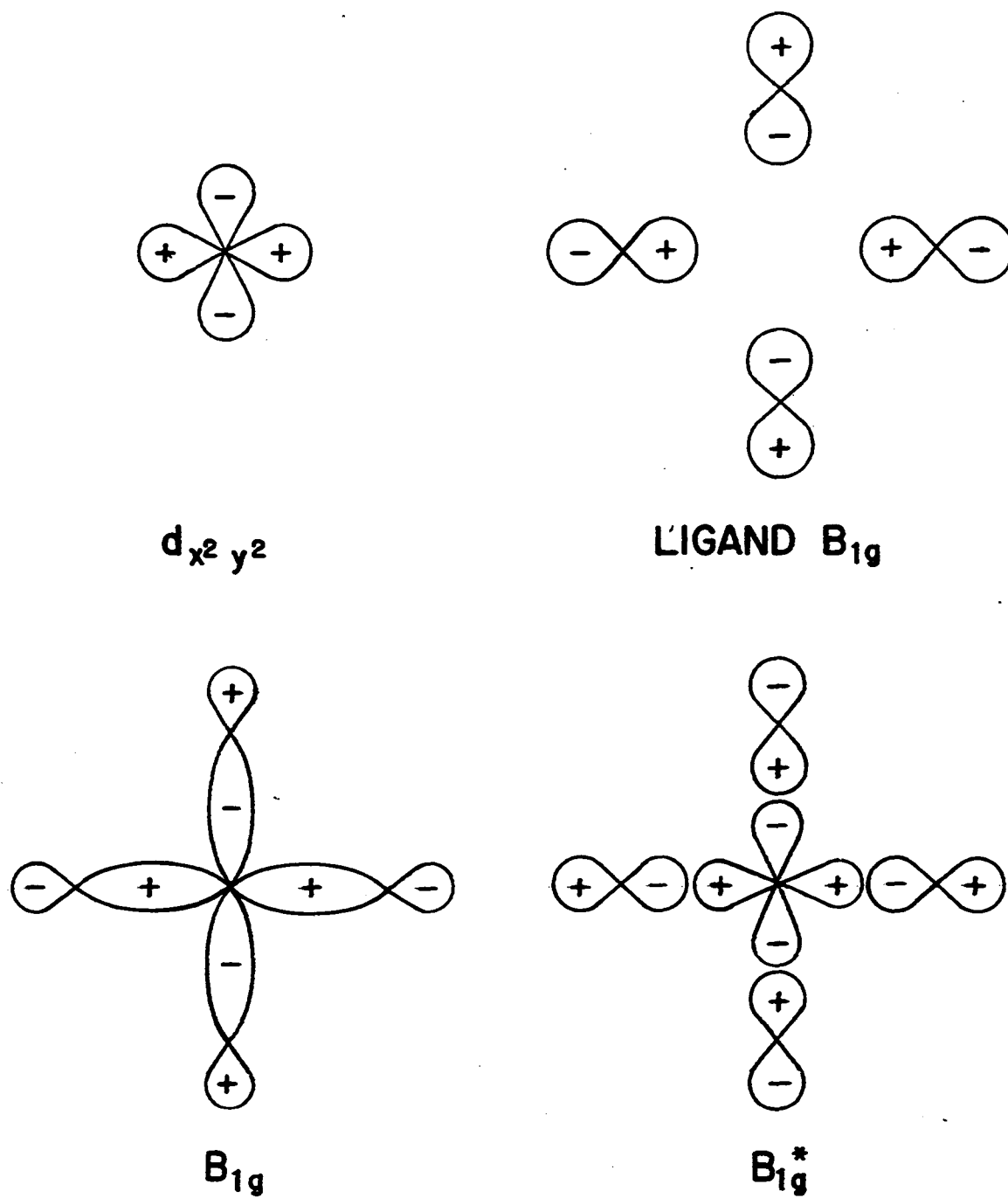


Figure 42. Illustration of the B_{1g} symmetry and molecular orbitals for the CuCl_4^{2-} ion

bonding and antibonding orbitals obtained will be filled. The inclusion of these other orbitals would only lead to a more complicated and confusing energy level diagram, and probably is not justified in a qualitative argument such as this.

The ligand orbitals contribute eight electrons to the molecular orbitals, and the metal atom contributes nine electrons. This gives seventeen electrons to distribute among the molecular orbitals for the ion. When the eight lowest orbitals are filled, it is found that the unpaired electron falls into the B_{1g} antibonding orbital. This orbital is formed from the ϕ_2 metal symmetry orbital and the σ_2 ligand symmetry orbital. These are illustrated in Figure 42, along with the bonding and antibonding orbitals.

There is contribution from the ligand orbitals as well as from the metal orbital in the antibonding orbital. This is in accordance with the experimentally observed fact that some of the electron density of the unpaired electron is distributed on the ligand atoms (19, 68) and is not localized on the metal atom. It is seen also that there is a node between the metal atom and each ligand atom, due to the fact that it is an antibonding orbital. Thus, in the neighborhood of the ligand atom, the electron essentially behaves as if it were in a ligand p-orbital.

C. Electronic Structure of the Cu_2Cl_6^- Ion

The simplest way to approach the bonding in the Cu_2Cl_6^- dimer is to consider it to consist of essentially two CuCl_4^- ions. In each half of the dimer the unpaired electron will be in a B_{1g} antibonding orbital as discussed in the previous section. Two molecular orbitals may then be formed by combining the two B_{1g} antibonding orbitals. Because of the essential p character of the B_{1g} antibonding orbital at the bridging ligand atoms, there is essentially zero overlap, and the two new orbitals formed will be degenerate for all practical purposes. These are illustrated in Figure 44f and Figure 44n. It is best to use the results of this crude argument mainly as a guide as to what might be expected from a more thorough analysis.

The group theoretical analysis of the Cu_2Cl_6^- dimer is much more complicated than that for the CuCl_4^- ion for two reasons. First, there are more orbitals and electrons involved, and second, the dimer belongs to a lower symmetry group, so that the group theory does not simplify the problem as much.

The symmetry group in this case is D_{2h} . That is, the dimer contains three mutually perpendicular two-fold axes, a center of symmetry, and three mirror planes perpendicular to the two-fold axes. Assuming that the molecule lies in

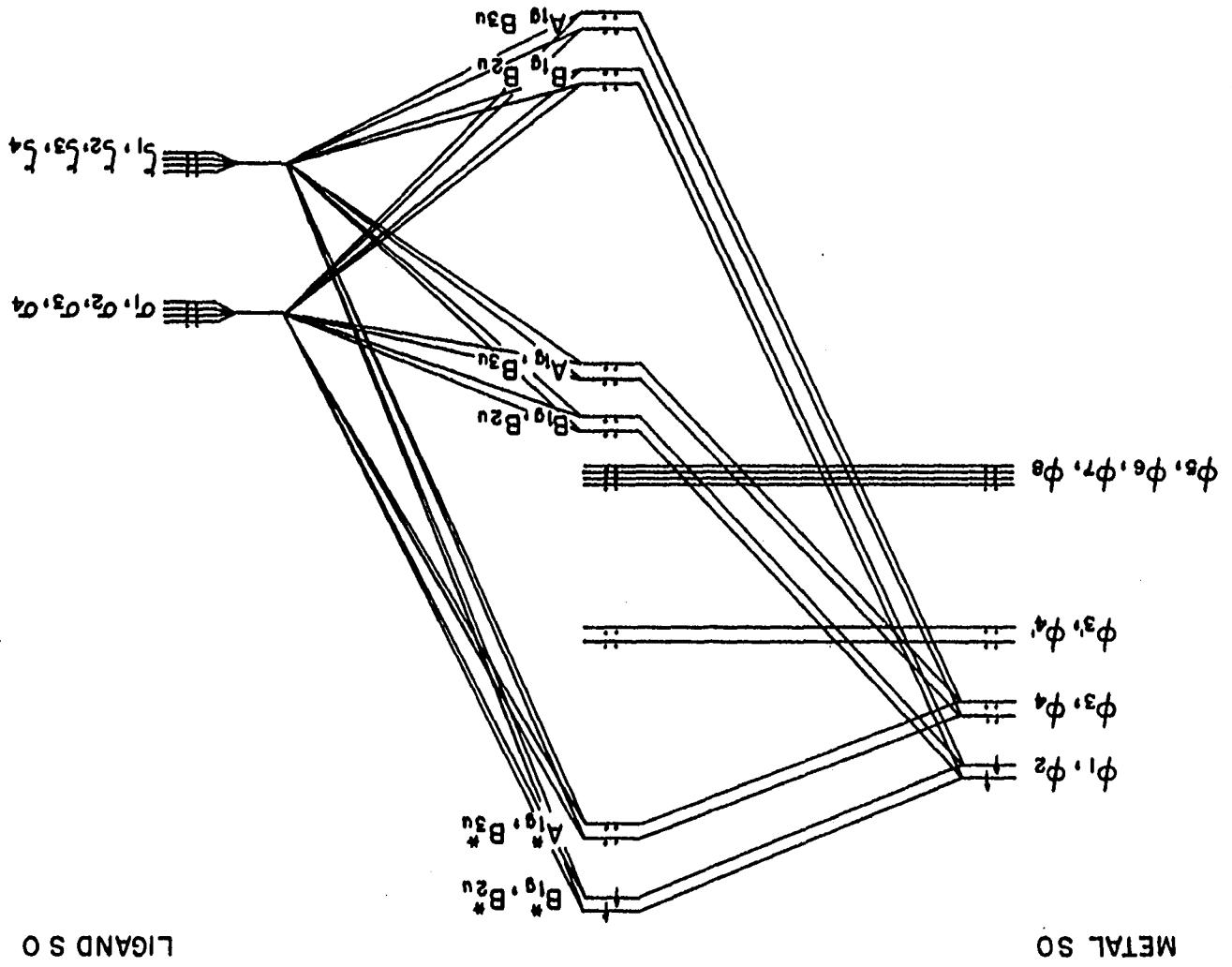
the xy-plane, with the x-axis parallel to the Cu-Cu direction, the symmetry orbitals for both the metal atoms and the ligand atoms can be formed. These are listed in Table 31 of Appendix B. Since there are two sets of equivalent chlorine atoms in the dimer (these two sets contain the four terminal chlorine atoms and the two bridging chlorine atoms respectively), there are two sets of ligand symmetry orbitals. The symmetry orbitals for the terminal chlorine atoms are denoted by σ_i and π_i while the symmetry orbitals for the bridging chlorine atoms are denoted by ζ_i . For the metal symmetry orbitals, the main difference between this case and that for the CuCl_4^- ion is that now each orbital is replaced by two orbitals. These two orbitals are linear combinations of the atomic orbitals on the two copper atoms. These two orbitals will be nearly degenerate since there is little overlap of the orbitals from the two atoms. It should also be noted that the d_{xz} and d_{yz} orbitals on a given metal atom are not required to be degenerate by the symmetry of the group. However, to the extent that the overlap between orbitals on the two metal atoms can be neglected, these degeneracies will exist due to the additional requirement that there exist a square planar coordination for both copper atoms.

To make the situation as simple as possible, only the metal symmetry orbitals obtained from the 3d orbitals will

be considered in the formation of the molecular orbitals. The metal symmetry orbitals will be split in energy in the manner illustrated in Figure 43, and thus the φ_5 and φ_6 orbitals (the two orbitals derived from the metal d_{xy} orbitals) have the highest energies. The ligand symmetry orbitals will be split in energy also. The atomic orbitals of the four terminal chlorine atoms are influenced by one metal ion, while the orbitals of the two bridging chlorine atoms are influenced by two metal ions. Hence, the symmetry orbitals constructed from the bridging chlorine atoms will be lower in energy than the symmetry orbitals constructed from the terminal chlorine atoms.

It seems reasonable to expect that the shift in the energy levels upon formation of the bonding and antibonding molecular orbitals will be similar to the shifts postulated for the CuCl_4^- ion. There is additional complication because of the existence of two ligand symmetry orbitals for the same irreducible representations in several instances. Thus, one bonding orbital, one antibonding orbital, and one intermediate orbital will be formed. Thus it will be necessary to solve a 3×3 secular determinant to obtain the coefficients for the three molecular orbitals. The molecular B_{1g} orbitals will be formed for the φ_1 , σ_1 , and ζ_1 orbitals (Figures 44a, 44c, and 44d respectively). The bonding orbital will be as illustrated in Figure 44e, the

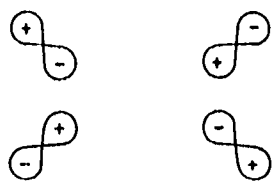
Figure 43. Scheme of the molecular orbital energy levels for the $\text{Cu}_2\text{Cl}_6^{=}$ ion



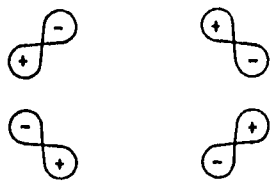
antibonding orbital will be as illustrated in Figure 44f, and the third molecular orbital will have one of the forms illustrated in Figures 44g and 44h. The orbital illustrated in Figure 44g is antibonding between the metal ion and the bridging ligands and bonding between the metal ion and the terminal ligands. For the orbital illustrated in Figure 44h, this situation is reversed. The orbital illustration in Figure 44g will most likely be the orbital which actually occurs since the ζ_1 orbital has a lower energy than the π_1 orbital, and thus will become antibonding sooner. It should be noted that the π_1 and π_2 ligand symmetry orbitals are nonbonding with respect to the φ_1 and φ_2 metal symmetry orbitals. However, they will have π -bonding characteristics with respect to metal symmetry orbitals derived from the metal p-orbitals. The various orbitals with B_{2u} symmetry are illustrated in Figures 44i - 44p.

The postulated energy levels for the molecular orbitals are illustrated in Figure 43. The π -bonding ligand orbitals are omitted for convenience. The degeneracies which existed for the metal symmetry orbitals will still exist when the molecular orbitals are formed. The ligand symmetry orbitals contribute sixteen electrons and the metal symmetry orbitals contribute eighteen electrons and thus there are thirty-four electrons to be distributed among the molecular orbitals. When the molecular orbitals are filled up, it is found that

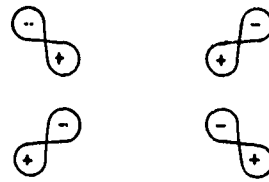
Figure 44. Illustration of the B_{1g} and B_{2u} symmetry and molecular orbitals for the Cu_2Cl_6^- ion



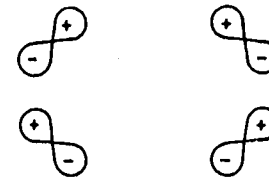
a σ_1



b π_1



i σ_2



j π_2



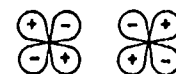
c ζ_1



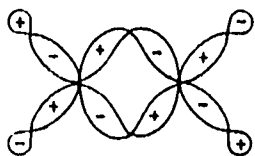
d ϕ_1



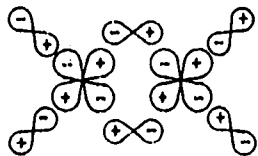
k ζ_2



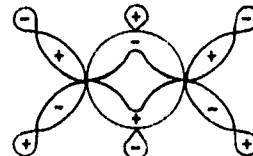
l ϕ_2



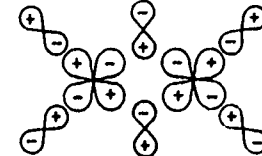
e B_{1g} (bonding)



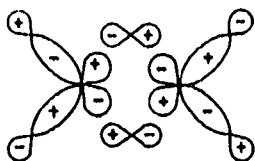
f B_{1g}^* (antibonding)



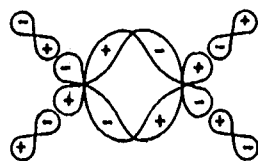
m B_{2u} (bonding)



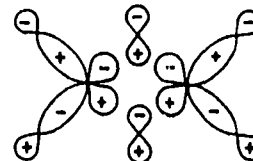
n B_{2u}^* (antibonding)



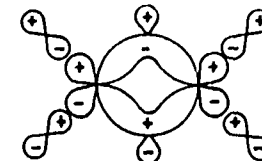
g B_{1g} (mixed)



h B_{1g} (mixed)



o B_{2u} (mixed)



p B_{2u} (mixed)

there are two electrons to be distributed between the nearly degenerate B_{1g}^* and B_{2u}^* antibonding orbitals. It is gratifying to note that these two orbitals are the same as the two orbitals obtained by the arguments presented at the very beginning of this section.

With the knowledge that these two electrons are in the essentially degenerate B_{1g}^* and B_{2u}^* orbitals, the question then arises as to whether the dimer exists in a singlet or a triplet configuration. At room temperatures certainly the thermal energy, kT , will be much greater than the energy separation between the various possible states. Hence the electrons should be statistically distributed and the magnetic susceptibility would be expected to obey the Curie law or the Curie-Weiss law. However, as the temperature is decreased so that kT becomes smaller than the energy separation, the electrons should occupy the lowest state, and thus an ordering of the spins of the electrons should occur. There are three possible singlet configurations, two in which the spins of the two electrons are paired antiparallel in either the B_{1g}^* or the B_{2u}^* orbital and the third in which they are paired antiparallel with one electron located in the B_{1g}^* orbital and the other one in the B_{2u}^* orbital. The only triplet configuration arises when one electron is located in each orbital with their spins aligned parallel. Applying the familiar Hund's rule (71, 72) to this situation,

it seems likely that the triplet state will be the lowest in energy. Experimentally, it is not known which is the ground state. For the case of $\text{LiCuCl}_3 \cdot 2\text{H}_2\text{O}$, where the magnetic unit cell is the same size as the chemical unit cell and, assuming that the magnetic interaction through the unsymmetric bridge is ferromagnetic as in $\text{CuF}_2 \cdot 2\text{H}_2\text{O}$, the magnetic interaction between copper atoms in the symmetrically bridged dimers must be ferromagnetic also since the connection between equivalent copper atoms in the $(\text{Cu}_2\text{Cl}_6)_n^{2n-}$ chains is through one symmetric bridge and one unsymmetric bridge. However, the negative Curie temperature (-10°K) is hard to explain if the main interactions within the chain are ferromagnetic unless it is assumed that the interactions between the chains are stronger than the interactions within the chains. It is also possible that the extrapolation of the susceptibility data from the very high temperature region may give a positive Curie temperature since the observed Curie temperature is so close to zero. In KCuCl_3 , where the stacking of the chains is different than in $\text{LiCuCl}_3 \cdot 2\text{H}_2\text{O}$, a ferromagnetic interaction through the unsymmetrical bridge would not require a ferromagnetic interaction through the symmetrical bridge in the dimer.

The red coloration is observed for all the compounds in which symmetrical type bridging chlorines exist. Mori (40) has found a transition at $525\overset{\circ}{\text{A}}$ in the reflection spectrum of

KCuCl₃. In addition, crystals of LiCuCl₃·2H₂O, KCuCl₃, and NH₄CuCl₃ appear red when examined by polarized light when the electric vector is parallel to the copper-copper direction of the dimer and yellow-green when the electric vector is perpendicular to this direction. It thus appears that an electronic transition within the Cu₂Cl₆⁼ dimer is responsible for this absorption band. If the assumption that the two unpaired electrons are located in the B_{1g}^{*} and B_{2u}^{*} orbitals is correct, then it seems reasonable to assume that this electronic transition involves a transfer of an electron from one of these orbitals to the other. The intensity of the transition suggests that it is at least partially forbidden and thus the transition is probably a triplet-singlet or singlet-triplet transition depending upon which state is the lowest in energy.

Moeller found a strong maximum in the absorption spectrum of a 2.0N CuCl₂ solution at approximately 5150⁰A. It was suggested that this absorption band was primarily due to the presence of the CuCl₄⁼ species in solution. Since the absorption maximum occurs at essentially the same wavelength in the spectrum of KCuCl₃, it appears that the absorption band is due to the presence of the Cu₂Cl₆⁼ species in the solution. This does not invalidate Mori's contention (40) that the CuCl₅³⁻ ion exists in solution since his absorption measurements were made on a very dilute

(.000124M solution of CuSO_4 in 10.0N HCl) solution.

D. Conclusion

The qualitative aspects of the electronic structure of the CuCl_4^- and the Cu_2Cl_6^- ions have been discussed in this section. It was found that the unpaired electron in the square planar CuCl_4^- ion should lie in a B_{1g}^* molecular orbital. The important feature is that the electron is no longer localized on the copper ion, but is distributed over the ligand atoms as well. This delocalization can be expected also where one or more of the chlorine ions has been replaced by other ligands, such as oxygen or nitrogen atoms. The existence of the unpaired electron in a B_{1g}^* molecular orbital has been used (68) to explain the electron paramagnetic resonance of organic complexes of copper(II) and it has been found that approximately 30% of the electron density has been delocalized unto the ligands.

For the planar Cu_2Cl_6^- ion, it was found that the two unpaired electrons should lie in the nearly degenerate B_{1g}^* and B_{2u}^* molecular orbitals. At low temperatures, the spins of these two electrons should become ordered and it was proposed that a ferromagnetic type ordering should be expected. It was also proposed that the deep red coloration of the compounds containing this ion was due to an electronic transition between these two molecular orbitals. If these

proposals are correct, it seems likely that a ferromagnetic interaction will occur within the infinite $(\text{CuCl}_2)_n$ chain in anhydrous cupric chloride and within the trimer and pentamer in $\text{Cu}_3\text{Cl}_6(\text{CH}_3\text{CN})_2$ and $\text{Cu}_5\text{Cl}_{10}(\text{C}_3\text{H}_7\text{OH})_2$ respectively. It is hoped that future work on the magnetic and optical properties of these compounds might give unambiguous answers to the electronic structure of the copper(II) halides.

V. LITERATURE CITED

1. Vossos, P. H., Fitzwater, D. R. and Rundle, R. E. Acta Cryst. (to be published) ca. 1963.
2. Vossos, P. H., Jennings, L. D. and Rundle, R. E. J. Chem. Phys. 32, 1590 (1960).
3. Vossos, P. H. and Rundle, R. E. Crystal Structure and Magnetic Properties of $\text{LiCuCl}_3 \cdot 2\text{H}_2\text{O}$. U. S. Atomic Energy Commission Report IS-1074. (Iowa State Univ., Ames, Iowa) 1958.
4. Dwiggins, Claudius W., Jr. Determination of the Crystal Structure of Potassium Trichlorocuprate(II). Microfilm copy. Unpublished Ph.D. thesis. Fayetteville, Ark., Library, University of Arkansas. 1958.
5. Wells, A. F. J. Chem. Soc. 1947, 1670.
6. Billy, C. and Haendler, H. M. J. Am. Chem. Soc. 79, 1049 (1957).
7. Helmholtz, L. J. Am. Chem. Soc. 69, 8861 (1947).
8. Wells, A. F. J. Chem. Soc. 1947, 1662.
9. Helmholtz, L. and Kruh, K. F. J. Am. Chem. Soc. 74, 1176 (1952).
10. Mori, M., Saito, Y. and Watanabe, T. Bull. Chem. Soc. Japan 34, 295 (1961).
11. Harker, D. Z. Krist. 93, 136 (1938).
12. Kabalkina, S. S. Dodeady Akad. Nank. SSR 110, 1013 (1956).
13. Geller, S. and Bond, W. L. J. Chem. Phys. 29, 925 (1958).
14. Chrobak, L. Zeit. Krist. 88, 35 (1934).
15. Freeman, H. C., Smith, J. E. W. L. and Taylor, J. C. Acta Cryst. 14, 407 (1961).

16. Van der Marel, L. C.; Van den Brock, J., Wasscher, J. D. and Gorter, C. J. *Physica* 21, 685 (1955).
17. Poulis, N. J. and Hardeman, G. E. G. *Physica* 18, 201 (1952).
18. _____. *J. Chim. Phys.* 50, 110 (1953).
19. Rundle, R. E. *J. Am. Chem. Soc.* 79, 3372 (1957).
20. Abrahams, S. C. *J. Chem. Phys.* 36, 56 (1962).
21. Shulman, R. G. *J. Chem. Phys.* 35, 1498 (1961).
22. Bozoth, R. M. and Nielson, J. W. *Phys. Rev.* 110, 879 (1958).
23. Marshall, W. *J. Phys. Chem. Solids* 7, 159 (1958).
24. De Haas, W. J. and Gorter, C. J. *Leiden Comm.* 215a (1931).
25. Starr, C., Bitter, F. and Kaufmann, A. R. *Phys. Rev.* 58, 134 (1956).
26. Perakis, N. and Serres, A. *J. Phys. Radium* 17, 134 (1956).
27. Spence, R. D. and Murty, C. R. K. *Physica* 27, 850 (1961).
28. Mori, M. *Bull. Chem. Soc. Japan* 34, 454 (1961).
29. Stoner, E. C. *Phil. Mag.* 8, 250 (1929).
30. Ray, P. and Sen, D. N. *J. Ind. Chem. Soc.* 25, 473 (1948).
31. Mookherji, A. and Chhonkar, N. S. *Ind. J. Phys.* 33, 74 (1959).
32. Dunn, T. N. *The Visible and Ultra-Violet Spectra of Complex Compounds*. In Lewis, J. and Wilkens, R. G., eds. *Modern Coordination Chemistry*, pp. 229-300. Interscience Publishers, Inc., New York, New York. 1960.
33. Moeller, T. *J. Phys. Chem.* 48, 111 (1944).

34. Getman, F. H. J. Phys. Chem. 26, 217 (1922).
35. Yamada, S. and Tsuchida, R. Bull. Chem. Soc. Japan 27, 436 (1954).
36. Felsenfeld, G. Proc. Roy. Soc. A326, 506 (1956).
37. Ballhausen, C. J. Dan. Mat. Fys. Med. 29, no. 4 (1954).
38. Ballhausen, C. J. and Liehr, A. D. J. Mol. Spectroscopy 2, 236 (1958).
39. _____. J. Mol. Spectroscopy 4, 190 (1960).
40. Mori, M. Bull. Chem. Soc. Japan (to be published) ca. 1962.
41. Busing, W. R. and Levy, H. A. A Crystallographic Least Squares Refinement Program for the IBM 704. U. S. Atomic Energy Commission Report ORNL 59-4-37. (Oak Ridge National Laboratory, Tenn.) 1959.
42. Busing, W. R. and Levy, H. A. A Crystallographic Function and Error Program for the IBM 704. U. S. Atomic Energy Commission Report ORNL 59-12-3. (Oak Ridge National Laboratory, Tenn.) 1959.
43. Sly, W. G. and Shoemaker, D. P. MIFR1: Two- and Three-Dimensional Crystallographic Fourier Summation Program for the IBM 704 Computer. Technical Reports DSR 7998 and DSR 7738-7740. (Massachusetts Institute of Technology, Cambridge, Mass.) 1960.
44. International Tables for X-Ray Crystallography. Vol. 2. The Kynoch Press, Birmingham, England. 1959.
45. Hamilton, W. C. Acta Cryst. 8, 185 (1955).
46. Meyerhoffer, W. Zeit. Phys. Chem. 3, 338 (1889).
47. _____. Zeit. Phys. Chem. 5, 102 (1890).
48. _____. Sitzber. Akad. Wein 102, 200 (1893).
49. Groger, M. Zeit. Anorg. Chem. 19, 328 (1899).
50. Bueger, M. J. X-Ray Crystallography. John Wiley and Sons, Inc., New York, N. Y. 1952.

51. Waser, J. Rev. Sci. Instr. 22, 563 (1951).
52. Engle, R. Compt. Rend. 106, 273 (1888).
53. _____. Compt. Rend. 107, 178 (1888).
54. Foote, H. W. and Walden, P. T. J. Am. Chem. Soc. 33, 1032 (1911).
55. Naumann, A. Ber. 47, 249 (1914).
56. Evans, R. C., Mann, F. G., Peiser, H. S. and Purdie, D. J. Chem. Soc. 1940, 1209.
57. Wells, A. F. Proc. Roy. Soc. 167A, 169 (1938).
58. Vand, V. and Bell, I. P. Acta Cryst. 4, 465 (1951).
59. Danford, M. D. and Livinston, R. L. J. Am. Chem. Soc. 77, 2944 (1955).
60. Thomas, L. F., Sherrard, E. I. and Sheridan, J. Trans. Fara. Soc. 51, 619 (1955).
61. Wang, F. E., Simpson, P. G. and Lipscomb, W. N. J. Chem. Phys. 35, 1335 (1961).
62. Reddy, J. and Lipscomb, W. N. J. Chem. Phys. 31, 610 (1959).
63. Thomas, J. T., Robertson, J. H. and Cox, E. G. Acta Cryst. 11, 599 (1958).
64. Lloyd, E., Brown, C. B., Glynwyn, D., Bonnell, R. and Jones, W. J. J. Chem. Soc. 1928, 658.
65. Peterson, S. and Levy, H. A. J. Chem. Phys. 26, 220 (1957).
66. Jennings, L. D. Rev. Sci. Instr. 31, 1269 (1960).
67. Gerstein, B. C. Heat capacity and magnetic susceptibility of thulium ethylsulfate. Unpublished Ph.D. thesis. Ames, Iowa, Library, Iowa State University of Science and Technology. 1960.
68. Gersmann, H. R. and Swalen, J. D. J. Chem. Phys. 36, 3221 (1962).

69. Richardson, J. W. and Rundle, R. E. A Theoretical Study of the Electronic Structure of Transition-Metal Complexes. U. S. Atomic Energy Commission Report ISC-830. (Iowa State Univ., Ames, Iowa) 1956.
70. Fenske, R. F. and Martin, D. S. Energy Levels of Platinum(II) Complexes on the Basis of Ligand Field Theory. U. S. Atomic Energy Commission Report IS-342. (Iowa State Univ., Ames, Iowa) 1961.
71. Herzberg, G. Atomic Spectra and Atomic Structure. Dover Publications, New York, N. Y. 1944.
72. Herzberg, G. Molecular Spectra and Molecular Structure I. Spectra of Diatomic Molecules. 2nd ed. Van Nostrand Co., New York, N. Y. 1950.
73. Eyring, H., Walter, J. and Kimball, G. E. Quantum Chemistry. John Wiley and Sons, Inc., New York, N. Y. 1944.

VI. ACKNOWLEDGMENTS

The author is pleased to express his appreciation to Dr. R. E. Rundle for his interest, suggestions, encouragement, and guidance during the course of this research work.

The assistance of Dr. Christian Scheringer and Mr. Lawrence Hoard with the magnetic susceptibility measurements is gratefully acknowledged, as is the assistance of Mrs. Jean Kestel in judging the crystallographic intensity data. Mr. H. F. Hollenbeck gave valuable assistance throughout the crystallographic portion of this research. The assistance of Mr. Robert Dillon, Mr. Galen Stucky, and Mr. Gordon Engebretson with the programming portion of the research work is also appreciated.

Finally, the patience and understanding of my wife was most helpful during the course of this research.

VII. APPENDIX A: GROUP THEORY APPLICATION TO
BONDING IN THE CuCl_4^- ION

The square planar ion CuCl_4^- belongs to the symmetry group D_{4h} . The character table for this group is given in Table 23. For a brief discussion of the meaning of the symbols, see Eyring, Walter and Kimball (73). The free atom wave functions with angular momentum l transform as do the spherical harmonics of order l , Y_l . The character, χ , of the reducible representations for the spherical harmonics for $l = 0, 1$, and 2 are given in Table 24. These are

Table 23. Character table for the group D_{4h}

	E	C_2	$2C_4$	$2C_2'$	$2C_2''$	i	σ_h	$2S_4$	$2\sigma_v'$	$2\sigma_v''$
A_{1g}	1	1	1	1	1	1	1	1	1	1
A_{1u}	1	1	1	1	1	-1	-1	-1	-1	-1
A_{2g}	1	1	1	-1	-1	1	1	1	-1	-1
A_{2u}	1	1	1	-1	-1	-1	-1	-1	1	1
B_{1g}	1	1	-1	1	-1	1	1	-1	1	-1
B_{1u}	1	1	-1	1	-1	-1	-1	1	-1	1
B_{2g}	1	1	-1	-1	1	1	1	-1	-1	1
B_{2u}	1	1	-1	-1	1	-1	-1	1	1	-1
E_g	2	-2	0	0	0	2	-2	0	0	0
E_u	2	-2	0	0	0	-2	2	0	0	0

derived for the formulae

$$\begin{aligned} \chi &= 2\ell + 1 && \text{for } E, \\ \chi &= \frac{\sin (\ell + \frac{1}{2})\pi}{\sin \pi/2} && \text{for } C_2, C_2^i, \text{ and } C_2'', \\ \chi &= (-1)^\ell (2\ell + 1) && \text{for } i, \\ \chi &= (-1)^\ell \frac{\sin (\ell + \frac{1}{2})\pi}{\sin \pi/2} && \text{for } \sigma_h, \\ \chi &= \frac{\sin (\ell + \frac{1}{2})\pi/2}{\sin \pi/4} && \text{for } C_4, \\ \chi &= \frac{\cos (\ell + \frac{1}{2})\pi/2}{\cos \pi/4} && \text{for } S_4, \\ \text{and } \chi &= 1 && \text{for } \sigma_v^i \text{ and } \sigma_v''. \end{aligned}$$

Table 24. Character table for the spherical harmonics of the symmetry group D_{4h}

	E	C_2	$2C_4$	$2C_2^i$	$2C_2''$	i	σ_h	$2S_4$	$2\sigma_v^i$	$2\sigma_v''$
$\ell = 0 (Y_0)$	1	1	1	1	1	1	1	1	1	1
$\ell = 1 (Y_1)$	3	-1	1	-1	-1	-3	1	-1	1	1
$\ell = 2 (Y_2)$	5	1	-1	1	1	5	1	-1	1	1

These reducible representations may be broken up into their irreducible representations through the use of the proper orthogonality conditions (or merely by inspection in simple cases). The orthogonality relation is

$$\sum_t \chi^i(t) \overline{\chi^j(t)} = h\sigma_{ij}$$

where $\chi^i(t)$ is the trace (character) of element t of the i^{th} irreducible representation of the group, $\overline{\chi^j(t)}$ is the complex conjugate of the trace of element t of a given reducible representation, h is the order of the group, and σ_{ij} is one if the i^{th} irreducible representation is contained in the reducible representation and zero otherwise. The summation is over all of the elements of the group.

For Y_0 the representation obviously contains only A_{1g} , while for Y_1 the representation contains A_{2u} and E_u and for Y_2 the representation contains A_{1g} , B_{1g} , B_{2g} , and E_g . The decomposition of these representations into their irreducible representations are given in Table 25. Thus the s-orbitals belong to the A_{1g} representations since Y_0 contains only the A_{1g} representation. The p_x orbital transforms in the same manner as the quantity x , since the p_x orbital has the form $\psi = Cf(r)x$, where C is a constant, and $f(r)$ is a function of the radius r only. To discover how the quantities x , y , and z transform, the group operations may be considered as 3×3 matrices, which when operated on by a positional vector (x,y,z) , transform the vector into a new vector (x', y', z') . For example, the identity operation, E , may be represented by the identity matrix, I . The

Table 25. Decomposition of the Y_1 and Y_2 representations into irreducible representations for the symmetry group D_{4h}

	E	C_2	$2C_4$	$2C_2'$	$2C_2''$	i	σ_h	$2S_4$	$2\sigma_v'$	$2\sigma_v''$
A_{2u}	1	1	1	-1	-1	-1	-1	-1	1	1
E_u	2	-2	0	0	0	-2	2	0	0	0
Y_1	3	-1	1	-1	-1	-3	1	-1	1	1
A_{1g}	1	1	1	1	1	1	1	1	1	1
B_{1g}	1	1	-1	1	-1	1	1	-1	1	-1
B_{2g}	1	1	-1	-1	1	1	1	-1	-1	1
E_g	2	-2	0	0	0	2	-2	0	0	0
Y_2	5	1	-1	1	1	5	1	-1	1	1

matrices are listed in Table 26. It is seen that these matrices have traces which are equal to the character of the representation Y_1 . This confirms that the quantities x , y , z transform in the same manner as the spherical harmonics of order 1.

Consider the operation of the group elements on a vector of the form $(0,0,z)$. The identity operation obviously does not change the vector. This may be represented by the equation

Table 26. Matrix representation of the group operations of the symmetry group D_{4h}

E	C_2	C_4	C_4^3
$\begin{pmatrix} 1 & 0 & 0 \\ 0 & 1 & 0 \\ 0 & 0 & 1 \end{pmatrix}$ $C_2^i(x)$	$\begin{pmatrix} -1 & 0 & 0 \\ 0 & -1 & 0 \\ 0 & 0 & 1 \end{pmatrix}$ $C_2^i(y)$	$\begin{pmatrix} 0 & -1 & 0 \\ 1 & 0 & 0 \\ 0 & 0 & 1 \end{pmatrix}$ $C_2^{ii}(xy)$	$\begin{pmatrix} 0 & 1 & 0 \\ -1 & 0 & 0 \\ 0 & 0 & 1 \end{pmatrix}$ $C_2^{ii}(-xy)$
$\begin{pmatrix} 1 & 0 & 0 \\ 0 & -1 & 0 \\ 0 & 0 & -1 \end{pmatrix}$ i	$\begin{pmatrix} -1 & 0 & 0 \\ 0 & 1 & 0 \\ 0 & 0 & -1 \end{pmatrix}$ σ_h	$\begin{pmatrix} 0 & 1 & 0 \\ 1 & 0 & 0 \\ 0 & 0 & -1 \end{pmatrix}$ S_4	$\begin{pmatrix} 0 & -1 & 0 \\ -1 & 0 & 0 \\ 0 & 0 & -1 \end{pmatrix}$ S_4^3
$\begin{pmatrix} -1 & 0 & 0 \\ 0 & -1 & 0 \\ 0 & 0 & -1 \end{pmatrix}$ $\sigma_v^i(x)$	$\begin{pmatrix} 1 & 0 & 0 \\ 0 & 1 & 0 \\ 0 & 0 & -1 \end{pmatrix}$ $\sigma_v^i(y)$	$\begin{pmatrix} 0 & -1 & 0 \\ 1 & 0 & 0 \\ 0 & 0 & -1 \end{pmatrix}$ $\sigma_v^{ii}(xy)$	$\begin{pmatrix} 0 & 1 & 0 \\ -1 & 0 & 0 \\ 0 & 0 & -1 \end{pmatrix}$ $\sigma_v^{ii}(-xy)$
$\begin{pmatrix} -1 & 0 & 0 \\ 0 & 1 & 0 \\ 0 & 0 & 1 \end{pmatrix}$	$\begin{pmatrix} 1 & 0 & 0 \\ 0 & -1 & 0 \\ 0 & 0 & 1 \end{pmatrix}$	$\begin{pmatrix} 0 & -1 & 0 \\ -1 & 0 & 0 \\ 0 & 0 & 1 \end{pmatrix}$	$\begin{pmatrix} 0 & 1 & 0 \\ 1 & 0 & 0 \\ 0 & 0 & 1 \end{pmatrix}$

$$E(0,0,z) = (0,0,z) \begin{pmatrix} 1 & 0 & 0 \\ 0 & 1 & 0 \\ 0 & 0 & 1 \end{pmatrix} = (0,0,z) = (1)(0,0,z).$$

Similarly the operation C_4 may be represented by the equation

$$C_4(0,0,z) = (0,0,z) \begin{pmatrix} 0 & -1 & 0 \\ 1 & 0 & 0 \\ 0 & 0 & -1 \end{pmatrix} = (0,0,-z) = (-1)(0,0,z).$$

The coefficient in front of the vector on the right hand side of the equation may be considered as a one-dimensional matrix representation of the group operation for the vector under consideration. The character of this representation will be equal to the trace of the matrix, and will be identical to the character of the representation to which the vector belongs. When this procedure is carried out for all the group elements, it is seen that the vector $(0,0,z)$ transforms according to the representation A_{2u} , and thus the p_z orbital belongs to the A_{2u} representation. The same procedure could be carried out for a vector of the type $(x,y,0)$ to determine which representation this vector belongs. However it is known that the representation of Y_1 contains only the two irreducible representations A_{2u} and E_u . Thus, the pair of orbitals p_x and p_y must belong to the representation E_u .

The situation for the d orbitals is a little more complex since they do not transform as the quantities x , y , or z , but as products of these quantities. This is because the d_{xy} orbital, for example, has the analytical form

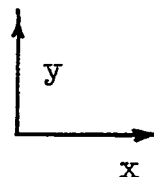
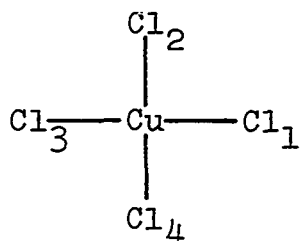
$$\psi = c \cdot R(r) \cdot xy$$

where c is a constant and $R(r)$ is a function of the radius r only. Thus the angular dependence of the function is determined by the product xy . First consider the d_{z^2} orbital, which transforms in the same manner as the product z^2 , which belongs to the product representation $A_{2u} \times A_{2u}$. That is, since z transforms as does the representation A_{2u} , the product z^2 transforms in the same manner as the product $A_{2u} \times A_{2u}$. In general the character for a given symmetry element in a product representation is given by the product of the character in the first representation and the complex conjugate of the character in the second representation, that is, $\chi(t) = \chi^1(t) \overline{\chi^2(t)}$. Since all of the characters of the representation A_{2u} are ± 1 , the characters of the product representation $A_{2u} \times A_{2u}$ are all $+1$. This is obviously the representation A_{1g} . Similarly the pair of orbitals d_{xz} and d_{yz} will transform like the product of the pair x and y with z , that is, they will transform like the product representation $E_u \times A_{2u}$. This product representation is E_g , as may be easily checked by doing the necessary multiplication. This means that the remaining two orbitals $d_{x^2-y^2}$ and d_{xy} must be split between the two representations B_{1g} and B_{2g} , since these two irreducible representations are contained in the representation for Y_2 , along with the two irreducible representations A_{1g} and E_g obtained above. The simplest method of assigning the symmetries of these last

two orbitals is to consider the effect of the group operations on the product $(x^2 - y^2)$. Any operation which changes x to $\pm x$ and y to $\pm y$ will leave the product unchanged, while any operation which changes x to $\pm y$ and y to $\pm x$ will change the sign of the product. Thus the character of the operations E , C_2 , C_2' , i , σ_h , and σ_v' will be ± 1 , while the operations C_4 , C_2'' , S_4 and σ_v'' will have character -1 . This means that the $d_{x^2-y^2}$ orbital belongs to the B_{1g} representation and therefore the d_{xy} orbital must belong to the B_{2g} representation.

For the ligand orbitals, linear combinations of the various orbitals must be constructed which transform in the same manner as the various irreducible representations. To assist in this, it is convenient to determine which irreducible representations will be present in the total representation for the ligand orbitals. But first this total representation must be determined.

Let the CuCl_4^- ion be situated as illustrated, with the chlorine atoms being numbered in a counterclockwise direction as indicated.



Under the group operations, the positions of the various chlorine atoms will be interchanged. Thus under the operation C_2 , atom 1 will be interchanged with atom 3, and atom 2 will be interchanged with atom 4. If the initial state is specified by a vector (1,2,3,4), then the final state can be specified by the vector (3,4,1,2). The number specifies which atom is being considered, and the position in the vector specifies the location of the atom. Now a matrix can be constructed, which, when operated on the first vector, will give the second vector. This can be done for each group operation, and these matrices will constitute a representation for the position of the ligands. The matrices for the various group elements are listed in Table 27. The trace of each of these matrices is the character for that group element. Thus the character table for the exchange of the positions of the ligands under the operations of the group is

E	C_2	$2C_4$	$2C_2'$	$2C_2''$	i	σ_h	$2S_4$	$2\sigma_v'$	$2\sigma_v''$
4	0	0	2	0	0	4	0	2	0

It is noted that the trace is equal to number of atoms left invariant by the operation.

However, it is also necessary to consider how the ligand orbitals themselves will be affected by the

Table 27. Matrix representation for the interchange of ligands in $\text{CuCl}_4^{=}$ under the symmetry operations of D_{4h}

E	C_2	C_4	C_4^3
$\begin{pmatrix} 1 & 0 & 0 & 0 \\ 0 & 1 & 0 & 0 \\ 0 & 0 & 1 & 0 \\ 0 & 0 & 0 & 1 \end{pmatrix}$	$\begin{pmatrix} 0 & 0 & 1 & 0 \\ 0 & 0 & 0 & 1 \\ 1 & 0 & 0 & 0 \\ 0 & 1 & 0 & 0 \end{pmatrix}$	$\begin{pmatrix} 0 & 1 & 0 & 0 \\ 0 & 0 & 1 & 0 \\ 0 & 0 & 0 & 1 \\ 1 & 0 & 0 & 0 \end{pmatrix}$	$\begin{pmatrix} 0 & 0 & 0 & 1 \\ 1 & 0 & 0 & 0 \\ 0 & 1 & 0 & 0 \\ 0 & 0 & 1 & 0 \end{pmatrix}$
$C_2^I(x)$	$C_2^I(y)$	$C_2^{II}(xy)$	$C_2^{II}(-xy)$
$\begin{pmatrix} 1 & 0 & 0 & 0 \\ 0 & 0 & 0 & 1 \\ 0 & 0 & 1 & 0 \\ 0 & 1 & 0 & 0 \end{pmatrix}$	$\begin{pmatrix} 0 & 0 & 1 & 0 \\ 0 & 1 & 0 & 0 \\ 1 & 0 & 0 & 0 \\ 0 & 0 & 0 & 1 \end{pmatrix}$	$\begin{pmatrix} 0 & 1 & 0 & 0 \\ 1 & 0 & 0 & 0 \\ 0 & 0 & 0 & 1 \\ 0 & 0 & 1 & 0 \end{pmatrix}$	$\begin{pmatrix} 0 & 0 & 0 & 1 \\ 0 & 0 & 1 & 0 \\ 0 & 1 & 0 & 0 \\ 1 & 0 & 0 & 0 \end{pmatrix}$
i	σ_h	S_4	S_4^3
$\begin{pmatrix} 0 & 0 & 1 & 0 \\ 0 & 0 & 0 & 1 \\ 1 & 0 & 0 & 0 \\ 0 & 1 & 0 & 0 \end{pmatrix}$	$\begin{pmatrix} 1 & 0 & 0 & 0 \\ 0 & 1 & 0 & 0 \\ 0 & 0 & 1 & 0 \\ 0 & 0 & 0 & 1 \end{pmatrix}$	$\begin{pmatrix} 0 & 1 & 0 & 0 \\ 0 & 0 & 1 & 0 \\ 0 & 0 & 0 & 1 \\ 1 & 0 & 0 & 0 \end{pmatrix}$	$\begin{pmatrix} 0 & 0 & 0 & 1 \\ 1 & 0 & 0 & 0 \\ 0 & 1 & 0 & 0 \\ 0 & 0 & 1 & 0 \end{pmatrix}$
$\sigma_V^I(x)$	$\sigma_V^I(y)$	$\sigma_V^{II}(xy)$	$\sigma_V^{II}(-xy)$
$\begin{pmatrix} 0 & 0 & 1 & 0 \\ 0 & 1 & 0 & 0 \\ 1 & 0 & 0 & 0 \\ 0 & 0 & 0 & 1 \end{pmatrix}$	$\begin{pmatrix} 1 & 0 & 0 & 0 \\ 0 & 0 & 0 & 1 \\ 0 & 0 & 1 & 0 \\ 0 & 1 & 0 & 0 \end{pmatrix}$	$\begin{pmatrix} 0 & 0 & 0 & 1 \\ 0 & 0 & 1 & 0 \\ 0 & 1 & 0 & 0 \\ 1 & 0 & 0 & 0 \end{pmatrix}$	$\begin{pmatrix} 0 & 1 & 0 & 0 \\ 1 & 0 & 0 & 0 \\ 0 & 0 & 0 & 1 \\ 0 & 0 & 1 & 0 \end{pmatrix}$

operations of the group. Since chloride ions are the ligands under consideration, only p orbitals will be involved, and the total representation for the ligand orbitals will be given by the product of the matrix representation

for the exchange of ligands and the matrix representation for the p orbitals on a single ligand. The character table for the representation for the ligand orbitals is

E	C_2	$2C_4$	$2C_2'$	$2C_2''$	i	σ_h	$2S_4$	$2\sigma_v'$	$2\sigma_v''$
12	0	0	-2	0	0	4	0	2	0

This representation can be shown to contain the irreducible representations A_{1g} , A_{2g} , A_{2u} , B_{1g} , B_{2g} , B_{2u} , E_g , and $2E_u$ through the use of the orthogonality relationship previously discussed.

The linear combinations of the p_x , p_y , and p_z orbitals on the four ligands atoms which correspond to the above representations must now be found. This may be simplified somewhat by recalling that the pair of orbitals p_x and p_y belong to the E_u representation while the p_z orbital belongs to the A_{2u} representation. Thus the linear combinations involving p_x and p_y orbitals will belong to irreducible representations contained in the product representation of E_u with that for the interchange of ligand positions, while the linear combinations involving p_z orbitals will belong to the product representation of A_{2u} with that for the interchange of ligand positions. Therefore, the linear combinations of p_x and p_y orbitals will belong to A_{1g} , A_{2g} , B_{1g} , B_{2g} , and $2E_u$, and those of the p_z orbitals will belong to

A_{2u} , B_{2u} , and E_g .

It will be assumed that the p_x orbitals on each ligand is pointed along the x-axis with the positive lobe in the direction of positive x values, and similarly for the p_y and p_z orbitals. Having obtained the breakdown of the representation of the ligand orbitals into its irreducible representations, the proper symmetry orbital for each irreducible representation can be constructed. These are listed in Table 28, and it is quite easy to check each symmetry orbital to see that it transforms as does the irreducible representation to which it corresponds.

Table 28. Symmetry orbitals for the CuCl_4^- ion

Symmetry	Metal orbital	Ligand orbital ^a
A_{1g}	$\varphi_1 = s$	$\sigma_1 = \frac{1}{2}(x_1+x_2-x_3-x_4)$
	$\varphi_1' = d_{z^2}$	
B_{1g}	$\varphi_2 = d_{x^2-y^2}$	$\sigma_2 = \frac{1}{2}(x_1-y_2-x_3+y_4)$
E_u	$\varphi_3 = p_x$	$\sigma_3 = 1/\sqrt{2}(x_1+x_3)$
	$\varphi_4 = p_y$	$\sigma_4 = 1/\sqrt{2}(y_2+y_4)$
		$\pi_3 = 1/\sqrt{2}(y_1-y_3)$
		$\pi_4 = 1/\sqrt{2}(x_2-x_4)$
A_{2g}		$\pi_5 = \frac{1}{2}(y_1-x_2-y_3+x_4)$
B_{2g}	$\varphi_6 = d_{xy}$	$\pi_6 = \frac{1}{2}(y_1+x_2-y_3-x_4)$
A_{2u}	$\varphi_7 = p_z$	$\pi_7 = \frac{1}{2}(z_1+z_2+z_3+z_4)$
B_{2u}		$\pi_8 = \frac{1}{2}(z_1-z_2+z_3-z_4)$
E_g		$\pi_9 = 1/\sqrt{2}(z_1-z_3)$
		$\pi_{10} = 1/\sqrt{2}(z_2-z_4)$

^aFor the ligand orbitals, x_1 denotes the p_x orbital on atom 1 with the positive lobe pointing in the positive x-direction located. The notations y_1 and z_1 have similar meanings.

VIII. APPENDIX B: GROUP THEORY APPLICATION TO
 BONDING IN THE Cu_2Cl_6^- ION

The planar dimer Cu_2Cl_6^- belongs to the symmetry group D_{2h} . The character table is given in Table 29, and the characters of the representations for the spherical harmonics of order 0, 1, and 2 are given in Table 30 along with the decomposition of the representations into their irreducible representations.

Table 29. Character table for the group D_{2h}

	E	$C_2(z)$	$C_2(y)$	$C_2(x)$	i	σ_z	σ_y	σ_x
A_{1g}	1	1	1	1	1	1	1	1
A_{1u}	1	1	1	1	-1	-1	-1	-1
B_{1g}	1	1	-1	-1	1	1	-1	-1
B_{1u}	1	1	-1	-1	-1	-1	1	1
B_{2g}	1	-1	1	-1	1	-1	1	-1
B_{2u}	1	-1	1	-1	-1	1	-1	1
B_{3g}	1	-1	-1	1	1	-1	-1	1
B_{3u}	1	-1	-1	1	-1	1	1	-1

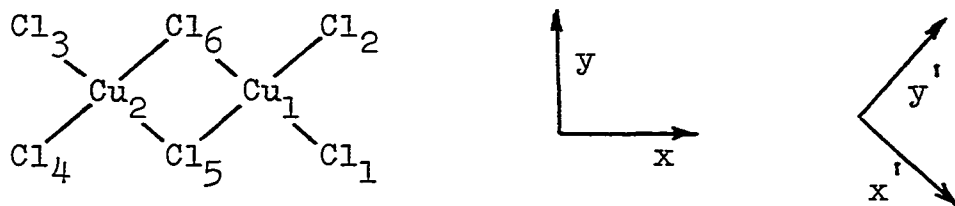
Table 30. Characters for the representations of the Y_0 , Y_1 , and Y_2 spherical harmonics and decomposition into their irreducible representations for the group D_{2h}

	E	$C_2(z)$	$C_2(y)$	$C_2(x)$	i	σ_z	σ_y	σ_x
A_{1g}	1	1	1	1	1	1	1	1
Y_0	1	1	1	1	1	1	1	1
B_{1u}	1	1	-1	-1	-1	-1	1	1
B_{2u}	1	-1	1	-1	-1	1	-1	1
B_{3u}	1	-1	-1	1	-1	1	1	-1
Y_1	3	-1	-1	-1	-3	1	1	1
A_{1g}	1	1	1	1	1	1	1	1
A_{1g}	1	1	1	1	1	1	1	1
B_{1g}	1	1	-1	-1	1	1	-1	-1
B_{2g}	1	-1	1	-1	1	-1	1	-1
B_{3g}	1	-1	-1	1	1	-1	-1	1
Y_2	5	1	1	1	5	1	1	1

The s orbital obviously belongs to the A_{1g} representation again. The p_z orbital must belong to the B_{1u} representation since this is the only p orbital which is invariant under the operation $C_2(x)$. Similarly, the p_y

orbital and the p_x orbital belong to the B_{2u} and B_{3u} representations respectively. For the d orbitals, the d_{z^2} and $d_{x^2-y^2}$ orbitals must be the two orbitals belonging to the two A_{1g} representations since these two orbitals are invariant under all the operations of the group. The d_{xy} orbital is invariant to reflection in the xy-plane, that is, it is invariant to the group operation σ_z , and must therefore belong to the representation B_{1g} . Similar arguments show that the d_{xz} and d_{yz} orbitals belong to the B_{2g} and B_{3g} representations respectively.

In the discussion on the formation of the symmetry orbitals for the Cu_2Cl_6^- dimer, it will be assumed that the dimer is oriented as indicated in the following illustration, with the chlorine atoms numbered as indicated. Again



it will be assumed that the positive lobe of the p_x orbitals is pointed in the positive x-direction, and similarly for the p_y and p_z orbitals.

In the Cu_2Cl_6^- dimer, there are two sets of equivalent chlorine atoms with the one set containing Cl_1 , Cl_2 , Cl_3 and

Cl_4 and the second set containing Cl_5 and Cl_6 . It will be necessary to construct symmetry orbitals for both sets of ligand atoms and also for the two metal atoms. It is recalled from the discussion in Appendix A that the character for each operation was equal to the number of atoms left invariant by that operation. For the set which consists of the ligand Cl_5 and Cl_6 atoms, the operations E , σ_z , $C_2(y)$, and σ_x leave both atoms invariant and thus have a character of two, while the other operations interchange the two atoms and have a character of zero. Thus the representation for this set of ligands contains the irreducible representations A_{1g} and B_{2u} . For the set which contains the four terminal chlorine atoms, the operations E and σ_z have a character of four, while all the other operations have a character of zero since no atoms are left invariant under these operations. The representation for the interchange of these four ligands contains the irreducible representations A_{1g} , B_{1g} , B_{2u} , and B_{3u} . The various ligand symmetry orbitals are listed in Table 31. These are constructed conveniently by the following procedure: choose one ligand orbital (or more precisely, choose the function defining this orbital), operate on this orbital by each of the group operations, multiple the result of this operation by the character of the irreducible representation, and sum over all operations. Mathematically, this may be expressed as

Table 31. Symmetry orbitals for the Cu_2Cl_6^- ion

Symmetry	Metal orbital	Ligand orbital ^a
B_{1g}	$\varphi_1 = 1/\sqrt{2}[d_{xy}(1) + d_{xy}(2)]$	$\sigma_1 = \frac{1}{2}(x_1^i - y_2^i - x_3^i + y_4^i)$ $\pi_1 = \frac{1}{2}(y_1^i - x_2^i - y_3^i + x_4^i)$ $\zeta_1 = 1/\sqrt{2}(x_5 - x_6)$
B_{2u}	$\varphi_2 = 1/\sqrt{2}[d_{xy}(1) - d_{xy}(2)]$	$\sigma_2 = \frac{1}{2}(x_1^i - y_2^i + x_3^i - y_4^i)$ $\pi_2 = \frac{1}{2}(y_1^i - x_2^i + y_3^i - x_4^i)$ $\zeta_2 = 1/\sqrt{2}(y_5 + y_6)$
A_{1g}	$\varphi_3 = 1/\sqrt{2}[d_{z^2}(1) + d_{z^2}(2)]$ $\varphi_3^i = 1/\sqrt{2}[d_{x^2-y^2}(1) + d_{x^2-y^2}(2)]$	$\sigma_3 = \frac{1}{2}(x_1^i + y_2^i - x_3^i - y_4^i)$ $\pi_3 = \frac{1}{2}(y_1^i + x_2^i - y_3^i - x_4^i)$ $\zeta_3 = 1/\sqrt{2}(y_5 - y_6)$
B_{3u}	$\varphi_4 = 1/\sqrt{2}[d_{z^2}(1) - d_{z^2}(2)]$ $\varphi_4^i = 1/\sqrt{2}[d_{x^2-y^2}(1) - d_{x^2-y^2}(2)]$	$\sigma_4 = \frac{1}{2}(x_1^i + y_2^i + x_3^i + y_4^i)$ $\pi_4 = \frac{1}{2}(y_1^i + x_2^i + y_3^i + x_4^i)$ $\zeta_4 = 1/\sqrt{2}(y_5 + y_6)$
B_{1u}	$\varphi_5 = 1/\sqrt{2}[d_{xz}(1) - d_{xz}(2)]$	$\pi_5 = \frac{1}{2}(z_1 - z_2 + z_3 - z_4)$ $\zeta_5 = 1/\sqrt{2}(z_5 + z_6)$
B_{2g}	$\varphi_6 = 1/\sqrt{2}[d_{xz}(1) + d_{xz}(2)]$	$\pi_6 = \frac{1}{2}(z_1 + z_2 - z_3 - z_4)$ $\zeta_6 = 1/\sqrt{2}(z_5 - z_6)$
A_{1u}	$\varphi_7 = 1/\sqrt{2}[d_{yz}(1) - d_{yz}(2)]$	$\pi_7 = \frac{1}{2}(z_1 + z_2 + z_3 + z_4)$
B_{3g}	$\varphi_8 = 1/\sqrt{2}[d_{yz}(1) + d_{yz}(2)]$	$\pi_8 = \frac{1}{2}(z_1 - z_2 - z_3 + z_4)$

^aFor the ligand orbitals, x_1 denotes the p_x orbital on atom 1 with the positive lobe pointing in the positive x direction while x_1^i denotes the p_x orbital on atom 1 with the positive lobe pointing in the positive x^i direction.

$$\varphi_i = \sum_t \chi^i(t) R(t) \psi$$

where φ_i is the symmetry orbital for the i^{th} representation, ψ is a wave function located on one ligand atom, $R(t)$ is the operation t , and $\chi^i(t)$ is the character of the operation t of the i^{th} irreducible representation and the sum is over all the operations of the group. If the sum is zero, there is no symmetry orbital which belongs to that particular irreducible representation. For the set containing the four ligand atoms, it will be convenient to use p-orbitals defined in a coordinate system rotated clockwise 45° around the z-axis of the previously defined coordinate system. These new coordinates will be denoted by (x', y', z) .

The metal symmetry orbitals are formed in the same manner as the ligand symmetry orbitals. The operations E , $C_2(x)$, σ_z , and σ_y leave the two atoms unchanged while the four other operations interchange the positions of these two atoms. The character for the first four operations mentioned is 2 and the character for the other four operations is 0 and the representation for the interchange of metal atoms thus contains the A_{1g} and B_{3u} irreducible representations. The various metal symmetry orbitals are listed in Table 31.